

**The Cellular and Molecular Investigation of Wnt/FZD  
Signalling During Spinal Cord Neurogenesis**

**Abdulmajeed Fahad Alrefaei**

**Doctor of Philosophy**

**University of East Anglia**

**School of Biological Sciences**

**April 2016**

This copy of the thesis has been supplied on condition that anyone who consults it is understood to recognize that its copyright rests with its author and due acknowledgement must always be made of the use of any material contained in, or delivered from, this thesis.

## **Acknowledgements**

I would like to thank my supervision team for their continuous support during my PhD and for their valuable discussion in regular meetings;

**Prof. Andrea Münsterberg and Dr Grant Wheeler**, for their excellent guidance, providing me an excellent environment for doing research, and for reading my thesis.

**Dr Tim Grocott**, who's always willing to answer my questions and for his help during my First year.

**Dr Paul Thomas**, for his much appreciated help on microscopy and imaging.

**Dr Geoff Mok**, for many scientific discussions and for reading some chapters of my thesis.

**Dr Niki Kennerly and Dr Dom McCormick**, for their help on molecular techniques at the beginning of my research.

### **Past and current members of the Münsterberg and Wheeler Laboratories:**

Danielle Blackwell, Nicole Ward, Ines Desanlis, Dr Kim Hanson, Camille Viaut, Marta Marin, Dr Angels Ruyra Ripoll, Katy Saide, Johannes Wittig, Dr James McColl, Dr Adam Hendry, Dr Vicky Hatch, Dr Connie Ochmann, Dr Kasia Goljanek-Whysall, Dr Amanda Barber, Andy Loveday, Chris Ford, Ayisha Ahmed, Dr Simon Moxon, Marlene Jahnke, Juliana Giusti and Amy Lyall for being such amazing Friends and for all the fun we have had during these four years.

Also, I would like to express my sincere gratitude to my parents and to my brothers and sisters for encouraging and supporting me throughout my study in the UK. Also I would like to thank all my Friends in the UK and in Saudi Students Society in Norwich.

Finally, I would like to thank **the Saudi Arabian Government** for funding my PhD research.

**-Memberships:**

- 1- Member of British Society of Cell Biology.
- 2- Member of British Society of Developmental Biology.

**-Rewards:**

- 1-Honor Fell/Company of Biologists Travel Awards 2012, 2014 and 2015.
- 2-Several awards from Saudi Arabian Cultural Bureau, London-UK.
- 3-Rewarded by Saudi Ambassador in United Kingdom 2015.

**-Publications:**

1-Mok GF, **Alrefaei AF**, McColl J, Grocott T, Münsterberg A. (2015) Chicken as a Developmental Model. In: eLS. John Wiley & Sons, Ltd: Chichester. DOI: 10.1002/9780470015902.a0021543.

2-Abou-Elhamd A, **Alrefaei AF\***, Mok GF\*, Garcia-Morales C, Abu-Elmagd M, Wheeler GN, Münsterberg A. (2015) Klf131 attenuates beta-catenin dependent Wnt signaling and regulates embryo myogenesis. *Developmental Biology* 402(1):61-71\*joint authorship.

3-Goljanek-Whysall K\*, Mok GF\*, **Fahad Alrefaei A**, Kennerley N, Wheeler GN, Münsterberg A. (2014) myomiR-dependent switching of BAF60 variant incorporation into Brg1 chromatin remodeling complexes during embryo myogenesis. *Development* 141(17):3378-87.

**-Conferences:**

- 1-Joint meeting of British Society of Cell biology, British society of developmental Biology and Japanese Society of Developmental Biology, spring 2012, Warwick University, the uk.
- 2- Xenpous meeting 2012, Sanger Institute, Cambridge.
- 3-4th the Young Embryologist Meeting, 2012, University College London.
- 4-Winter enrichment program, 2013, KAUST, Saudi Arabia.
- 5- Xenpous meeting 2013, Oxford.
- 6-4th the Young Embryologist Network Annual Meeting, 2014, University College London.
- 7-EMBO Conference on “Spinal cord development and regeneration”, 2014, Spain. Presented a poster.
- 8-8th the Saudi Student Conference 2015, Imperial College London. One of the organizers and presented a poster.
- 9- Joint meeting of Portuguese Society of Developmental Biology, British Society of Cell Biology and British Society of Developmental Biology, 2015, Portugal. Presented a poster.
- 10-9th the Saudi Student Conference 2016, University of Birmingham. Presented a poster titled “Frizzled-10 receptor is involved in neurogenesis of the Spinal cord”.

## Abstract

Spinal cord development has been studied extensively and is a model for embryonic patterning and cell differentiation. These processes are governed by extracellular and intracellular signaling and require gene transcription. Wnt signaling has been shown to be involved in dorsal-ventral patterning of the spinal cord, where it affects cell proliferation and specification. Wnt ligands bind to Frizzled receptors and Lrp5/6 co-receptors and initiate canonical,  $\beta$ -catenin-dependent, Wnt signaling. To determine important FZD receptors in chick spinal cord we analysed FZD expression patterns using *in situ* hybridization. In situ cryosections showed that FZD expression patterns are dynamic and specific along the dorsal-ventral axis of the spinal cord. Previous work in *Xenopus* showed that FZD10 acts through canonical Wnt signaling. However, which Wnt ligands activate FZD10 during neurogenesis remains unclear. Here, we investigate FZD10 expression, regulation and function in the chick developing spinal cord using *in situ* hybridization, *in ovo* electroporation and immunohistochemistry.

FZD10 is expressed in the dorsal neural tube and overlaps with expression of Wnt1, Wnt3a, markers of dorsal progenitors and of interneurons. To examine Wnt1 and Wnt3a interactions with FZD10 *in vivo*, developing spinal cords were electroporated with Wnt1 and Wnt3a individually. Targeted mis-expression of Wnt1 up-regulated FZD10 expression whereas Wnt3a did not. This may suggest that FZD10 exclusively interacts with Wnt1 to mediate its function during spinal cord development.

Furthermore, the role of FZD10 was studied *in vivo* in developing spinal cords. FZD10 regulated cell proliferation and differentiation, suggesting that it is required for Wnt1 signal transduction and for spinal cord development.

Lrp6 is involved in central nervous system development including spinal cord. In this study, *in vivo* experiments revealed that Lrp6 complements Wnt1/FZD10 mediated activation of dorsal markers during spinal cord neurogenesis. This could explain how Wnt signalling regulates sensory neuron formation in the dorsal spinal cord.

<b>Table of Contents</b>	<b>Page number</b>
<b>Chapter1</b>	1-34
<b>1 Introduction</b>	1
<b>1-1 Wnt signalling pathways</b>	1
<b>1-2 Neural development:</b>	5
<b>1-3 Dorsal-ventral neural tube patterning and signalling pathways</b>	9
1-3-1 The ventral neural tube and Shh	11
1-3-2 The dorsal neural tube and Wnt/BMP	13
1-3-2-1 BMP signalling	14
1-3-2-2 Wnt signalling	15
<b>1-4 Dorsal neural tube development and the canonical Wnt signalling pathway</b>	16
<b>1-5 FZD receptors</b>	19
1-5-1 FZD structure and signalling	19
1-5-2 FZDs and Wnt specificity	21
1-5-3 Wnt/FZD signalling and diseases	24
1-5-3-1 FZDs and cancer	24
1-5-3-2 Wnt/FZD signalling and neural tube defects	25
<b>1-6 Expression and function of FZDs during development</b>	28
<b>1-7 The project background and aims</b>	33
<b>Chapter2</b>	36-57
<b>2- Materials and Methods</b>	36
<b>2-1-RNA extraction and purification</b>	36
<b>2-2-cDNA synthesis</b>	37
<b>2-3-Cloning of full length of FZD10</b>	37
<b>2-4-Primer design to clone FZD10</b>	37
<b>2-5-PCR reaction and conditions</b>	38
<b>2-6-Agarose gel electrophoresis</b>	38
<b>2-7-DNA extraction from agarose gel</b>	39
<b>2-8-Cloning of FZD10 into plasmid vector</b>	39

2-8-1-Ligation of FZD10 into pGEM-T easy vector	40
2-8-2-Ligation of FZD10 into pCAB expression vector	41
<b>2-9-Plasmid transformation</b>	42
<b>2-10-DNA purification and preparation</b>	42
2-10-1-Mini preparation of DNA plasmid	42
2-10-2-Midi preparation of DNA plasmid	43
<b>2-11 Cloning of short fragments of FZD receptors</b>	45
2-11-1 Designed primers for FZD cloning	46
2-11-2 PCR reaction and condition	46
<b>2-12 Electroporation</b>	48
<b>2-13 FZD10 knockdown using shRNA</b>	49
<b>2-14 Whole mount in situ hybridization (WISH)</b>	50
2-14-1 Probe synthesis	50
2-14-2 Antisense transcription	51
2-14-3 Probe purification	51
2-14-4 Embryo preparation and staging	52
2-14-5 Rehydration	53
2-14-6 Proteinase K treatment	53
2-14-7 Hybridisation	53
2-14-8 Post-hybridisation	53
2-14-9 Post-antibody washes and colour reaction	54
2-14-10 Double in situ hybridisation	54
<b>2-15 Cryosectioning</b>	55
<b>2-16 Immunostaining</b>	56
<b>Chapter3</b>	59-69
<b>3-1 Introduction</b>	59
<b>3-2 Results</b>	
3-2 FZDs are expressed in the chick developing spinal cord	62
3-3 FZD7 and FZD10 are expressed during spinal cord neurogenesis	66
<b>3-4 Summary</b>	68
<b>Chapter4</b>	71-81
<b>4-1 introduction</b>	71

<b>4-2 Results</b>	
4-2 FZD10 expression pattern during chick embryo development	73
4-3 FZD10 is expressed in the dorsal domain of the spinal cord during neurogenesis	75
4-4 FZD10 expression overlaps with dorsal progenitors markers	77
4-5 FZD10 expression overlaps with dorsal Wnts (Wnt1 and Wnt3a) in the spinal cord	79
<b>4-6 Summary</b>	81
<b>Chapter5</b>	83-96
<b>5-1 Introduction</b>	83
<b>5-1 Results</b>	
5-2 Wnt1 and Wn3a regulate FZDs expression in the dorsal-ventral axis of the spinal cord	85
5-3 Wnt1 and Wnt3a affect spinal cord patterning and Wn1 overexpression up-regulates FZD10 expression	88
<b>5-4 Summary</b>	95
<b>Chapter6</b>	98-127
<b>6-1 Introduction</b>	98
<b>6-2 Results</b>	
6-2 Knockdown of FZD10 led to a decrease in cell proliferation in the spinal cord	100
6-3 Knockdown of FZD10 affected neurogenesis in the spinal cord	103
6-4 Knockdown of FZD10 rescued the Wnt1 overexpression phenotype	107
6-5 Overexpression of FZD10 affected the patterning of neural progenitors and inhibited neurogenesis	112
6-6 Overexpressed FZD10 affected the cytoskeleton structure of the spinal cord	119

6-7 Co-overexpression of Lrp6 and FZD10 strongly enhanced the Wnt1 phenotype, leading to overgrowth and striking dorsalization in the spinal cord	121
<b>6-8 Summary</b>	126
<b>Chapter7</b>	129-144
<b>7 Discussion</b>	
<b>7-1 Introduction</b>	129
<b>7-2 Wnt1 and Wnt3a expression and function during spinal cord development</b>	129
<b>7-3 FZDs are expressed during spinal cord development</b>	132
<b>7-4 FZD10 expression during spinal cord neurogenesis</b>	133
<b>7-5 Dorsally expressed Wnts (Wnt1/Wnt3a) regulates the expression of FZD7 and FZD10 in the spinal cord</b>	134
<b>7-6 Wnt1 up-regulates FZD10 expression in the spinal cord</b>	136
<b>7-7 FZD10 function during spinal cord neurogenesis</b>	137
7-7-1 FZD10 knockdown reduces cell proliferation and inhibits neurogenesis in spinal cord	137
7-7-2 FZD10 knockdown rescues the Wnt1 phenotype	138
7-7-3 FZD10 overexpression affects neural progenitors and neural differentiation markers	139
7-7-3 FZD10 overexpression severely affects the actin cytoskeleton in the spinal cord	141
7-7-4 FZD10 interacts with Lrp6 to mediate Wnt1 activity in vivo in the spinal cord	142
<b>7-8 Conclusion</b>	144
<b>8- References Appendixes</b>	145
<b>9- Appendixes</b>	162

<b>List of Figures</b>	
<b>Chapter1</b>	
Fig. 1.1 Wnt signalling pathways	2
Fig. 1.2 Neural tube and neural crest formation	6
Fig. 1.3 Cross section of the developing spinal cord	10
Fig. 1.4 This Diagram shows a cross section of the developing spinal cord	11
Fig. 1.5 Schematic illustration of FZD structure	20
<b>Chapter2</b>	
Fig. 2.1 Electroporation approach in chick neural tube	48
Fig. 2.2 RFP expression was detected after electroporation of scrambled shRNA	50
<b>Chapter3</b>	
Fig. 3.1 Expression patterns of cFZDs in the developing spinal cord were detected by in situ hybridization at stage HH14-15	63
Fig. 3.2 Whole mount in situ shows expression patterns of FZD4 at different stages	64
Fig. 3.3 Whole mount in situ shows expression patterns of FZD6 and FZD8	65
Fig. 3.4 Expression patterns of FZD7 and FZD10 in the spinal cord at stage HH24	67
<b>Chapter4</b>	
Fig. 4.1 Whole mount in situ hybridization of FZD10 expression during chick embryo development in HH9-28 embryos	74
Fig. 4.2 FZD10 expression in the dorsal spinal cord during dorsal neurogenesis	76
Fig. 4.3 Comparison of the expression patterns of FZD10 and neural markers	78
Fig. 4.4 Expression profile of Wnt1, Wnt3a and FZD10 in chick embryo at HH14 and HH20	80
<b>Chapter5</b>	
Fig. 5.1 Wnt1 and Wn3a affect FZD10 and 7 expression in chick spinal cord (24hours PE)	87
Fig. 5.2 Wnt1 and Wn3a electroporation in chick spinal cord after 48hours	90
Fig. 5.3 Analysis of protein expression patterns after Wnt1 misexpression in spinal cord	91
Fig. 5.4 Analysis of protein expression patterns after Wnt3a misexpression in spinal cord	92
Fig. 5.5 FZD10 expression is up-regulated following Wn1 misexpression	94
<b>Chapter6</b>	
Fig. 6.1 FZD10 was knocked down after electroporating FZD10 sh-RNA vector in the spinal cord	101
Fig. 6.2 Knockdown of FZD10 led to a reduction in spinal cord size and a decrease in proliferative cells	102
Fig. 6.3 FZD10 knockdown affects neural markers in spinal cord (24hours PE)	105
Fig. 6.4 The effect of FZD10 knockdown on spinal cord after 48hours PE	106
Fig. 6.5 Schematic illustration of rescue experiments in the spinal cord	108
Fig. 6.6 FZD10 knockdown by sh-RNA rescues Wnt1 overexpression phenotype	109

Fig. 6.7 Knockdown of FZD10 did not affect the phenotype of Wnt3a overexpression	110
Fig. 6.8 Summary of phenotypes that shows percentage of embryos after rescue experiments	111
Fig. 6.9 Ectopic expression of FZD10 is detected in the spinal cord after electroporation	113
Fig. 6.10 FZD10 overexpression affects neural progenitor patterning the in D-V axis of the spinal cord	114
Fig. 6.11 FZD10 overexpression leads to inhibition in neurogenesis of the spinal cord 48 hours PE	117
Fig. 6.12 FZD10 overexpression reduces neurogenesis of the spinal cord 72 hours PE	118
Fig. 6.13 overexpressed FZD10 affected the structure of the cytoskeleton in the spinal cord 48 hours PE	120
Fig. 6.14 LRP6 misexpression does not affect dorsal progenitor patterning in the spinal cord	122
Fig. 6.15 FZD10 interacts with Lrp6 to mediate Wnt1 activity in vivo in the spinal cord	124
Fig. 6.16 the size of ventral expansion of Pax7 after 48 hours PE	125
<b>Chapter7</b>	
Fig.7.1 proposed model for Wnt1 and Wnt3a signaling in the spinal cord	138
Fig. 7.1 Schematic representation of Wnt1/FZD10/Lrp6 signalling model	140

<b>List of Tables</b>	
<b>Chapter2</b>	
Table. 1.1 Summary of FZDs expression in Xenopus	29
Table. 1.2 Summary of FZDs expression in mouse	31
Table 2.1 Primers were used for cloning and sequencing	45
Table 2.2 Plasmids used for electroporation	47
Table 2.3 In situ probes were made and used in this project	52
Table 2.4 Antibodies used in this project	57
<b>Chapter3</b>	
Table. 3.1 Summary of FZD receptor expression in the spinal cord	66

**Abbreviations:**

APC: Adenomatous polyposis coli

ATP: Adenosine Triphosphate

BBR: Boehringer Blocking Reagent

BCIP: 5-Bromo-4-chloro-3-indolyl phosphate

BMP: Bone morphogenetic proteins

BSA: Bovine serum albumin

cDNA: Complementary DNA

CHAPS: 3-[(3-Cholamidopropyl)dimethylammonio]-1-propanesulfonate

CNS: Central nervous system

D/V: Dorsal-Ventral

DAPI: 4',6-Diamidino-2-Phenylindole, Dihydrochloride

DEPC: Diethyl Bicarbonate

DiG: Digoxigenin

DKK1: Dickkopf-related protein 1

dn: Dominant negative

DNA: Deoxyribonucleic Acid

dNTP: Deoxynucleotide

DTT: Dithiothreitol

DVI: Dishevelled

E.coli: Escherichia coli

EP: Electroporation

EtOH: Ethanol

FGF: Fibroblast growth factors

FITC: Fluorescein

FITC: Fluorescein

FZD: Frizzled

GFP: Green fluorescent protein

GSK3b: Glycogen Synthase Kinase 3

In Situ: In situ hybridization

IPTG: Isopropyl Beta-D-Thiogalactoside

LB: Luria Bertani medium

LRP: low-density related lipoprotein receptor

MAB: Maleic acid buffer

MABT: Maleic acid buffer-Tween20

MeOH: Methanol

MgCl<sub>2</sub>: Magnesium chloride

Min: Minutes

NaCl: Sodium chloride

NBT: Nitroblue tetrazolium

NC: Neural crest

NT: Neural tube

O/N: Over night

PAGE-SDS: Polyacridamide Gel electrophoresis sodium dodecyl sulphate

PBS: Phosphate Buffer Saline

PBST: Phosphate Buffer Saline Tween-20 or Triton

PCP: Planar cell polarity

PCR: Polymerase Chain reaction

RFP: Red fluorescent protein

ShRNA: Short hairpin RNA

SSC: Sodium Chloride/Sodium Citrate

TAE: Tris Acetata-EDTA

TBE: Tris/Borate/EDTA

TBST: Tris buffer saline -Tween20

Wnt: Wingless-type MMTV integration site

WT: Wild type

X-Gal: 5-bromo-4-chloro-3-indolyl-beta-D- galacto-pyranoside

## **1.Introduction**

### **1-1 Wnt signalling pathways:**

Wnt signalling regulates many embryonic and developmental processes in both invertebrates and vertebrates, from fruit flies to humans. Wnt signalling has been shown to be involved in the regulation of a wide variety of biological processes, such as cell proliferation, cell polarity, cell differentiation, cell fate specification and cell death (Moon et al., 2004; Logan and Nusse, 2004). It also plays several roles in the development of the central nervous system (CNS), such as in neural induction, neurulation, patterning, neural cortical migration, neuronal differentiation in the spinal cord, neural stem cells, axon guidance and synaptogenesis (Yoshikawa et al., 1997; Pöpperl et al., 1997; Muroyama et al., 2004; Muroyama et al., 2002; Lee et al., 2004; Chenn and Walsh, 2003; Lyuksyutova et al., 2003; Hall et al., 2000; Alvarez-Medina et al., 2008; Le Dréau and Martí, 2012).

Development of the vertebrate CNS requires cell-to-cell communication, intracellular signalling and gene transcription. Wnt signalling is also involved in these events because it can function as a morphogen, which means that it can regulate cell-to-cell communication and other processes that require extracellular signalling pathways (Zecca et al., 1996; Neumann and Cohen, 1997).

The Wnt ligands belong to a family of secreted glycoproteins that bind to the N-terminal extracellular cysteine-rich domain of the Frizzled (FZD) receptor family of seven-pass transmembrane proteins (Komiya and Habas, 2008). Wnt ligands and their receptors are normally classified into those that activate canonical or non-canonical signalling pathways (Fig 1.1). Canonical signalling is also called Wnt/ $\beta$ -catenin signalling because  $\beta$ -catenin is a major player in this pathway (Komiya and Habas, 2008). The

non-canonical signalling pathways are divided into planar cell polarity (PCP) pathways and Wnt/Ca<sup>2+</sup> pathways. The division of Wnt signalling relies on the fact that canonical Wnts bind to FZDs and activate  $\beta$ -catenin, which then activates target genes of the signalling pathway, whereas the non-canonical Wnts bind to FZDs and activate small Rho GTPases but the pathways are independent of  $\beta$ -catenin activity (Saijun and Zongbin, 2012; Komiya and Habas, 2008). It is worth mentioning that canonical and non-canonical Wnt signalling pathways are able to regulate each other (Saijun and Zongbin, 2012).

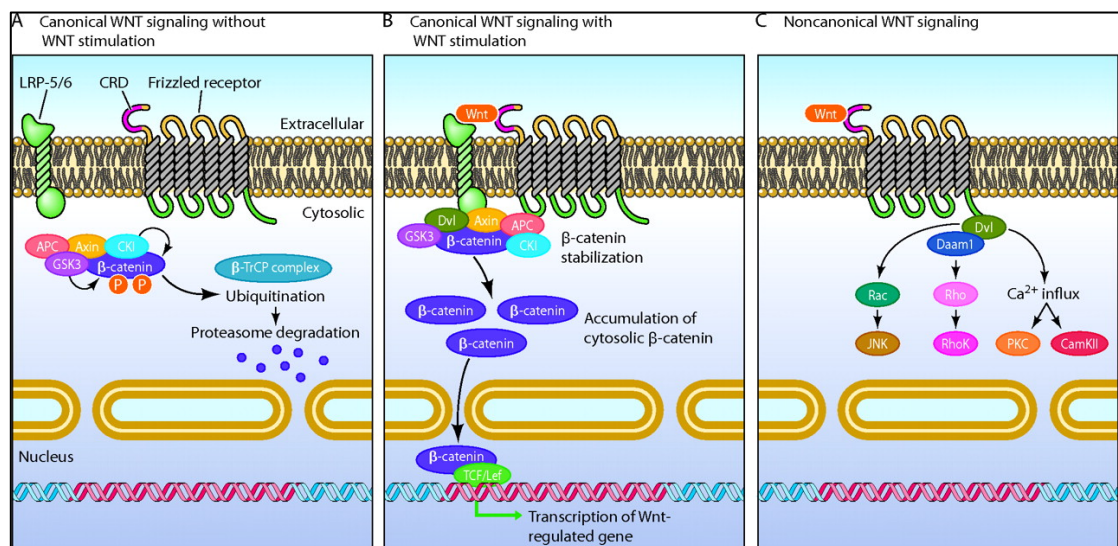


**Fig. 1.1 Wnt signalling pathways.** (A) Canonical Wnt signalling without Wnt activation. (B) Canonical Wnt signalling with Wnt activation. (C) Non-canonical Wnt signalling (planar cell polarity (PCP) pathways and Wnt/Ca<sup>2+</sup> pathways). (Adapted from Masckauchán and Kitajewski, 2006).

In this study, I focus only on the canonical Wnt signalling pathway.

### **-Canonical Wnt signalling:**

The canonical Wnt signalling pathway consists of several components, including several ligands (Wnts) and receptors, FZDs (FZD1-10); a co-receptor, the low-density lipoprotein-related receptor protein (LRP5/6); dishevelled (Dvl), a cytoplasmic protein;  $\beta$ -catenin destruction complex; glycogen synthase kinase 3 $\beta$  (GSK-3 $\beta$ ); adenomatous polyposis coli (APC); Axin proteins and casein kinase I (CKI) and nuclear transcription factors of the lymphoid enhancer factor/T-cell factor (LEF/TCF) family as well as Wnt target genes (Fig. 1). In addition, canonical Wnt signalling is inhibited by antagonists such as sFRP, WIF-1, Cerberus and DKKs (Saijun and Zongbin, 2012). Furthermore, Kremen genes are known as inhibitors for canonical Wnt signalling (Mao et al., 2002).

$\beta$ -catenin is a key player in the canonical Wnt signalling pathway. The stability of  $\beta$ -catenin relies on the presence of Wnt ligands (He et al., 2004). Without Wnt ligand binding to a cognate receptor,  $\beta$ -catenin is degraded by the destruction complex Axin/APC/GSK-3/CKI (Fig. 1.1A). The destruction complex mediates  $\beta$ -catenin degradation through the proteasomal machinery (He et al., 2004), leading to the association of LEF/TCF transcription factors with transcriptional co-repressors in the nucleus, which represses Wnt target genes (Saijun and Zongbin, 2012; Komiya and Habas, 2008).

$\beta$ -catenin is stabilised when Wnt ligands bind to cell surface receptors FZD/LRP5/6, leading to inhibition of the destruction complex (Fig. 1.1B) (Masckauchán and Kitajewski, 2006). The binding of Wnt ligands to FZD/LRP5/6 receptors leads to the activation of dishevelled (Dvl), a cytoplasmic protein containing three domains: a DIX, a PDZ and a DEP domain (Wallingford and Habas, 2005). The DIX and PDZ domains

are required for canonical Wnt signalling and for the Dvl-mediated inhibition of the destruction complex Axin/APC/GSK-3/CKI (Wallingford and Habas, 2005). When the destruction complex is inhibited by Dvl, the degradation of  $\beta$ -catenin is also stopped, resulting in the accumulation and stabilisation of  $\beta$ -catenin in the cytoplasm (Saijun and Zongbin, 2012; Komiya and Habas, 2008). After accumulation,  $\beta$ -catenin enters the nucleus and then interacts with LEF/TCF DNA-binding transcription factors (Fig. 1.1B). This results in the activation of Wnt target genes such as *Twin* and *Myc* (Reya and Clevers, 2005; Harland and Gerhart, 1997) (Fig. 1.1B).

More than 18 Wnt ligands have been identified in vertebrates (Wang et al., 2006). In this study, the Wnt ligands that are expressed in the dorsal neural tube will be examined, in particular Wnt1 and Wnt3a. These are the best candidates to start with because of their important role in the development of the dorsal neural tube. However, their specific receptors have not been identified in the dorsal neural tube.

Also, 10 FZDs receptors have been identified in vertebrates (Wang et al., 2006). The FZD family consists of 7-pass transmembrane proteins, which are members of G-protein-coupled receptors (Wang et al., 2006) (see below 1-5.)

## **1-2 Neural development:**

Development of the vertebrate nervous system is complex, requiring multiple interactions between tissues and signalling pathways. The nervous system's development starts during gastrulation, in which the embryo is rearranged into three germ layers, called the ectoderm, mesoderm and endoderm. These germ layers give rise to specific tissues. For example, the ectoderm gives rise to the epidermis, the neural tube and the neural crest. During late gastrulation neural induction takes place, and this gives the dorsal ectoderm neural identity. Neural induction is a key event for neural development, which is directed by Hensen's node in chick embryos (equivalent of Spemann's organiser) (Colas and Schoenwolf, 2001). Hensen's node is located at the anterior end of the primitive streak and plays an important role in neural induction, controlling the movement of cells during gastrulation and producing numerous signals that specify neural cells. Rapid proliferation leads to expansion of the dorsal ectoderm, which then becomes a neural plate. The neural plate gives rise to all central nervous system tissues, the brain and the spinal cord (Gilbert, 2010). Initially the neural plate will generate the neural tube. The formation of the neural tube is called neurulation, and there are two types: primary and secondary neurulation (Fig. 1.2) (Gilbert, 2010; Colas and Schoenwolf, 2001). In primary neurulation, the edge of the neural plate thickens and elevates, and the epidermal cells move toward the dorsal midline. This leads to the formation of the neural folds (Fig. 1.2), which meet and fuse at the midline, forming a hollow tube. The process of primary neurulation leads to the formation of the anterior neural tube, which is separated from the epidermis by the neural crest (Fig. 1.2) (Gilbert, 2010). The posterior end of the neural tube and tail bud are formed through the process of secondary neurulation. In chick embryos, the closure of the neural tube begins at the level of the midbrain and zips up in both directions. Failure of neural tube

closure causes many malformations in the central nervous system, called neural tube defects (Greene and Copp, 2009).

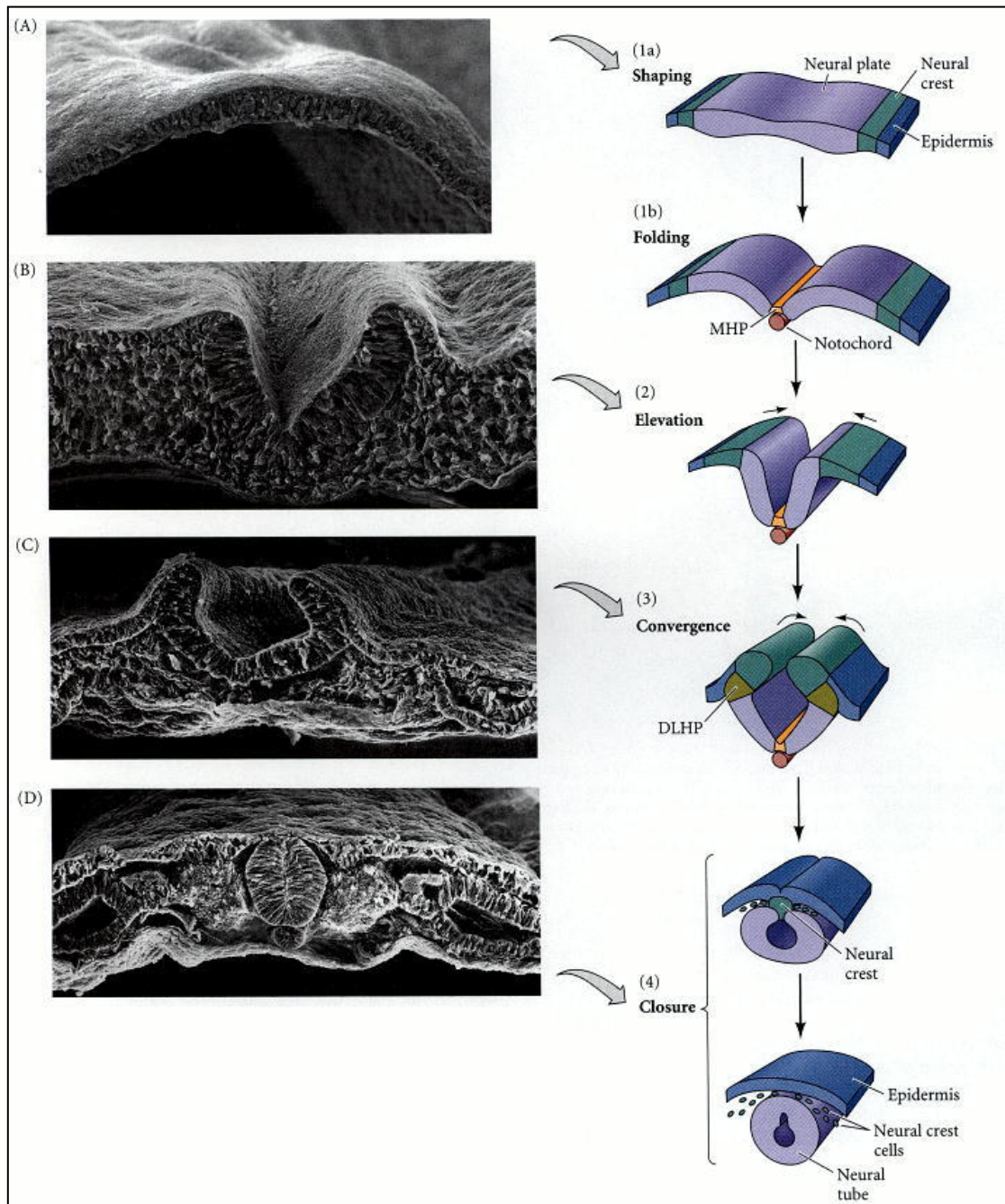


**Fig. 1.2 Neural tube and neural crest formation.** (A) Neural plate. (B) Neural groove. (C) Neural folds. (D) Neural tube. 1 to 4 illustrates the processes of neurulation from neural plate bending to neural tube closure. (Adapted from Gilbert, 2010).

Through the process of neurulation, the neural tube and crest are formed. The neural tube gives rise to the forebrain, midbrain and hindbrain as well as the spinal cord, which in combination form the functional central nervous system in vertebrates. The neural crest is formed during the process of neurulation from dorsal ectoderm, and it is first induced in the region of the neural plate border (Fig. 1.2). After neural tube formation, the neural crest delaminates from the region between the dorsal neural tube and the epidermis and migrates out following a number of different routes. Also, it gives rise to many types of cells, such as peripheral and enteric neurons and glia (Le Douarin and Kalcheim, 1999).

Many signalling pathways play important roles in neural development in vertebrates. Bone morphogenic proteins (BMPs), fibroblast growth factors (FGFs) and the Wnts are the major players during neural induction and neurulation. BMP signalling is blocked by the organiser activity (Hensen's node in chicks), which generates BMP inhibitors from the dorsal mesoderm (chordin, noggin and follistatin) (Muñoz-Sanjuán and Brivanlou, 2002; Stern, 2005). The inhibitory signals block BMP4 activity, leading to the activation of neural cell specification and inhibiting epidermal cells in the dorsal ectoderm (Piccolo et al., 1996; Zimmerman et al., 1996). This process leads to the formation of the neuroectoderm, resulting in the formation of the neural plate. This is called the default model of neural induction (Wilson and Edlund, 2001; Stern, 2005).

As mentioned above, FGFs are involved in neural induction and neurulation. Many studies have reported the involvement of FGF signalling in neural induction (Bertrand et al., 2003; Streit and Stern, 1999; Stern, 2005). Streit et al. (2000) showed that FGF signalling is important for the initiation of neural induction before gastrulation in chick

embryos. FGFs are also involved in secondary neurulation, which is the mechanism that generates the posterior end of neural tube and tail bud (Storey et al., 1998; Shamim and Mason, 1999).

Wnt signalling pathways play a critical role in many developmental processes, including neural induction and neurulation. In addition, Wnt signalling pathways have been shown to play a role in the formation of the dorsal Spemann–Mangold organiser in early *Xenopus* embryos, which mediates neural induction (De Robertis, 2000; Tao et al., 2005). Also, it has been shown that activation of canonical Wnt signalling leads to formation of a secondary dorsal axis when RNA encoding components such as dnGSK3 $\beta$ ,  $\beta$ -catenin, or Wnt1/3a is microinjected into the prospective ventral side of early *Xenopus* embryos (Du et al., 1995). Moreover, canonical Wnt signalling can regulate anterior–posterior axis formation and neural patterning (De Robertis and Kuroda, 2004; Logan and Nusse, 2004; Yamaguchi, 2001; Kawano and Kypta, 2003).

The integration of Wnt signals with FGFs and BMPs is important for the selection of cell fates during neural induction, through which embryonic ectoderm cells are directed to become neural or epidermal cells (Wilson and Edlund, 2001; Muñoz-Sanjuán and Brivanlou, 2002; Stern, 2005). It has also been shown that Wnt activity is required for neural induction through  $\beta$ -catenin signals (Baker et al., 1999), and Wnt signalling is also involved in neural tube and neural crest formation (Muroyama et al., 2002; Ikeya et al., 1997; Dorsky et al., 1998; Calisto et al., 2005). Moreover, many studies have shown that Wnt signalling plays a critical role in neural tube patterning along the anterior-posterior and dorsal-ventral axes (Baker et al., 1999; Robertis et al., 2000; Domingos et al., 2001; Kiecker and Niehrs, 2001; Ulloa and Martí, 2010; Le Dréau and

Martí, 2012). Therefore, Wnt signalling is one of the key signals that pattern the central nervous system.

### **1-3 Dorsal-ventral neural tube patterning and signalling pathways:**

The neural tube is the precursor of the central nervous system, which develops from the neural plate through the process of neurulation, giving rise to the brain and spinal cord. After neural induction, the neural tube differentiates and is patterned in anterior-posterior (AP) and dorsal-ventral (DV) axes (Wilson and Maden, 2005). The differentiation of the neural tube results in the formation of the forebrain, midbrain and hindbrain in the anterior portion of a developing embryo as well as the formation of the spinal cord in the posterior portion. The patterning of the AP neural tube is controlled by many developmental signals, including BMPs, FGFs, Wnts and retinoic acid (RA) (Blumberg et al., 1997; Wodarz and Nusse, 1998; Gamse and Sive, 2000; Holowacz and Sokol, 1999; Momoi et al., 2003; Villanueva et al., 2002).

The DV patterning of the neural tube occurs after neural induction and during the elongation of the embryonic axis, while the organiser (Hensen's node in chicks) is regressing (Wilson and Maden, 2005). Through neurulation, the roof plate is formed on the dorsal side of the neural tube, where sensory neurons will form, and the floor plate is formed on the ventral side of the neural tube, where motor neurons will form (Zhuang and Sockanathan, 2006; Wilson and Maden, 2005). The roof plate and floor plate act as signalling centres, which interact in a reciprocal fashion by secreting different morphogen proteins, to establish the DV neural tube pattern. Also, the somites and the notochord are required for patterning the DV axis.

The neural tube is divided into eleven domains of neural progenitor cell populations along the DV axis using transcription factors (TFs) [the home-domain (HD) and the

basic-helix-loop-helix (bHLH) families] as molecular markers for specific neural progenitors (Ulloa and Martí, 2010; Le Dréau and Martí, 2012; Wilson and Maden, 2005). The dorsal TFs divide the dorsal neural tube into six domains (dP1-dP6), and the ventral TFs divide the ventral half into five domains (p0, p1, p2, pMN and p3) (Ulloa and Martí, 2010) (Fig 1.3). The expression of these TFs is controlled by several patterning signals, which are secreted from the tissues surrounding the neural tube.

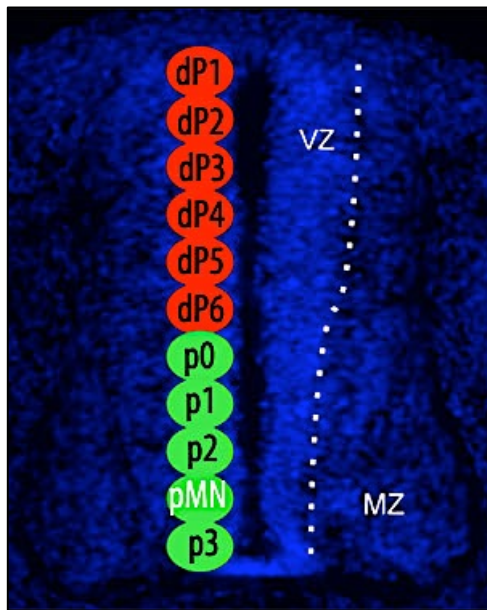


**Fig. 1.3 Cross section of the developing spinal cord, at stage HH24 stained with DAPI; red circles mark six dorsal progenitor domains (dP1-dP6), while green circles represent five ventral progenitor domains (p0, p1, p2, pMN and p3). VZ, the ventricular zone; MZ, the mantle zone.**

Several extracellular signalling pathways are active in the DV neural tube, including FGFs, RA, BMPs, Wnts, and sonic hedgehog (Shh) (Fig. 1.4) (Ulloa and Martí, 2010; Le Dréau and Martí, 2012; Wilson and Maden, 2005). These patterning signals are produced by different tissues; FGFs are generated by the mesoderm, RA is expressed by somites, BMPs and Wnts are expressed and secreted by the roof plate and Shh is produced by the notochord and then by the floor plate (Ulloa and Martí, 2010; Wilson and Maden, 2005). In this study, the focus is mainly on Wnts, but I will briefly mention

BMPs and Shh because of their known interactions with Wnt signalling pathways. All of these signals act as morphogens, specifying neural cell types along DV axis of spinal cord.

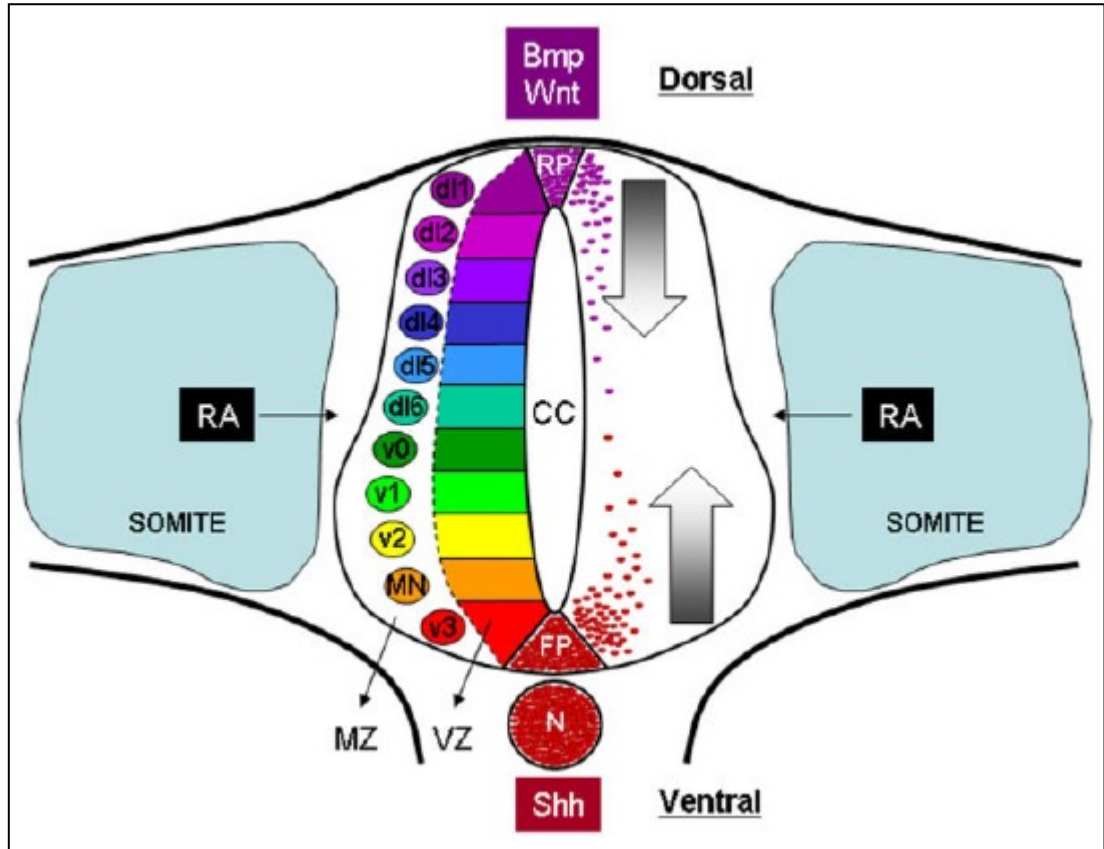


**Fig. 1.4** This Diagram shows a cross section of the developing spinal cord. The ventricular zone (VZ) is a layer of proliferative progenitor cells surrounding the lumen. The mantle zone (MZ) consists of differentiated neurons in specific order along DV axis. The neural tube is patterned by gradients of Wnts and Bmps, secreted by the roof plate (RP), and Shh, produced by the notochord (N) and the floor plate (FP). Retinoic acid (RA) is produced in somites (Adapted from Ulloa and Martí, 2010).

### 1-3-1 The ventral neural tube and Shh:

The ventral neural tube is patterned by the notochord and the floor plate, which generate a Shh gradient, which in turn specifies ventral neural cell fates (Martí et al., 1995; Placzek et al., 1990). The notochord is necessary for the specification of the ventral

neural tube and removal of the notochord results in a loss of the floor plate and motor neurons (Placzek, 1995). Moreover, it is sufficient to induce the floor plate of the neural tube because grafting it beside the neural tube results in the induction of an ectopic floor plate and motor neurons (Placzek 1990). Thus, the notochord is required for the formation of the floor plate, which acts as a signalling centre for Shh activity.

Shh is generated by the notochord and then by the floor plate, and it controls the ventral patterning of the neural tube. Shh is a member of the hedgehog (Hh) family of proteins and is involved in many developmental processes. For example, Shh is sufficient and necessary to specify the ventral neural tube (Martí et al., 1995; Roelink et al., 1995). The gradient concentration of Shh patterns the ventral neural tube by inducing and repressing particular homeo-domain (HD) proteins (Briscoe et al., 2000; Jessell, 2000). The HD proteins that are activated by high-level concentrations of Shh are called Class II and include Nkx2.2 and Olig2, and the HD proteins that are repressed by Shh are called Class I and include Pax3, Pax7, Pax6 and Irx3 (Briscoe et al., 2000; Dessaud et al., 2008; Jessell, 2000). Cross-repression between Class I and Class II HD proteins refines their boundary domains and maintains their expression (Zhuang and Sockanathan, 2006; Briscoe et al., 2000; Wilson and Maden, 2005). This in turn establishes five neural progenitors in the ventral neural tube: p0, p1, p2, pMN and p3 (Le Dréau and Martí, 2012) (Fig 1.3). For example, cross-repressive interaction of the Olig2 and Nkx2.2 leads to the creation of the pMN and p3 progenitors boundary in the ventral half of the neural tube (Sun et al., 2003).

The Shh gradient activity is mediated through the Gli transcription factors (Stamatakis et al., 2005). Gli genes are expressed in the neural tube (Gli1, Gli2, Gli3) and the proteins exist in an activator (GliA) or a repressor form (GliR), which either activate or repress target genes of Shh (Ulloa and Martí, 2010). Knockout of Gli2 led to many alternations in the ventral neural tube (floor plate and V3 progenitors were lost) (Matise et al., 1998), and knockout of Gli3 led to a normal ventral pattern but intermediate dorsally expanded interneurons (Persson et al., 2002). It has been proposed that Shh creates a balance between the Gli activator (Gli2) and repressor activities (Gli3R) in the neural tube (Ulloa and Martí, 2010). Furthermore, Gli3 transcription factor has been considered as an inhibitor for Shh activity (Wang et al., 2000; Jacob and Brisco, 2003).

### **1-3-2 The dorsal neural tube and Wnt/BMP:**

The dorsal neural tube is patterned by the activity of the roof plate, which generates many extracellular signals, including BMPs and Wnts (Helms and Johnson, 2003; Zhuang and Sockanathan, 2006). The dorsal neural tube is divided into six domains characterized by expression of dorsal TFs (dI1, 2, 3, 4, 5, 6) (Le Dréau and Martí, 2012). Also, dorsal interneurons are divided into two groups according to their dependency on the roof plate; dI1-3 are dependent on roof plate activity (called Class A) and dI4-6 are independent of roof plate activity (called Class B) (Zhuang and Sockanathan, 2006). At least for Class A, the roof plate is required for the dorsal patterning of the neural tube. Two studies have shown the requirement for the roof plate. The first showed that the lack of a roof plate in Dreher mutant mice, in which *Lmx1a* gene was affected, led to a loss of dorsal interneurons (Millonig et al., 2000). The second study showed that when the roof plate was genetically ablated in mouse embryo by introducing conditional expression of diphtheria toxin A subunit from the *Gdf7* locus

in the roof plate cells resulted in a loss of dorsal interneurons (dI1-3) in the neural tube (Lee et al., 2000).

The roof plate is essential for dorsal neuron specification, especially for Class A (dI1-3). It is a signalling centre that expresses many members of the BMP and Wnt families, which play important roles in the dorsal patterning of the neural tube (Timmer et al., 2002; Ikeya et al., 1997; Le Dréau and Martí, 2012; Wilson and Maden, 2005).

### **1-3-2-1 BMP signalling:**

BMPs are members of the transforming growth factor beta family (TGF $\beta$ ). BMPs play an important role throughout neural development, including the DV patterning of the neural tube. Many TGF $\beta$  family members are expressed in the roof plate, including BMP4, BMP5, BMP7, Activin B, Dorsalin1 and GDF7 (Chesnutt et al., 2004; Zhuang and Sockanathan, 2006). This suggests that BMPs are involved in dorsalizing the neural tube. In fact, findings from in vitro and in vivo studies have demonstrated that BMP signalling is required for dorsal neural tube specification (Helms and Johnson, 2003). Two groups of researchers have demonstrated this requirement, and both studies were conducted on chick embryos using electroporation (Timmer et al., 2002; Chesnutt et al., 2004). Timmer et al. (2002) showed that overexpression of BMP receptors (BMPR-Ia and BMPR-Ib) led to an expansion of dorsal interneurons (dI1-3), whereas inhibition of BMP signalling resulted in a loss or reduction of dI1-3. They also showed that BMPs pattern the neural tube through the regulation of bHLH and HD proteins. The authors concluded that BMP signalling positively regulates dorsal expression of Pax7 and negatively regulates Pax6 in intermediate regions, both Pax7 and Pax6 are homeo- and paired-domain containing proteins. This regulation leads to refinement of expression boundaries of these proteins in the dorsal neural tube.

In another study, Chesnutt et al. (2004) overexpressed noggin (BMP inhibitor) in chick neural tubes using electroporation, which led to a loss of roof plate and dorsal cell fates, indicating that BMP signalling is required for roof plate maintenance and dorsal interneurons. Also, they showed that the dorsal neural progenitors that express bHLH proteins are required for BMP signalling. Moreover, the study demonstrated that Wnt family members and FZD receptors that are expressed in the dorsal neural tube (Wnt1 and FZD10) are positively regulated by BMP signalling, whereas those that are expressed on the ventral side (Wnt7a, FZD7, sFRP1) are negatively regulated. Chesnutt et al. (2004) proposed that BMP signalling regulates dorsal neural tube patterning while Wnt signalling regulates proliferation. In other words, BMP signalling controls patterning and growth in coordination with canonical Wnt signalling. This means that canonical Wnt signalling is regulated by BMP signalling and acts as a mitogenic rather than a patterning signal. Wnt ligands are downstream of BMP signalling, and their expressions are enhanced by BMP signalling, especially Wnt1/3a (Chesnutt et al., 2004). For example, Wnt1 is induced by BMPR overexpression.

Recently, Le Dréau et al. (2012) demonstrated that BMP7 is required for dorsal neural tube neurogenesis (dI1-dI3-dI5) but it is not required for patterning in chick and mouse embryos.

### **1-3-2-2 Wnt signalling:**

Wnt signalling is involved in dorsal neural tube patterning (see 1-4). Many Wnt family members are expressed in the dorsal neural tube, including Wnt1/3a, which are expressed in the roof plate, which acts a signalling centre for BMP/Wnt.

In summary, the DV neural tube axis is established by interactions between Shh, BMP and Wnt. Shh sets up the ventral side of the neural tube and functions against BMP/Wnt activity in that location. BMP and Wnt establish the dorsal side of the neural tube and repress Shh activity on that side. Shh, BMP and Wnt pattern the neural tube through the complex regulation of HD and bHLH transcription factors along the DV axis.

#### **1-4 Dorsal neural tube development and the canonical Wnt signalling pathway:**

Wnt genes are involved in the development of the central nervous system in vertebrates. Several Wnt genes are expressed in the neural tube, namely, Wnt1, Wnt3, Wnt3a, Wnt4, Wnt7a and Wnt7b (Parr et al., 1993). Wnt1 and Wnt3a are known as canonical and exclusively expressed in the roof plate, and they are implicated in the DV axis development of the neural tube (Chesnutt et al., 2004; Dickinson et al., 1994; Megason and McMahon, 2002; Muroyama et al., 2002; Alvarez-Medina et al., 2008).

In fact, many studies have reported a proliferative role for Wnt signalling in the neural tube. Dickinson et al. (1994) showed that overexpression of Wnt1 led to an increase in proliferation in the CNS without pronounced changes in patterning, meaning that Wnt1 acts as a mitogenic signal. Megason and McMahon (2002) findings agreed with that study, concluding that Wnt1 and Wnt3a act as a mitogenic signal in neural progenitors. Chesnutt et al. (2004) data confirmed the mitogenic activity of Wnts using in ovo chick electroporation assays. They also proposed that Wnt activity is dependent on BMP activity (which couples growth with patterning). Ille et al. (2007) agreed with the model proposed by Chesnutt et al. (2004), suggesting an inhibitory crosstalk between Wnt/BMP signalling in the neural tube. Wnt signalling induces proliferation and

inhibits differentiation, whereas BMP signalling induces differentiation and inhibits proliferation (Ille et al., 2007). This inhibitory crosstalk links patterning and growth, whereby the dorsal half of the developing spinal cord is refined.

However, several reports have suggested a patterning role for Wnt signalling in the neural tube. Muroyama et al. (2002) showed that in the Wnt1/Wnt3a double mutant mouse, dorsal interneurons 1 and 2 were lost or reduced, whereas dorsal interneuron 3 was expanded. Also, they showed that Wnt3a protein is able to induce dI1 and dI2 markers. This suggests that Wnts are required for dorsal interneuron specification, at least for dI1-3. Moreover, this phenotype is consistent with the phenotype of roof-plate-ablated embryos, which show a loss of dI1-3 (Lee et al., 2000). As a result, Wnt1 and Wnt3a play an essential role in dorsal spinal cord patterning (Muroyama et al., 2002).

Additionally, it has been shown that canonical Wnt signalling is sufficient to induce the bHLH transcription factor Olig3, which is required for dI1-3 progenitors (Zechner et al., 2007). Zechner et al. (2007) demonstrated that Olig3 expression is lost from neural progenitors in  $\beta$ -catenin conditional mutant mice. Also, they showed that Olig3 is ectopically expressed when  $\beta$ -catenin is constitutively expressed in the entire spinal cord axis. Clearly, canonical Wnt signalling is involved in DV patterning.

In a study using chick electroporation assays, the overexpression of Wnt1 and Wnt3a led to the expansion of dorsal genes (Pax6 and Pax7) and to the inhibition of ventral genes (Olig2 and Nkx2.2) (Alvarez-Medina et al., 2008). On the other hand, the inhibition of the Wnt signalling pathway led to an opposite phenotype: the dorsal genes were inhibited, and the ventral genes were expanded dorsally (Alvarez-Medina et al.,

2008). Interestingly, Alvarez-Medina et al. (2008) reported that Wnt signalling could regulate DV neural tube patterning through the regulation of Gli3 expression, which represses Shh signalling. They showed that Gli3 is expressed in dorsal spinal cord, and it was ventrally expanded when Wnt1/3a was overexpressed in the chick neural tube, its expression seemed to be directly regulated by canonical Wnt signalling. Furthermore, in Wnt1/3a double mutant mice Gli3 expression was reduced. These results indicate that canonical Wnt signalling can regulate Gli3 expression in spinal cord. They have proposed that the patterning activity of canonical Wnt signalling is dependent on Gli3 repressor form to antagonize Shh signalling in dorsal spinal cord. Also, the authors showed that Wnt activity in DV patterning is independent of BMP activity. Thus, Wnt signalling can control patterning in the DV neural tube through regulating Shh/Gli signalling.

In addition, a 'gain and loss of function' study of zebrafish spinal cord concluded that Wnt signalling regulates patterning and proliferation: canonical Wnt signalling regulates patterning through TCF7 (transcriptional mediator) and proliferation through TCF3 (Bonner et al 2008), indicating that canonical Wnt signalling plays roles in both proliferative and patterning activities.

Recently, an *in vivo* experiment showed that  $\beta$ -catenin regulates the cell fate and polarity of the neuroblasts in chick neural tubes via atypical protein kinase C (aPKC) expression and localisation (Herrera et al., 2014). Therefore, canonical Wnt signalling is required for proper development of the neural tube. However, Wnt-FZD interactions *in vivo* in the neural tube have not been investigated. Hence, studying the FZD receptors of canonical Wnt signalling (Wnt1/3a) could provide an understanding of the

mechanism through which canonical Wnt signalling is able to regulate neural tube development.

### **1-5 FZD receptors:**

FZDs are receptors for Wnts and other ligands. They are involved in the regulation of developmental processes such as cell polarity, neural patterning, cell proliferation and neural synapsis development (Clevers, 2006; Medina et al., 2000). The deregulation of FZDs causes many diseases including cardiac hypertrophy, cancer, neural tube defects and neural degeneration (Luo et al., 2007; Malaterre et al., 2007; Ueno et al., 2013; Wang et al., 2006).

### **1-5-1 FZD structure and signalling:**

FZD receptors have been identified in both vertebrates and invertebrates. There are only four FZDs in *Drosophila* and *C. elegans*, whereas ten FZDs have been characterised in vertebrates, including mice and humans (Amerongen and Nusse, 2009). FZD receptors are classified into four groups based on amino acid sequence similarity (FZD1, 2 and 7; FZD3 and 6; FZD5 and 8; FZD4, 9 and 10) (Huang and Klein, 2004).

FZDs are 7-pass transmembrane proteins and members of the G-protein-coupled receptor (GPCR) superfamily (Barnes et al., 1998; Wang et al., 2006) (Fig. 1.5). The length of FZD proteins is around 500–700 amino acids. FZDs consist of the N-terminal extracellular cysteine-rich domain (CRD), a linker region, the seven hydrophobic domains and C-terminal intracellular domain (MacDonald and He, 2012; Wang et al., 1996; Barnes et al., 1998) (Fig. 1.4). The CRD length is around 120 amino acids, and it is conserved in all FZDs and binds to Wnts with great affinity (Bhanot et al., 1996;

Dann et al., 2001). The KTXXXW motif in C-terminal is necessary for activation of the canonical Wnt pathway (Umbhauer et al., 2000) (Fig. 1.5).

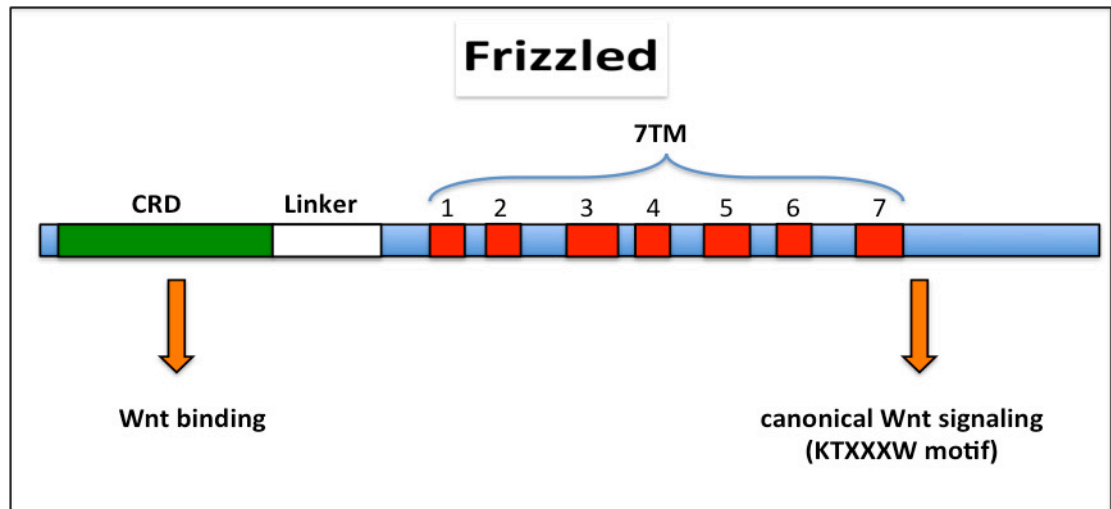


**Fig. 1.5 Schematic illustration of FZD structure;** CRD is extracellular domain where Wnts bind to FZDs followed by a linker region. 7TM are seven transmembrane domains. C-terminal is intracellular domain where KTXXXW motif is located.

FZDs are expressed on the surface of Wnt-responsive cells and act as receptors for Wnt ligands (Bhanot et al., 1999). FZDs were first studied in *Drosophila*, in which dFZD1 mutant flies exhibit cell polarity defects. The first evidence showing that FZDs bind to Wnts also came from studies of *Drosophila*: dFZD2 overexpression in non-sensitive Wnt cell cultures leads to Wnt binding and activation of canonical Wnt (Bhanot et al., 1996). Furthermore, dFZD1/2 depletion mimics the Wingless mutant phenotype in *Drosophila* (Bhanot et al., 1999; Bhat, 1998). In addition, FZD receptors synergise with Wnts in axis duplication assays in *Xenopus* (Deardorff et al., 2001; Garcia-Morales et al., 2009; Yang-Snyder et al., 1996). Also, many reports have documented that FZD CRDs are required for Wnt binding (Hsieh et al., 1999; Wu and Nusse, 2002; Cadigan

et al., 1998; Rulifson et al., 2000; Zhang and Carthew, 1998). Furthermore, the crystal structure of FZD8-CRD and XWnt8-mFZD8CRD complex has confirmed and explained the mechanism of Wnt–FZD interactions (Hsieh et al., 1999; Dann et al., 2001; Janda et al., 2012). Therefore, FZD receptors are needed for Wnt reception and signal transductions.

FZDs mainly bind to Wnts, but they can also bind to other ligands including sFRPs and R-spondin (Rodriguez et al., 2005; Nam et al., 2006). Binding of FZDs leads to Wnt signalling activation (Liu et al., 2003; Li and Bu, 2005). Therefore, FZDs are able to activate both Wnt signalling pathways: the canonical (Wnt/ $\beta$ -catenin signalling) and the non-canonical (Wnt/PCP signalling and Wnt/calcium signalling). In FZD/ $\beta$ -catenin signalling, FZD binding with other co-receptors (LRP5/6) leads to the stabilisation and accumulation of  $\beta$ -catenin (Gordon and Nusse, 2006). In FZD/PCP signalling, this binding results in the activation of the c-Jun N-terminal kinase (JNK) pathway (Seifert and Mlodzik, 2007). In FZD/ $\text{Ca}^{2+}$  signalling, FZD binding leads to increased calcium levels inside cells, which results in the activation of calcium-responsive enzymes such as protein kinase C (PKC) (Kohn and Moon, 2005; Slusarski et al., 1997).

### **1-5-2 FZDs and Wnt specificity:**

Wnt–FZD specificity is complicated and poorly understood for many reasons, including the ability of FZDs to activate multiple pathways. For example, FZD7 is able to mediate canonical Wnt and non-canonical Wnt signalling, as reported in chick somite and other systems (Medina et al., 2000; Gros et al., 2009). Furthermore, Wnts can bind to multiple FZDs, and FZDs can engage with more than one Wnt ligand (19 Wnts– 10 FZDs) (Hsieh et al., 1999b; Carmon and Loose, 2010). As an example, Wnt9a can bind to CRDs of FZD4, 7 and 9, as shown by immunoprecipitation assays in COS7 cells

(Matsumoto et al., 2008). Also, redundancy is common among FZD receptors, which makes it difficult to study an independent function for each FZD. In *Drosophila*, dFZD1 and dFZD2 function redundantly, and both have to be mutant to produce a wingless-like phenotype (Chen and Struhl, 1999; Muller et al., 1999). Mouse genetic studies have reported that FZD1 and 2 exhibit redundancy in their function, as do FZD3/6 (Wang et al., 2006; Yu et al., 2010).

However, several reports have documented the specificity of certain Wnts and their receptors. For example, in *Drosophila*, dFZD2-CRD has stronger binding affinity for Wg (ten-fold) than dFZD1-CRD (Rulifson et al., 2000). In addition, dFZD1 has a primary role in PCP signalling, whereas dFZD2 does not have a role in polarity (Rulifson et al., 2000).

In *Xenopus*, axis duplication assays have shown many examples of Wnt-FZD selectivity. For instance, XWnt5a can only induce axis duplication when it is co-injected with FZD5, but other examined FZDs do not have this effect (He et al., 1997). This suggests that FZD5 is a receptor for XWnt5a and mediates its activity in axis induction. FZD10 shows interaction with Wnt1 but not Wnt3a, as reported in axis duplication assays (Garcia-Morales et al., 2009). Also, FZD8 has the ability to synergise with XWnt8, leading to induction of complete axes in *Xenopus* (Deardorff et al., 1998). Moreover, XWnt8 protein can interact with FZD8 protein, and FZD8-CRD binds to XWnt8 with higher affinity compared to other FZDs (Janda et al., 2012).

In zebrafish, FZD3a interacts with Wnt8b and regulates the formation of forebrain commissures, and their independent knock-down leads to the same phenotype; commissural defects (Hofmeister and Key, 2013).

Luciferase assays have been used to dissect Wnt–FZD interactions in different cell lines. FZD9 (Rfz9) strongly activates TCF transcription (Wnt/ $\beta$ -catenin reporter) when it is co-expressed with Wnt2, but not when it is co-expressed with other Wnts, as shown in 293T cells (Karasawa et al., 2002). This indicates that FZD9 is a receptor for Wnt2 and mediates its function through canonical Wnt signalling. Additionally, a recent study using the same cell line showed that Wnt2 can increase TCF activity more than fifteen-fold when it is co-transfected with FZD8 or 9, but not with the other eight FZDs (Bravo et al., 2013).

Recently, Dijksterhuis et al. (2015) characterised a novel cell line called the mouse myeloid progenitor (32D). This cell line does not express FZD receptors, but it expresses LRP5 and 6. Therefore, the authors generated an overexpressing cell line for each individual FZD (FZD2, 4 and 5) and investigated their function and selectivity with multiple Wnts (Wnt3a, Wnt4, Wnt5a and Wnt9b). Interestingly, only Wnt3a could increase  $\beta$ -catenin stability and induce LRP6 phosphorylation (PS) in a dose-dependent manner in 32D/FZD2, 4 and 5 cells. However, a high concentration of Wnt5a was able to induce  $\beta$ -catenin stability in 32D/FZD5-expressing cells, but not in 32D/FZD2 or 32D/FZD4 cells. This suggests Wnt5a prefers binding to FZD5. The authors also showed that phosphorylation (PS) of DVL2/3 was affected by Wnt–FZD selectivity. For instance, stimulation of Wnt3a and Wnt5b led to the formation of PS-DVL3 but not PS-DVL2 in 32D/FZD5 cells. Obviously, Wnt–FZD pair binding has a different biological activity, as reported in this cell line. Therefore, this cell line and other approaches could help dissect receptor–ligand interactions and explain the downstream effects of each Wnt–FZD pair. Additionally, studies of Wnt–FZD signalling are necessary to tackle Wnt-related diseases, such as cancer, neural tube defects and neurodegenerative diseases.

### **1-5-3 Wnt/FZD signalling and diseases:**

#### **1-5-3-1 FZDs and cancer:**

Wnt signalling is known to regulate cell Proliferation and reportedly, Wnt components are highly expressed in human cancers, such as lung, breast and colon cancer (Amerongen and Nusse 2009; Bravo et al., 2013; Gurney et al., 2012; Ueno et al., 2013). Moreover, FZDs are overexpressed and involved in several human cancer types (Ueno et al., 2013). For example, FZD1 is overexpressed in colon cancer (Holcombe et al 2002), and a high expression of FZD3 has been found in chronic lymphocytic leukaemia cells and in lymphoma cells (Lu et al., 2004; Qiang et al., 2003). Also, FZD5 overexpression is seen in kidney and prostate cancer (Janssens et al., 2005; Thiele et al., 2011). FZD7 is highly expressed in more than six colorectal cancer lines (Ueno et al., 2008) while FZD8 is upregulated in several types of lung cancer (Bravo et al., 2013). FZD10 is strongly expressed in colon, lung and sarcoma cancer (Terasaki et al., 2002; Nagayama et al., 2005).

FZD knockdown approach was used in different cell lines. FZD7-siRNA reduced invasion activity and cell viability in colorectal cancer lines (Ueno et al., 2008). In lung cancer cell lines, the targeting of FZD8 by shRNA resulted in a significant reduction in proliferation (Wang et al., 2012). Moreover, FZD8-shRNA inhibited tumour growth in vivo, as seen in xenograft mouse models. Notably, both studies showed that knockdown of either FZD7 or FZD8 reduced the canonical Wnt signalling. In addition, FZD10-siRNA suppressed tumour growth in synovial sarcomas cell lines (Nagayama et al., 2005). Therefore, FZDs are involved in many cancer types, so targeting these receptors could be a valuable tool for treating cancer.

Additionally, antibodies can be used against FZDs in cancerous cells. MAb 92-13 antibody is specifically bound to FZD10-overexpressing tumours, allowing these tumours to be targeted by radio-immunotherapy (Fukukawa et al., 2008). Another antibody called OMP-18R5 (a human IgG2 isotype) has been identified that can bind to five different FZDs (FZD1, 2, 5, 7 and 8) through a conserved epitope (Gurney et al., 2012). OMP-18R5 inhibits the canonical Wnt signalling by preventing Wnt ligands from binding to FZD receptors. This antibody suppresses several kinds of human tumours including breast, colon and pancreatic cancer. Furthermore, it has shown strong synergy with many chemotherapy drugs, such as taxol.

It has also been shown that microRNAs are able to regulate FZD expression (Ueno et al., 2013). For instance, FZD1 is inhibited by miR-204 overexpression (Li et al., 2011), and miR-23b regulates FZD7 in colon cancer cells (Zhang et al., 2011). Thus, microRNAs can be used to suppress tumour growth that result from overexpression of Wnt pathway components, including FZDs.

### **1-5-3-2 Wnt/FZD signalling and neural tube defects:**

Neural tube is formed through the process of primary and secondary neurulation. Primary neurulation leads to neural tube formation and closure, while in secondary neurulation the interior of a solid precursor is hollowing out to form the caudal end of the neural tube. Most neural tube defects (NTDs) are a result of the failure of neural tube closure during primary neurulation in the brain or spinal cord (Greene and Copp, 2009).

Both canonical and non-canonical Wnt signalling are implicated in NTDs. Disruption of

non-canonical Wnt (PCP) components leads to NTDs, as shown in mutant mice of *Vangl2*, *Celsr1* and *Scrb1* (Curtin et al., 2003; Murdoch et al., 2003). Also FZDs, Wnt receptors, are involved in neural tube closure, as *FZD1/2* and *FZD3/6* mutant mice exhibited NTD phenotypes (Yu et al., 2010; Wang et al., 2006). In addition, DVL is involved in neural tube closure, as *Dvl1–Dvl2* double-knockout mice show severe NTD phenotypes in which the neural tube fails to close along the anterior–posterior axis (Hamblet et al., 2002).

A recent study showing the importance of canonical Wnt signalling (Wnt/ $\beta$ -catenin) in neural tube closure reports that spina bifida aperta, a NTD, was observed in  $\beta$ -catenin conditional knockout in *Pax3*-expressing cells in the dorsal neural tubes of mice (Zhao et al., 2014). Caudal axis bending and tail truncation were present in this mutant. *Pax3* and *Cdx2* play a very important role in caudal neural tube closure, and their expression was repressed in this mutant (Zhao et al., 2014).

In addition, the gain or loss of function of LRP6 (FZD co-receptor) affects neural tube closure, resulting in NTDs (Allache et al., 2014; Gray et al., 2013; Pinson et al., 2000). In both mutants, LRP6-dependent NTDs are linked to disruption of apical–basal cell polarity in the neural folds through RhoA activity (Gray et al., 2013). Recently, three mutations in LRP6 orthologs were found in NTDs in humans (285 patients were studied that have different forms of open and closed phenotypes of NTDs such as Myelomeningocele) (Allache et al., 2014). These mutations have an effect on Wnt pathways (Allache et al., 2014). Thus, Wnt signalling plays a crucial role in the process of neural tube development, including closure during neurulation.

It is worth mentioning that the dysregulation of Wnt signalling is also implicated in neurodegenerative diseases such as Huntington's, Alzheimer's and Parkinson's disease (Galli et al., 2014; Inestrosa and Toledo, 2014; Salinas, 2012). In Alzheimer's disease (AD), it was found that  $\beta$ -catenin levels are reduced in AD brains, whereas Wnt/ $\beta$ -catenin inhibitors (GSK-3 $\beta$ ) are active (Pei et al., 1999). The activation of Wnt/ $\beta$ -catenin signalling can stop  $\beta$ -amyloid peptide (A $\beta$ )-induced neurotoxicity in cultured rat hippocampal neurons (De Ferrari et al., 2003; Alvarez et al., 2004). In addition, it was reported that Wnt3a can activate Wnt/ $\beta$ -catenin signalling through FZD1 (not FZD2) and has a protective effect against A $\beta$  toxicity in hippocampal neurons and PC12 cells (Chacon et al., 2008). FZD1 overexpression along with Wnt3a leads to a significant increase in cell survival and prevents caspase-3 activation and degradation of  $\beta$ -catenin in the same cell line. This protective effect seems to be a result of Wnt/ $\beta$ -catenin signalling activation which in turn down-regulates Wnt inhibitors such as DKK1 and GSK-3 $\beta$ . These inhibitors are found to be overexpressed in AD brains (Galli et al., 2014; Inestrosa and Toledo, 2014).

Furthermore, DKK1 expression level is upregulated in AD brains (Caricasole et al., 2004). Interestingly, the blockade of DKK1 suppresses A $\beta$ -induced synaptic degeneration (Purro et al., 2012). On the other hand, inducible expression of DKK1 in the striatum of adult mice leads to a Wnt/ $\beta$ -catenin signalling blockade as well as synaptic defects and degeneration (Galli et al., 2014). Therefore, sustained Wnt/ $\beta$ -catenin signalling is important for adult neurogenesis. Also, targeting Wnt inhibitors such as GSK-3 $\beta$  and DKK-1 could be a useful approach for the treatment of neurodegenerative diseases (Purro et al., 2012; Inestrosa and Toledo, 2014; Salinas,

2012).

### **1-6 Expression and function of FZDs during development:**

FZDs are expressed in different embryonic tissues and are implicated in many developmental processes. In *Drosophila*, dFZD1 expression has been found in the epidermis and other tissues, such as the wing (Adler and Lee, 2001). dFZD2 expression has been reported during embryogenesis in many cell types, such as in the epidermis and mesoderm. In late stages, dFZD2 expression was seen exclusively in the hindgut, dorsal vessel and the CNS (Bhanot et al., 1996).

The function of FZDs has been investigated in flies via genetic screens and RNA interference. The loss of dFZD1 function affects cell polarity in the sensory bristles, dorsal epidermis and wings (Vinson and Adler, 1987; Gubb and Garcia-Bellido, 1982). Also, flies lacking both dFZD1 and dFZD2 show abnormalities in embryo patterning, neuroblast specification and heart formation (Bhat, 1998; Muller et al., 1999).

In zebrafish, Nikaido et al. (2013) performed a comprehensive expression analysis, and studied the function of zFZD genes during embryogenesis. They identified thirteen FZD members and showed that their expression patterns are dynamic and overlapping in zebrafish embryo. For example, zFZD3a/9b/10 expression is overlapping in the dorsal neural tube, and zFZD7b/10 are expressed in the neural plate border. In this study, it was reported that zFZD7a/7b knockdown affected convergent extension movement during gastrulation. Also, the inhibition of zFZD7a, zFZD7b and zFZD10 by morpholino leads to severe defects in mesodermal convergent extension.

In *Xenopus*, xFZDs show dynamic expression in the early and late stages of developing

embryos. They are involved in different cellular processes including axis formation, patterning and neurogenesis. Some xFZDs are expressed while neurogenesis takes place, for example: xFZD2/3/4/7/10 are expressed in developing neural tissues (Deardorff et al., 2001; Moriwaki et al., 2000; Shi and Boucaut, 2000; Wheeler and Hoppler, 1999); xFZD2 expression is found in the otic vesicle, the somite and the eye (Deardorff and Klein, 1999); and xFZD3 is detected in the neural plate, the neural tube and the eye (Shi et al., 1998), where it is able to regulate eye formation during development. The overexpression of xFZD3 results in ectopic eye formation, whereas the overexpression of a dominant negative form of xFZD3 inhibits the expression of eye markers such as Pax6 and Otx2 and eyes were malformed in *Xenopus* embryos (Rasmussen et al., 2001). It has also been shown that xFZD3 knockdown by morpholino inhibits neural crest induction (Deardorff. et al., 2001). In addition, xFZD4 is expressed during gastrulation and in the forebrain (Shi and Boucaut, 2000).

	FZD2	FZD3	FZD4	FZD7	FZD8	FZD10
Spemann organiser					X	
Neural tissues	X	X	X	X	X	X
Otic Vesicle	X					
Eye	X	X				
Somite	X					
Heart				X		

Table. 1.1 Summary of FZDs expression in *Xenopus*.

The expression of xFZD7 was found to be expressed in many tissues, including the neural tube, the neural crest and the heart (Wheeler and Hoppler, 1999), and it plays roles in early patterning, proliferation and morphogenesis (Medina et al., 2000; Zhang et al., 2013). Furthermore, xFZD7 overexpression or knockdown affects neural crest

development and neural tube patterning (Abu-Elmagd et al., 2006; Carla-Morales, 2008). xFZD8 is expressed in early developing cells including the Spemann organiser. The injection of xFZD8 RNA into ventral blastomeres leads to secondary axis formation, and it also synergises with XWnt8 (Deardorff et al., 1998). This report concluded that xFDZ8 is a receptor for Wnts and is involved in the morphogenesis of developing embryos.

In chickens, FZDs are expressed in the developing embryo in different tissues including the eye, somite, limb bud and neural tube (for more details see Chapter 3).

In mice, mFZDs are expressed during embryogenesis and adulthood and show specific and complex expression patterns (Borello et al., 1999; Summerhurst et al., 2008). Their expression is detectable by in situ hybridisation during the early stage of development (5.5 days). For example, mFZD5/8 are expressed in the visceral endoderm, and mFZD7 is expressed in the epiblast during gastrulation (Lu et al., 2004; Kemp et al., 2007).

Borello et al. (1999) performed a complete expression profile for mFZDs during the segmentation stage by in situ hybridisation. They showed that mFZDs are expressed in different tissues including somites, neural tube and limb bud. For instance, mFZD1/3/6/7/8/9 are present in developing somites as well as in the neural tube, except for mFZD6. Notably, mFZD3 is expressed in the dorsal neural tube while mFZD7 expression is restricted to the intermediate-ventral region of the neural tube. mFZD4/5 are detected in the ventral telencephalon. Moreover, Borello et al. (1999) reported that some mFZDs (1/3/5/6) are expressed during eye development, suggesting a role for these receptors in eye formation.

mFZD 3, 5 and mFZD8 were shown to be expressed in the mouse developing hippocampus (Davis et al., 2008). Therefore, the dynamic and specific expressions of mFZDs in different embryonic tissues suggest important roles for these receptors during development.

	FZD1	FZD3	FZD4	FZD5	FZD6	FZD7	FZD8	FZD9	FZD10
Visceral endoderm				X			X		
The epiblast						X			X
Somite	X	X			X	X	X	X	
Eye	X	X		X	X				X
Neural tube		X				X	X	X	X
Hippocampus		X		X			X		

Table. 1.2 Summary of FZDs expression in mouse.

FZD knockout produces different developmental defects. mFZD1/2 mutant exhibits developmental defects in the ventricular septum and the palate closure (Yu et al., 2010). Furthermore, the loss of mFZD2 in developing lung epithelium causes defects in branching morphogenesis (Kadzic et al., 2014). mFZD3 knockout mice show severe defects in axon development in the central nervous system (Hua et al., 2014; Wang et al., 2001; Wang et al., 2006). The loss of mFZD4 leads to abnormalities in the cerebellum, retina and cochlea (Xu et al., 2004; Wang et al., 2001). mFZD5 knockout causes yolk defects, leading to embryonic lethality (Ishikawa et al., 2001). Moreover, mFZD5 conditional loss-of-function results in many defects in the eye, such as

increased cell death in the ventral retina (Liu et al., 2008). The loss of mFZD6 results in a polarity defect in which hair is mis-orientated (Guo et al., 2004). mFZD3/6 double mutant leads to defects in tissue closure, where the neural tube and eyelid fail to close (Wang et al., 2006). Also, the patterning and polarity of inner-ear sensory hair cells are affected by the mFZD3/6 double mutant. The loss of mFZD9 produces abnormal B-cells, which implies that mFZD9 controls B-cell development (Ranheim et al., 2005). Thus, these phenotypes indicate that mFZDs plays many important roles during mouse embryo development. However, which specific Wnt ligands bind to which of these FZDs must still be investigated *in vivo*.

In this project, we used chick embryo as a model system. Chick embryos allow researchers to study genes expression and function at the molecular level during development (Mok et al., 2015). The chick neural tube is a widely used model system to study tissue patterning and in particular spinal cord development and to perform transient genetic manipulations. Spinal cord model allows researchers to study many biological events during neural development such as proliferation, patterning, specification and neural tube closure (Becker and Corral, 2015). Therefore, we used chick neural tube as a model system to study Wnt/FZD signalling during dorsal-ventral spinal cord neurogenesis.

### **1-7 The project background and aims:**

FZD10 is expressed in the dorsal neural tube in *Xenopus*, chicken, zebrafish and mouse (Wheeler and Hoppler, 1999; Yan et al., 2009; Kawakami et al., 2000; Nasevicius et al., 2000). This could suggest a role for FZD10 during spinal cord development. Previous studies on FZD10 in the Wheeler lab in *Xenopus* showed that FZD10 is expressed in the dorsal neural ectoderm and neural folds in the region where primary sensory neurons develop (Garcia-Morales et al., 2009). Their studies into loss of function in *Xenopus* showed that FZD10 is required for sensory neurons to form. Also, FZD10 mediates canonical Wnt signalling and interacts with Wnt1 and Wnt8 but not Wnt3a, as shown in synergy assays. Therefore, they proposed that FZD10 functions through canonical Wnt signalling and may mediate Wnt1 activity to determine sensory neural differentiation in *Xenopus*.

However, further study is needed to examine the role of FZD10 in proliferation and differentiation of neurons and investigate its interaction with Wnts, FZDs and the FZD co-receptor (Lrp6) in vivo during spinal cord neurogenesis.

So, this project aimed to study FZDs expression in chick neural tube and to investigate the regulation of FZD10 by dorsal Wnts. Wnt1 and Wnt3a are co-expressed in the roof plate and they show a complete overlapping expression pattern. Many studies have shown that Wnt1 and Wnt3a are required for neural tube development (e.g., Chesnutt et al., 2004; Dickinson et al., 1994; Megason and McMahon, 2002; Muroyama et al., 2002; Alvarez-Medina et al., 2008).

We also aimed to determine whether FZD10 only interacts with Wnt1 and not with Wnt3a in vivo, similar to what had been observed in *Xenopus laevis*.

**-The objectives of the project were:**

1-To characterise FZDs expression in chick neural tube.

2- To establish FZD10 expression pattern using in situ hybridisation.

3-To compare FZD10 expression to dorsal Wnt ligands expression (Wnt1, Wnt3a) during chick neural tube development.

4-To investigate the regulation of FZD10 by dorsal Wnts (Wnt1/3a) in the spinal cord using electroporation and in situ hybridization.

5-To study the function of FZD10 in spinal cord. In vivo approaches (electroporation) were used.

6-To investigate Wnt1, FZD10 and Lrp6 interactions in vivo during spinal cord neurogenesis using electroporation.

# Chapter 2

## **Materials and Methods**

## **2- Materials and Methods:**

### **2-1-RNA extraction and purification:**

Chicken eggs (White leghorn) were obtained from Henry Stuart and Co. Lincolnshire. They were incubated at 38°C until desired stages and the embryos were staged according to Hamburger and Hamilton (1992).

After three (HH18) or four days (HH24) of development, embryos were dissected in cold DEPC-PBS. Then, the dissected embryos were transferred into Eppendorf tubes containing 1ml of Trizol on ice, tubes were then vortexed until all embryonic tissues were completely dissolved in Trizol.

To purify the RNA, 200µl of chloroform was added to 1ml of Trizol. The mixture was incubated for 5mins, then centrifuged at 4°C for 25 minutes. The upper phase of the mixture was transferred into a new tube and 500µl of isopropanol was added. This was followed by adding 1.2M of NaCl and tubes were incubated for 15mins at room temperature after which the mixture was centrifuged for 20mins at 4°C. The supernatant was discarded and the pellet was washed with 100µl of fresh 70% EtOH. Tubes were centrifuged for 10mins and the supernatant was discarded. The pellet was left to dry at room temperature or in a heat-block at 37°C. The pellet was dissolved in 20ul of Sigma water. To check the RNA concentration, the nanodrop spectrophotometer was used. Purified RNA was stored at -20°C for short storage (up to 3 days) or at -80°C for long-term storage.

### **2-2-cDNA synthesis:**

To prepare 20µl of cDNA for PCR cloning, SuperScript™ II Reverse Transcriptase protocol was followed:

- 1ng of RNA
- 1µl of Oligo dTs
- 1µl of dNTPs
- 9µl of Sigma H<sub>2</sub>O

Incubate the mixture at 65°C or 75°C for 5mins using the PCR machine, then place the tube on ice. Then add:

- 4µl of 5X FSB (5x First strand buffer)
- 2µl of DTT
- 1µl of RNasin

Incubate at 47°C for 2mins in the PCR machine. Then add

- 1µl of SSII (SuperScript II)

Incubate at 42°C for 50mins, followed by 15mins at 70°C in the PCR machine. Store the 20µl of cDNA at -20°C and check successful synthesis using GAPDH primers in a PCR reaction. A product of the correct size was obtained.

### **2-3-Cloning of full length of FZD10:**

The full length cDNA sequence for FZD10 was obtained from the National Center for Biotechnology Information (NCBI; <http://www.ncbi.nlm.nih.gov>) with accession numbers (NM\_204098.2). Also, FZD10 full sequence is available from The Ensembl database (<http://www.ensembl.org/index.html>). Two pairs of primers were designed using online software such as Primer3Plus.

### **2-4-Primer design to clone FZD10:**

**-Forward primer:** Not1+FZD10

FW: 5' **GCGGCCGC**ATGTGCGAGTGAAGAGGTG 3'

**-Reverse primer:** EcoR1+ HA tag +FZD10

RW: 5'GAATTCTCAAGCGTAATCTGGAACATCGTATGGGTA-  
TCATACACAGGTGGGTGGTTG 3'

**2-5-PCR reaction and conditions:**

-PCR reaction-mix (30µl):

2µl cDNA

20µl BioMix (BioMix™ Red) (<http://www.bioline.com/uk/biomix-red.html>)

1µl 10µM Forward primer

1µl 10 µM reverse primer

1µl DMSO

5µl H<sub>2</sub>O

-PCR condition:

1-95°C 1min

2-95°C 1min

3-65°C 2mins

4-72°C 1min

5-go to step 2 for 29 more times

6-72°C for 10 mins.

After that, PCR product was checked using agarose gel electrophoresis.

**2-6-Agarose gel electrophoresis:**

0.5g of agarose was mixed with 50ml of TAE buffer in a flask. The agarose was dissolved using a microwave for 1-2mins. Then the agarose was left to cool down and 3.5µl of Ethidium bromide was added to the agarose, mixed and then poured in a gel tank containing well comb and left to set for 5mins. TAE buffer was added until the agarose gel was covered. All samples, 20 ul of PCR product, were mixed with loading buffer, containing dye, before being run in the gel at 75V, electrophoresis for 30mins.

(<https://www.addgene.org/plasmid-protocols/gel-electrophoresis/>)

### **2-7-DNA extraction from agarose gel:**

Agarose gel was run for 30mins until DNA fragments were separated. DNA was visualized using UV illumination (around 210-285nm). The agarose gel containing the DNA fragment (PCR product) was extracted using a clean razor blade and was purified following GeneJET Gel Extraction Kit protocol (Life Technologies). The agarose gel containing the DNA band was placed into a pre-weighed 1.5 mL tube then the tube was weighed with the agarose gel. 1:1 volume of Binding Buffer was added to the agarose gel. The gel:buffer mixture was incubated at 50-60°C for 10 min. The tube was vortexed every few minutes to mix and dissolve the gel then 800 µl of the mixture was loaded into the GeneJET purification column. The column was centrifuged for 1 min and the flow through was discarded. 100 µl of Binding Buffer was added to the column and centrifuged for 1 min. The flow through was discard and the column was placed back into the same collection tube. 700 µl of Wash Buffer was added to the column and centrifuged for 1 min. The flow through was discard and the column was placed back into the tube. The empty column was centrifuged for an additional 1 min to completely remove residual wash buffer. The column was transferred to a clean 1.5 ml Eppendorf tube. 20-50 µl of Elution Buffer or dH<sub>2</sub>O was added to the centre of the purification column membrane. The column was incubated for 1min then centrifuged for 1 min. The column was discarded and the purified DNA was stored at -20°C. ([https://tools.lifetechnologies.com/content/sfs/manuals/MAN0012661\\_GeneJET\\_Gel\\_Extraction\\_UG.pdf](https://tools.lifetechnologies.com/content/sfs/manuals/MAN0012661_GeneJET_Gel_Extraction_UG.pdf)).

### **2-8-Cloning of FZD10 into plasmid vector:**

FZD10 fragment was first ligated into pGEM-T easy vector and was then subcloned into pCAB-IRES-GFP vector.

### **2-8-1-Ligation of FZD10 into pGEM-T easy vector:**

pGEM-T easy vector is commonly used in cloning and makes the PCR product ligation efficient and quick because of 3'-T overhangs at the insertion site (Promega). FZD10 fragment was ligated into pGEM-T easy vector by assembling the following reaction mix:

- Ligation reaction (10 $\mu$ l):
- 0.5 $\mu$ l of pGEM-T easy vector (25ng)
- 2 $\mu$ l of FZD10
- 5 $\mu$ l 2X rapid ligation buffer
- 1 $\mu$ l T4 DNA ligase
- 1.5 $\mu$ l H<sub>2</sub>O

-Incubate for 2-4hours at room temperature.

The ligated DNA was transformed into competent DH5 $\alpha$  E-Coli (see 2-9). We took advantage of blue/white screening that is available for the pGEM-T easy vector system. For this, X-gal and IPTG were added to LB-CARB plates. Successful ligation of the insert will disrupt the production of  $\beta$ -galactosidase enzyme so the colonies' colour will be white. Unsuccessful ligation will result in blue colonies. After 24hours of incubation at 37°C, the LB plates were checked and then white colonies were picked up to do colony PCR, which was performed using FZD10 primers to screen many colonies. The colonies that contained FZD10 fragment were grown in LB-CARB media for future use. Mini prep was performed (see 2-10-1) in order to purify FZD10 DNA. The plasmid insert was confirmed by sequencing and pGEM-T-FZD10 was used to generate in situ

probe for FZD10. After that, the full length sequence of FZD10 was subcloned into pCAB-IRES-GFP for functional studies.

### **2-8-2-Ligation of FZD10 into pCAB expression vector:**

The full length of FZD10 was digested with restriction enzymes (Not1+EcoRI) from pGEM-T easy vector. The expression vector (pCAB-IRES-GFP) was cut with the same enzymes to generate compatible ends.

-Digestion reaction (20 $\mu$ L):

1 $\mu$ g DNA (pGEM-T-FZD10 or pCAB-IRES-GFP)

1 $\mu$ l of Not1

1 $\mu$ l EcoRI

4 $\mu$ l 10x Buffer

X  $\mu$ l dH<sub>2</sub>O up to 20  $\mu$ L

-Incubate for 4 hour at 37°C or overnight.

Then both, the full length of FZD10 and the linearized plasmid were run on an agarose gel (see 2-6) the relevant bands were extracted and purified from the gel (see 2-7).

After purification of FZD10 and pCAB-IRES-GFP, ligation was performed at a vector to insert ratio of 1:1 or 1:3. To determine the volumes needed the Ligation Calculator was used ([http://www.insilico.uni-duesseldorf.de/Lig\\_Input.html](http://www.insilico.uni-duesseldorf.de/Lig_Input.html)).

-Ligation reaction (10 $\mu$ l):

X  $\mu$ l of pCAB-IRES-GFP

X  $\mu$ l of FZD10

5 $\mu$ l 2X rapid ligation buffer

1 $\mu$ l T4 DNA ligase

X  $\mu$ l H<sub>2</sub>O up to 10 $\mu$ l

-Incubate for 2-4hours at room temperature or O/N.

Ligated plasmid was transformed into competent DH5 E-Coli (2-9).

### **2-9-Plasmid transformation:**

1µl of DNA plasmid was added to 200µl of competent E. coli cells and incubated on ice for 30mins. The cells were heat-shocked for 5mins at 37°C to take up the plasmid, and then they were incubated on ice for 5mins. 600µl of SOC medium was added and the cells were incubated for 1hour at 37°C to recover. The transformants were spun down briefly and most of the supernatant was removed. The bacterial pellet was suspended by pipetting and was plated out on a LB agar plate containing the appropriate antibiotic (i.e. Carbenicillin). The plate was incubated overnight at 37°C.

### **2-10-DNA purification and preparation:**

A single colony of transformed cells was picked and used to inoculate 5 or 50ml of LB/antibiotic medium to be incubated in a shaker (approx. 300 rpm) overnight at 37°C. The LB/antibiotic medium was then transferred to a 15 or 50ml tube to be spun down for 10/30 mins at 4°C. The DNA plasmid was purified using Plasmid Mini/Midi Kits. The concentration of the purified DNA was measured using a Nanodrop and checked on an agarose gel (electrophoresis).

#### **2-10-1-Mini preparation of DNA plasmid:**

DNA purification was performed according to the manufacturer's instructions of the reSource Plasmid Mini Kit protocol. Briefly, a single colony was picked from a LB medium plate and was incubated in 5 ml LB medium/antibiotic in a 20ml tube. The tube was incubated over night at 37°C with shaking. The bacterial cells were harvested by

centrifugation for 10 mins at 4°C. the supernatant was removed and the bacterial cells pellet was re-suspend in 250µl Buffer1+RNaseA then was transferred to a clean Eppendorf tube. The cell pellet was completely suspended by vortexing. 250 µl of Buffer2 was added that lysed the bacterial cells and mixed by inverting the tube 4–6 times. 350 µl of Buffer3 was added that led to DNA precipitation and the mixture was inverted 4–6 times. The tube was centrifuged for 10mins at 13,000 rpm. The spin column was placed in 2ml collection tube. The supernatant was transferred to the spin column by pipetting in the collection tube. Then, it was centrifuged for min and the supernatant was discarded. The spin column was washed with 0.5ml buffer B and was spun for 1min. after discarding the supernatant, the spin column was washed by adding 0.75ml bufferE (ethanol ???) and was centrifuged for 1min. The supernatant was discarded and the spin column was centrifuged again to get rid of residual ethanol.

The spin column was placed in a clean 1.5 ml Eppendorf tube. DNA was eluted by adding 50µl Elution Buffer or 50µl water to the centre of the column. After 1min, the Eppendorf tube was centrifuged for 1min and the column was discarded. The eluted DNA was stored at -20°C for further use

<http://www.lifesciences.sourcebioscience.com/clientupload/productinfo/sbs27104.pdf>).

#### **2-10-2-Midi preparation of DNA plasmid:**

Electroporation requires highly purified and concentrated DNA. For this, we used Midi prep kit (NucleoBond Xtra Plasmid Plus). The DNA purification was performed according to NucleoBond Xtra Plasmid Midi Kit protocol. A single colony was picked from a LB medium plate containing antibiotic and was incubated in 5 ml LB medium+ appropriate antibiotic in a 20ml tube overnight. Then, 1ml of LB medium was transferred to 50ml LB medium+ appropriate antibiotic in a flask and then was

incubated over night at 37°C with shaking. The LB medium was transferred to 50ml tube. The tube was centrifuged for 15min at 4°C to harvest the bacterial cells. Then the LB medium was discarded and the bacterial cell pellet remained in the tube.

The pellet was completely re-suspended in 8ml Resuspension Buffer (RES) + RNaseA by pipetting and vortexing. 8ml Lysis Buffer (LYS) was added and mixed by inverting many times. The mixture was incubated for 5min at room temperature. While incubating, a NucleoBond® Xtra Column was equilibrated by adding 12ml Equilibration Buffer (EQU) and the column was allowed to empty by gravity.

After the incubation, 8ml Neutralization Buffer (NEU) was added to the mixture and suspended by inverting until the mixture turned colorless, indicating that the completion of precipitation of SDS, protein, and genomic DNA. After that, the mixture was transferred to the NucleoBond® Xtra Column. The column was allowed to empty by gravity.

The NucleoBond® Xtra Column Filter and NucleoBond® Xtra Column was washed with 5ml Equilibration Buffer (EQU). The NucleoBond® Xtra Column Filter was removed and the NucleoBond® Xtra Column was washed with 8ml Buffer WASH. DNA was eluted by adding 5ml Elution Buffer (ELU) and was collected in a 15ml tube.

To concentrate eluted DNA, 3.5ml isopropanol was added to the DNA at room-temperature. The mixture was vortexed and left for 2min. The plunger of a 30ml syringe was removed and NucleoBond® Finalizer was attached to the syringe. The precipitation mixture was loaded into the syringe, then the plunger was inserted. The plunger was used to push the mixture slowly through the NucleoBond® Finalizer. The NucleoBond® Finalizer was removed and the plunger was pulled out from the syringe.

The NucleoBond<sup>®</sup> Finalizer was reattached to the syringe and 2ml of freshly prepared 70% ethanol was loaded into the syringe. Then, the plunger was inserted and pressed to discard the supernatant. The NucleoBond<sup>®</sup> Finalizer was dried by inserting the plunger into the syringe many times.

To elute DNA, The NucleoBond<sup>®</sup> Finalizer was removed from the 30ml syringe and attached to a 1ml syringe after removing the plunger. 100-200ul of Buffer TRIS or water was loaded into the syringe. Then the plunger was inserted to press DNA into the collection tube. The eluted DNA concentration was measured using the nanodrop spectrophotometer and was stored at -20°C for electroporation. (NucleoBond Xtra Plasmid DNA Purification User Manual (PT4011-1)\_Rev\_12-2.pdf)

### 2-11-cloning of short fragments of FZD receptors:

Frizzleds sequence was obtained from NCBI; (NCBI; <http://www.ncbi.nlm.nih.gov>)

with the following accession numbers:

-FZD2 (NM\_204222)

-FZD3 (NM\_001271940)

-FZD6 (NM\_001271931)

-FZD7 (NM\_204221)

-FZD10 (NM\_204098.2)

#### 2-11-1- designed primers for FZD cloning:

N	Name	Forward	Reverse
1	FZD2	CTGGA <sup>AA</sup> AGCTGGAAATGGA	TAACGTGAGCTGATGGCTTG
2	FZD3	GCGGCCGCATGGCTGTTAGCTGGATG TTCTGC	ACTGCCAGCCATGGTAAAGA
3	FZD6	CACTGCTCCTGTAACCA	TGACCCACCATATTGTTCTG
4	FZD7	CAGAGCGACCCATCATCTTC	TGCGGAACAAGGACACAAAG
5	FZD10	CCTCAGCGTTTCAAGTACCC	GGCCACAAAACCAGAAAGAA
6	M13	GTAAAACGACGGCCAG	CAGGAAACAGCTATGAC
7	pCaB	GGCAGGAAGGAAATGGGCGGGGA	GGCCCTCACATTGCCAAAAGACG
8	GapDH	CCTCTCTGGCAAAGTCCAAG	CATCCACCGTCTTCTGTGTG

Table 2-1: Primers were used for cloning and sequencing.

### **2-11-2-PCR reaction and condition:**

Chick FZD receptors were amplified by PCR from cDNA made from 3 or 4 days old chick embryos (see 2-1 and 2-2).

-PCR reaction (20ul):

1µl cDNA

10µl BioMix (Sigma)

1µl Forward primer

1µl Reverse primer

7µl H<sub>2</sub>O

-PCR condition:

1- 95°C 3mins

2- 95°C 1min

3- 56°C 1min

4- 72°C 1min

5- go to step 2 for 29 more times

6- 72°C 8mins.

Then the PCR products were purified (see 2-6 and 2-7) and cloned into pGEM-T easy vector (see 2-8-1). All FZD receptor fragments were confirmed by sequencing and then in situ probes were made (see 2-14).

### **2-12-Electroporation:**

After Nakamura et al (2004), the white eggs were incubated at 38°C until the embryos reached the desired Stage HH12-14. The eggs were opened at the broad end and ink/PBS/ penicillin/streptomycin mix was injected underneath the embryo to improve contrast and ease targeting. Embryos were injected by micro-injector into the neural

tube with the plasmid DNA mixed with 1% fast green. After injection, electroporation was performed by placing the electrodes on both sides of the embryo (i.e., the positive electrode on the right-hand side of the embryo and the negative one on the left) (Fig. 2-1B). The conditions for electroporation 20 or 24Voltage, Pulse number: 5, Pulse length: 50msec, Pulse interval: 100msec. After the electroporation, PBS/P/S was added onto the top of the embryos and the eggs were sealed with clear tape. They were then re-incubated for 24 or 48 hours at 38°C. Lastly, the electroporated embryos were dissected and GFP/RFP expression was visualised (Fig. 2-1C-D).

Number	Name	Obtained from
1	pCiG-Wnt1-IRES-GFP	Elisa Martí. (Megason and McMahon, 2002)
2	pCiG-Wnt3a-IRES-GFP	Elisa Martí (Megason and McMahon, 2002)
3	pCaB-dnWnt3a-IRES-GFP	Andrea Münsterberg lab
4	pCaB-FZD10-IRES-GFP	PCR
5	pCS2-GFP	Andrea Münsterberg lab
6	FZD10 shRNAs (A, B and C) see 2-13	Origene
7	Scrambled shRNA see 2-13	Origene
8	pCiG-IRES-GFP	(Megason and McMahon, 2002)
9	pCAB-IRES-GFP	Andrea Münsterberg lab
10	pCS2-hLrp6	Addgene

Table 2-2: Plasmids used for electroporation.

## Electroporation

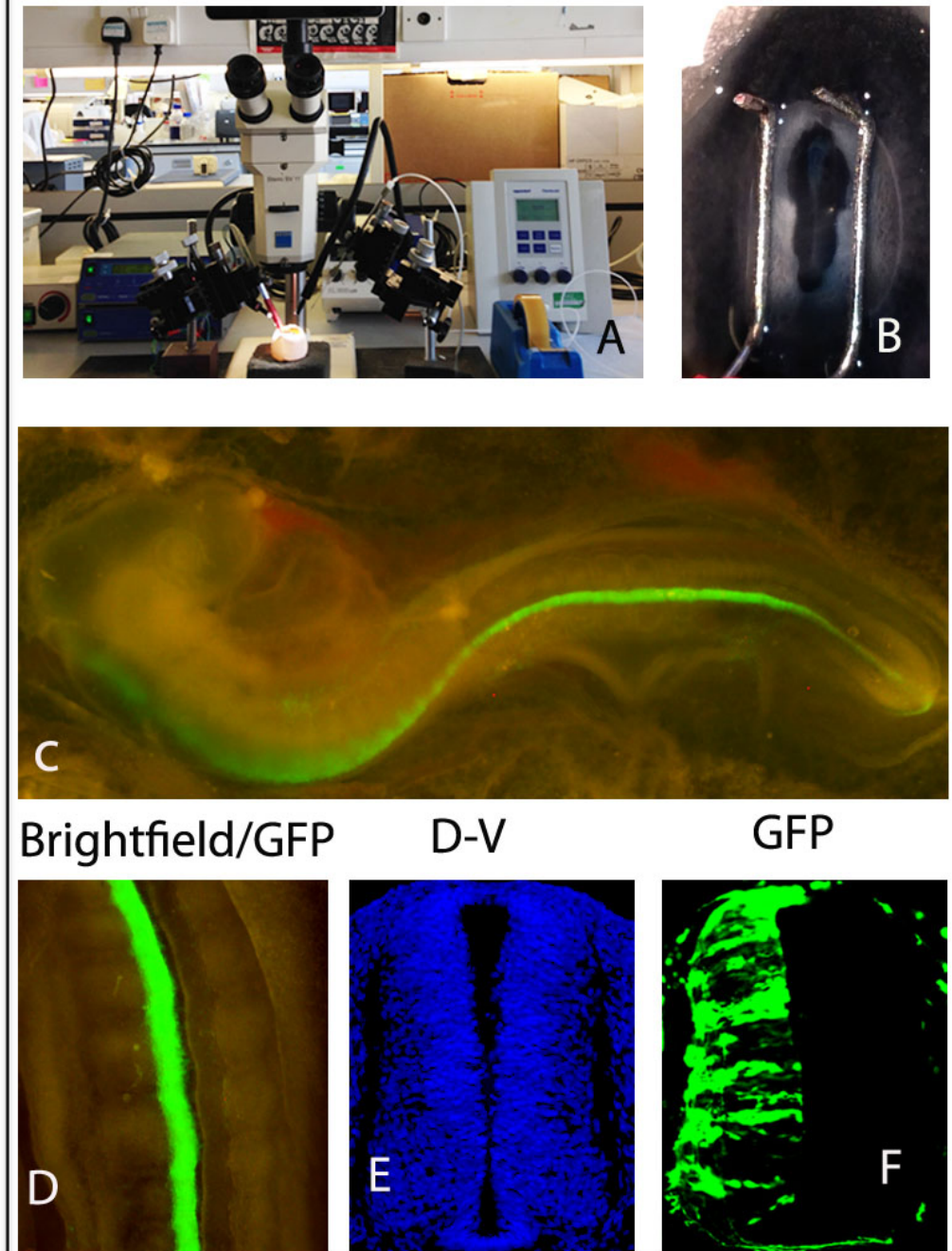


**Figure 2-1: Electroporation approach in chick neural tube.** (A) Showing equipment used for electroporation such as dissecting microscope and micro-injector. (B) Shows electrode position during electroporation. (C-D) Whole mount picture of electroporated embryo showing GFP expression. (E) Cross section of chick neural tube stained with DAPI. (F) GFP expression in one half of electroporated neural tube.

### **2-13- FZD10 knockdown using shRNA:**

To knock down FZD10 in the neural tube, we obtained three short hairpin RNAs (shRNA) that were designed and inserted in expression plasmid (pRFP-C-RS), which has U6 promoter (ORiGene). U6 promoter works in chick and is able to generate a small RNA transcript by RNA polymerase III (Islam et al., 2013;Katahira and Nakamura, 2003).

The shRNA expression was designed as follow, a 29 bp target gene specific sequence, a 7 bp loop, and another 29 bp reverse complementary sequence, all under U6 promoter. A termination sequence (TTTTTT) was located downstream of the second 29 bp reverse complementary sequence to terminate the transcription by RNA Pol III. All three shRNA expression plasmids were confirmed by sequence (ORiGene).

- Exact-ShRNA chick FZD10:

A- GTACAACATGACGAGAATGCCGAACCTGA

B- TGGATTGCCATCTGGTCCATTCTGTGCTT

C- GCAAGCGTTATTACCAGTAGTGGAATCTA

After obtaining the shRNA expression plasmids, electroporation was performed (Fig. 2-2) and FZD10 knockdown was checked for each shRNA plasmid by in situ hybridization (see 2-14). B and C shRNA plasmids showed better knockdown. So, B+C were used in all experiments and are referred to as (FZD10 shRNA).

Also scrambled shRNA was used as control and it did not show any effect of FZD10 expression after electroporation.

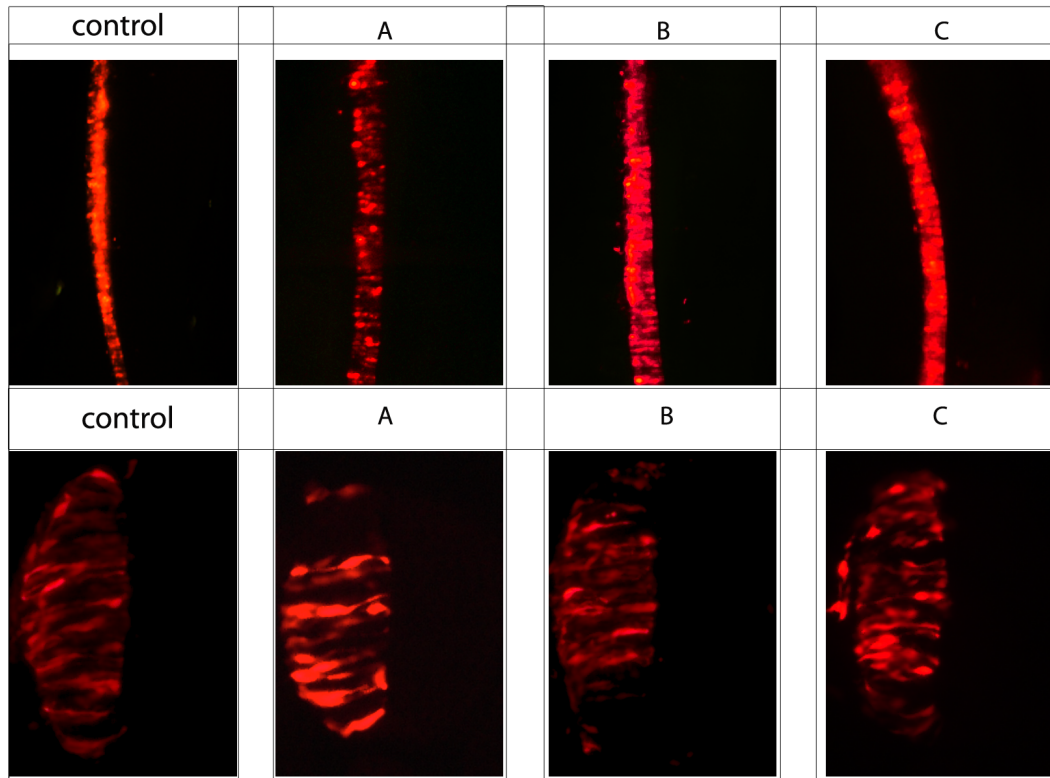


**Figure 2-2: RFP expression was detected after electroporation of scrambled shRNA (control) and FZD10 shRNA (A, B, C) in chick neural tube (24hrs).**

## 2-14- Whole mount in situ hybridization (WISH):

### 2-14-1-Probe synthesis:

(PCR method):

DNA template preparation: Some plasmids have M13 forward and M13 reverse sequences together with T3, T7 or SP6 promoter sequences on either side of the insert of interest. We took advantage of that to generate template by PCR. The PCR reaction was made up of 5 $\mu$ l of BiO mix, 1 $\mu$ l of M13 forward primer, 1 $\mu$ l of M13 reverse primer, 1 $\mu$ l of plasmid DNA and 2 $\mu$ l of Sigma water.

-The PCR reaction conditions:

- 1- 95°C for 3 minutes,
- 2- 95°C for 1 minute,
- 3- 55°C for 1 minute,

4-72°C for 1 minute,

5- go to step 2 for 24 more times for 1min

6- 72°C for 10 minutes.

1/10<sup>th</sup> of the PCR reaction was run on an agarose gel to ensure that a single sharp PCR product of the right size was obtained.

#### **2-14-2- Antisense transcription:**

The PCR product was transcribed using the appropriate RNA polymerase. The transcription reaction was in 50µl volume, containing the following mixture: 1µl PCR product (=DNA template), 10µl Promega transcription buffer, 5µl DTT, 5µl DIG or FITC-UTP plus NTP labelling mix, and 1µl RNasin, 2µl T3 or T7 or SP6 polymerase. The transcription reaction was incubated for 2-4 hours at the appropriate temperature for the polymerase used (T3/7 at 37°C, SP6 at 40°C). The DNA template was degraded by adding 1µl of RQ DNase and incubated for 30 minutes at 37°C. 1/20<sup>th</sup> of the transcription reaction was run on an agarose gel to examine the probe.

#### **2-14-3-Probe purification:**

The volume of the transcription reaction was made up to 80µl with Sigma water and precipitated by adding 220µl of 100% EtOH and 8µl LiCl, after which the reaction was incubated overnight at -20°C. This was centrifuged for 20 mins at 4°C and the supernatant was removed. The pellet was washed with 300µl 70% EtOH and centrifuged for 5mins. It was washed with 50µl 100% EtOH and spun down; then, the pellet was allowed to dry at room temperature, following which it was dissolved in 100ul Sigma water by incubating for 15mins at 65°C. The probe was denatured for 3mins at 95°C and quickly cooled on ice for 5mins. The probe was diluted by 10 volumes of hybridization buffer and stored at -20°C. Sometimes, G50 column used to purify the probe.

-illustra™ MicroSpin™ G-50 column:

The Column Preparation; the resin was resuspended in the column by vortexing. The cap of the column was loosened and then the column was placed in the collection tube. The collection tube was spun for 1min at  $735 \times g$ . The column was placed in a 1.5ml Eppendorf tube and the probe was applied to the top centre of the resin. The Eppendorf tube was spun for 2mins at  $735 \times g$ . The purified probe was collected in the Eppendorf tube and stored at  $-20^{\circ}\text{C}$  (<http://www.gelifesciences.com>).

N	Name	Vector	Sense	Antisense	Source
1	Wnt1	pBS	T3	T7	Andrea Münsterberg lab
2	Wnt3a	pGEM-T	T7	SP6	PCR (Qaiyun Yue)
3	FZD1	pBS-KS	T3	T7	C. Tabin
4	FZD2	pGEM-T	Sp6	T7	PCR
5	FZD3	pGEM-T	T7	Sp6	PCR
6	FZD4	pBS	T7	T3	C. Tabin
7	FZD5	pBS-Sk+	T7	T3	Sabine Fuhrmann
8	FZD6	pGEM-T	T7	Sp6	PCR
9	FZD7	pGEM-T	T7	Sp6	PCR
10	FZD8	pBS	T3	T7	C. Tabin
11	FZD9	pBS	T7	T3	C. Tabin
12	FZD10	pGEM-T	T7	Sp6	PCR
13	Ngn1	pBS-sk	T7		Cristina Pujades

Table 2-3: In situ probes were made and used in this project.

#### 2.14-4 Embryo preparation and staging:

White fertilized chicken eggs were obtained from local farms and incubated at  $37^{\circ}\text{C}$  until the desired stages had been reached. The embryos were staged according to Hamburger and Hamilton (1951) and harvested in PBS under a dissecting microscope. The embryos were then fixed in 4% PFA for 1hour at room temperature or overnight at  $4^{\circ}\text{C}$ , following which they were washed twice PBST for 5mins per wash. After that, they were dehydrated by passing them through ascending grades of MeOH (25%, 50%

and 70% MeOH in PBST), finishing at 100% MeOH, after which they were stored at –20°C.

#### **2.14-5 Rehydration:**

The embryos were rehydrated from 100% MeOH by passing them through descending grades of MeOH (70%, 50% and 25% MeOH in PBST) for 5mins each, followed by 2 washes with PBST; all of these steps were performed at room temperature with gentle rocking.

#### **2-14-6 Proteinase K treatment:**

Embryos younger than HH25 do not need to be treated with proteinase K (PK), but embryos older than HH25 were treated with 10µg/ml PK for different times depending on the embryo's stage. Then, the embryos were washed twice in PBST, and then fixed in 4% PFA containing 0.1% glutaraldehyde for 20 minutes with rocking. After that, the embryos were washed twice in PBST for 5mins per wash.

#### **2-14-7 Hybridisation:**

PBST was removed and 1:1 PBST/hybridisation buffer was added to the embryos. The embryos were kept until they sank in the solution, after which they were rinsed in hybridisation buffer for 15mins at room temperature. The embryos were incubated in the hybridisation buffer for 2hours at 65°C. Following this, the embryos were incubated in the probe of interest overnight at an appropriate temperature (65°C).

#### **2-14-8 Post-hybridisation:**

After hybridisation, the probes were removed and stored at -20°C. Then, the embryos were washed with hybridisation buffer for 10mins and washed in wash buffer twice for 30mins per wash. The embryos were then washed in 1:1 wash buffer/MABT for

10mins (all these washes were done at 65°C). After these steps, embryos were rinsed with 2x MABT at room temperature for 30mins per wash and washed in MABT/2% BBR solution for 1hour; this was followed by one wash in MABT/2% BBR/20% goat serum for 2hours to block non-specific binding. The embryos were incubated overnight in the cold room with rocking in MABT/2% BBR/20% goat serum/ant-digoxigenin-AP (1:2000) or anti-fluorescein-AP (1-1000).

#### **2-14-9 Post-antibody washes and colour reaction:**

The antibody solution was removed and the embryos were rinsed in MABT 5 times for 1hour each at room temperature with rocking, and then incubated in MABT overnight at 4°C. The following day, embryos were washed twice in freshly made NTMT buffer for 10mins each; they were then incubated in 7ul BCIP/9ul NBT/1ml NTMT or in fast red solution in the dark in order to develop the colour. The colour reaction was halted when the background had started to develop by washing many times in 5x TBST detergent mix. After background removal, embryos were fixed in 4% PFA and then washed twice in PBS in order to be photographed.

#### **2-14-10 Double in situ hybridisation:**

For double in situ hybridisation, embryos were incubated with two different labelling probes (1:1ml DIG labelling probe/FITC labelling probe). After this, the same protocol was followed, but after the first colour was developed the embryos were fixed in 4% PFA for 1hour at room temperature and then washed twice in PBS for 5mins each. Following this, embryos were incubated in MABT for 1hour at 65°C followed by two washes in MABT for 10mins each at room temperature. To block unspecific binding, embryos were treated in MABT/2% BBR solution for 1hour followed by one wash in MABT/2% BBR/20% goat serum for 2hours. Lastly, the embryos were incubated with the second antibody overnight in the cold room with rocking (in MABT/2% BBR/20%

goat serum/ant-fluorescin-AP (1-1,000)). The second colour was developed as mentioned earlier (see subsection 2.5.5) but with fast red.

Embryos were photographed as whole-mount double in situ hybridisation or sectioned to see the two different colours.

### **2-15- Cryosectioning:**

The embryos were fixed in 4% PFA for 1 hour at room temperature and then washed twice in PBS for 5 minutes each. The embryos were incubated with 30% sucrose for 4 hours at room temperature or overnight at 4°C. After this, they were mounted in OCT compound in plastic capsules then left for 2 hours at room temperature. Then, the embryos were positioned with needles, frozen by dry ice and then stored at -20°C for sectioning. The embryos were sectioned with a Leica cryostat and the sections' thicknesses were between 20 and 30 µm. The sections were collected in TESPA slides and left to dry at room temperature. The sections were washed twice in PBS for 5 minutes, after which they were covered with coverslips using a hydromount. The slides were kept overnight at room temperature to dry. Finally, the sections were imaged with a Zeiss CCD upright microscope using a colour camera. The pictures were imported from AxioVision Rel 4.8 to Adobe Photoshop CS for adjustment and labelling.

## **2-16-Immunostaining:**

Embryos were fixed in 4% PFA for 1 hour at room temperature, or overnight at 4°C. Different fixatives and fixation times may be needed for different antigens. The embryos were washed well with PBS to remove fixative. Then, They were transferred to 30% sucrose in PBS and kept for 2 hours at room temperature or at 4°C overnight. After that, they were embedded in OCT and sectioned using cryostat as normal. The cryosections were collected in slides. Fixo Gum was used to make a ring around sections. The Sections were rinsed in a jar of PBST (PBS 0.1%Triton). Sections were treated with a blocking buffer for 1 hour at room temp, or overnight at 4°C (blocking buffer: PBS + 5% BSA + 0.1% Triton + 5% Serum). After blocking, primary antibodies were prepared by diluting into blocking buffer to give the appropriate concentration. This was determined for each antibody. Sometimes, two different antibodies were combined together if they were raised in different species. 50-100ul antibody solution was applied to the slide, and then incubated at 4 °C overnight in a humidified chamber to prevent the sections from drying out. Next step, slides were washed 3 x 5 mins in a jar of PBST (PBS Triton). Suitable secondary antibodies and DAPI were Prepared and applied to the slides. The slides were incubated at room temp for 1 or 2 hours in a dark humidified chamber. Then the slides were washed 3 x 5 minutes or longer in a jar of PBST (PBS Triton) in the dark. A Final wash with PBS only for 2 x 5 mins and then the ring was removed before mounting. The slides were mounted with hydromount and kept overnight at 4°C in the dark. After that, the sections were imaged using Widefield microscope Zeiss AxioPlan 2ie. Then, the images were analysed.

<b>Number</b>	<b>Name</b>	<b>Species raised in</b>	<b>Dilution</b>	<b>Company</b>
1	Pax3	Mouse	1:50	DSHB
2	Pax6	Mouse	50:1000	DSHB
3	Pax7	Mouse	1:50	DSHB
4	Nkx2.2	Mouse	1:50	DSHB
5	Lhx1/4	Mouse	1:50	DSHB
6	Islet1	Mouse	1:50	DSHB
7	Tuj1	Mouse	2:1000	Covance
8	RFP	Rabbit	2:1000	Abcam
9	DAPI		1:2000	Life Technologies
10	H3	Rabbit	5:1000	Abcam
11	Anti-mouse Alexa Fluor 568	Goat	4:1000	Life Technologies
12	Anti-Rabbit Alexa Fluor 568	Goat	4:1000	Life Technologies
13	Anti-mouse Alexa Fluor 488	Goat	2:1000	Life Technologies
14	Anti-Rabbit Alexa Fluor 488	Goat	2:1000	Life Technologies
15	Anti-mouse Alexa Fluor 350	Goat	5:1000	Life Technologies
16	Alexa Fluor 568 Phalloidin		1:500	Invitrogen
17	Laminin	Mouse	1:500	DSHB

Table 2-4: Antibodies used in this project

# Chapter 3

**Expression of chick  
Frizzled receptors (cFZD)  
during spinal cord development**

### **3-1 Introduction**

Frizzleds (FZDs) are known as receptors for Wnt ligands. They have been shown to be involved in regulation of several embryogenesis events such as, cell proliferation, neural patterning, and neural synapse development (Clevers, 2006; Medina et al., 2000).

In chicken, ten Frizzled receptor genes have been identified and numbered from 1 to 10. Expression of FZDs is dynamic during chick embryogenesis and is found in different developing tissues (Chapman et al., 2004; Fuhrmann et al., 2003; Stark et al., 2000; Quinlan et al., 2009; Theodosiou and Tabin, 2003). Most of the cFZDs are expressed in early stages of development during patterning and neural specification. Six cFZD receptors show overlapping expression in the primitive streak and Hensen's node, including cFZD1, 2, 4, 7 and cFZD9 (Chapman et al., 2004). cFZD8 is exclusively expressed in Hensen's node.

Moreover, all cFZDs, with the exception of cFZD10, are expressed in the developing eye and their expression is specific in different parts of the eye (Fuhrmann et al., 2003). It was found that, cFZD1, 2 and 7 are present in the cranial placodes and in the somite during development (Stark et al., 2000). Their expression patterns are shown in early forming somites and overlap with myogenic markers such as MyoD (Linker et al., 2003). This group reported that *in vivo*, blockade of FZD signalling by cFZD7-CRD electroporation reduces MyoD expression, indicating the importance of FZDs during myogenesis. Also the same group showed that, cFZD7 mediates Wnt6 function through the canonical Wnt signalling in the dorsal part of the somite (linker et al., 2005). Another study by Gros and colleagues, 2009 documented that FZD7 inhibition *in vivo* affects cell polarity and elongation of myocytes in the myotome of chick somites. This was not dependent on canonical mechanisms and suggested that FZD7 might act as

Wnt11 receptor through non-canonical Wnt signalling (PCP).

A number of cFZDs, including cFZD1, 2, 4 and 7, are expressed strongly in the limb bud at different stages of development (Kengaku et al., 1997; Nohno et al., 1999; Stark et al., 2000). cFZD2 is found in the proximal limb mesenchyme and cFZD4 exhibits a specific expression pattern in the apical ectodermal ridge of the limb (Nohno et al., 1999). By stage HH30, cFZD4 shows high expression in the cartilage and in the interdigital spaces (Stark et al., 2000). cFZD1 and 7 expression is dynamic and distinct; cFZD1 expression is located on the ventral side of ectoderm and mesenchyme, whilst cFZD7 is expressed in the proximal-distal axis of the limb bud (Kengaku et al., 1997). cFZD1 and 7 are expressed during chondrogenesis in the limb and their misexpression in chick wing reduces chondrogenesis (Hartmann and Tabin, 2000). This study suggested that cFZD7 mediates Wnt4 signal in the articular chondrocytes. Another study showed that cFZD7 misexpression reduced chondrogenesis in chick limb culture (micromass), but cFZD1 misexpression did not have any effects (Tufan et al., 2002).

Some cFZD receptors have been shown to be expressed in kidney, liver and the gut during the development of chick embryo (Theodosiou and Tabin 2003; Matsumoto et al 2008; Stark et al 2000). cFZD4 shows a striking expression pattern in chick kidney and colocalizes with Wnt4 and other kidney markers (Stark et al 2000). FZD1, 4, 7 and 9 expression is detected in the chick liver, and FZD7/9 expression overlaps with Wnt9a expression and they seem to transfer its signal as shown by co-immunoprecipitation in COS7 cells (Matsumoto et al 2008).

cFZDs are expressed during the development of the central nervous system (Chesnutt et al., 2004; Kawakami et al., 2000; Galli et al., 2014; Quinlan et al., 2009). It has been reported that cFZDs exhibit complex and dynamic expression patterns in different

regions of the developing brain (Quinlan et al., 2009). For example, cFZD1, 2 and 7 show strong expression in the ventral of midbrain, while cFZD4 and 8 are expressed in the forebrain. In addition, cFZDs expression patterns overlap with many Wnt ligands in the mid and forebrain including Wnt1, Wnt3a, Wnt5A, and Wnt8B. This illustrates that Wnts and their receptors are present during the development of the brain.

In addition, cFZDs are expressed in the developing spinal cord (Chesnutt et al., 2004; Kawakami et al., 2000) and in this project we analyzed the expression patterns of all known FZDs during chick neurogenesis.

-Aims of this chapter:

- To clone and generate in situ probes for all chick FZDs (see chapter2).
- To establish a complete expression profile for all cFZDs in spinal cord.

### **3-2-FZDs are expressed in the chick developing spinal cord:**

To identify which FZDs mediate Wnt signalling that may be involved in the development of the spinal cord, an analysis of the expression patterns of these receptors was performed in chick embryos. To study the spatial expression of FZDs specific antisense RNA probes were generated for each FZD then whole mount in situ hybridization was used followed by cryo-sections as mentioned in materials and methods. FZD1 expression was seen in the dorsal spinal cord covering the roof plate and was graded dorsal to ventral at stage HH14-15 (Fig. 3.1D,E). FZD2 transcripts were detected in the intermediate ventral spinal cord and high level of expression was observed in the floor plate (Fig. 3.1F). FZD3 was strikingly expressed throughout the dorsal ventral spinal cord and it was restricted in the ventricular zone (Fig. 3.1G). FZD4, 5 and 6 were not present in the developing spinal cord at stage HH14-15 but they were expressed in other tissues (Fig. 3.1 H,I,J). For example, FZD4 is expressed in head, limb bud and nephrogenic ridge (Fig. 3.2). FZD6 was detected in the developing somite (Fig. 3.3A,A'). FZD7 showed specific and strong expression in the intermediate and ventral spinal cord (Fig. 3.1H). FZD8 did not appear to be expressed in the posterior neural tube, but it was found in nephrogenic ridge and limb bud (Fig. 3.1I and Fig. 3.3B,B',B''). FZD9 was ubiquitously expressed and seemed to be strongly expressed around the lumen of the chick spinal cord (Fig. 3.1J). FZD10 transcripts were specifically expressed in the dorsal spinal cord and strong signal was seen in the dorsal neural progenitors (Fig. 3.1K).

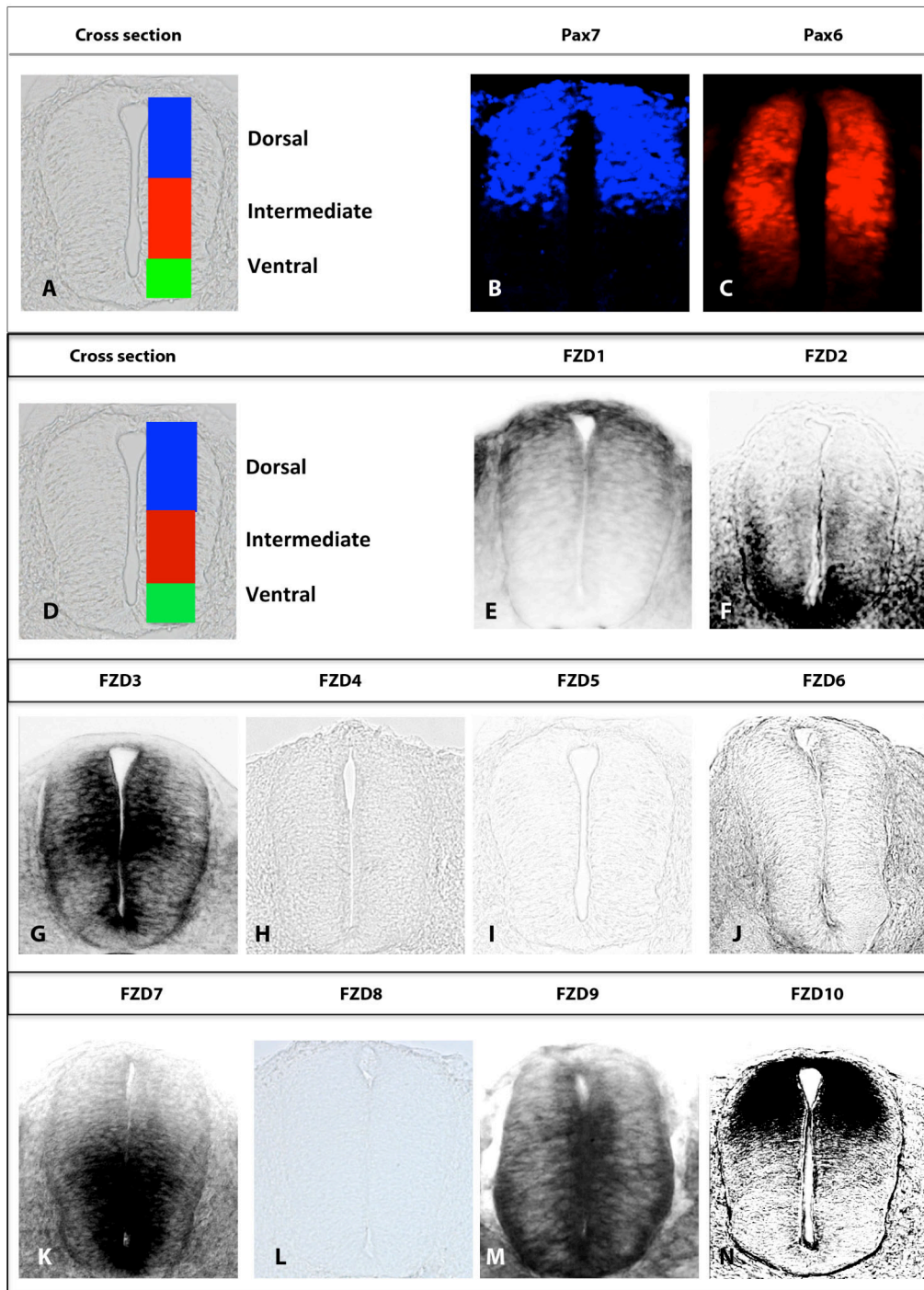


**Fig. 3.1.** Expression patterns of cFZDs in the developing spinal cord were detected by in situ hybridization at stage HH14-15.

(A and D) Cross section of spinal cord with three domains of neural progenitors indicated. (B) Pax7 stained 6 dorsal progenitors (C) Pax6 is a marker for intermediate progenitors. (E) Expression of FZD1. (F) FZD2 expression in the ventral spinal cord. (G) FZD3 expression throughout the spinal cord. (H,I J, L) FZD4, 5, 6 and 8 are not expressed in the spinal cord. (K) Expression of FZD7. (M) FZD9 expression. (N) FZD10 expression in the dorsal spinal cord.

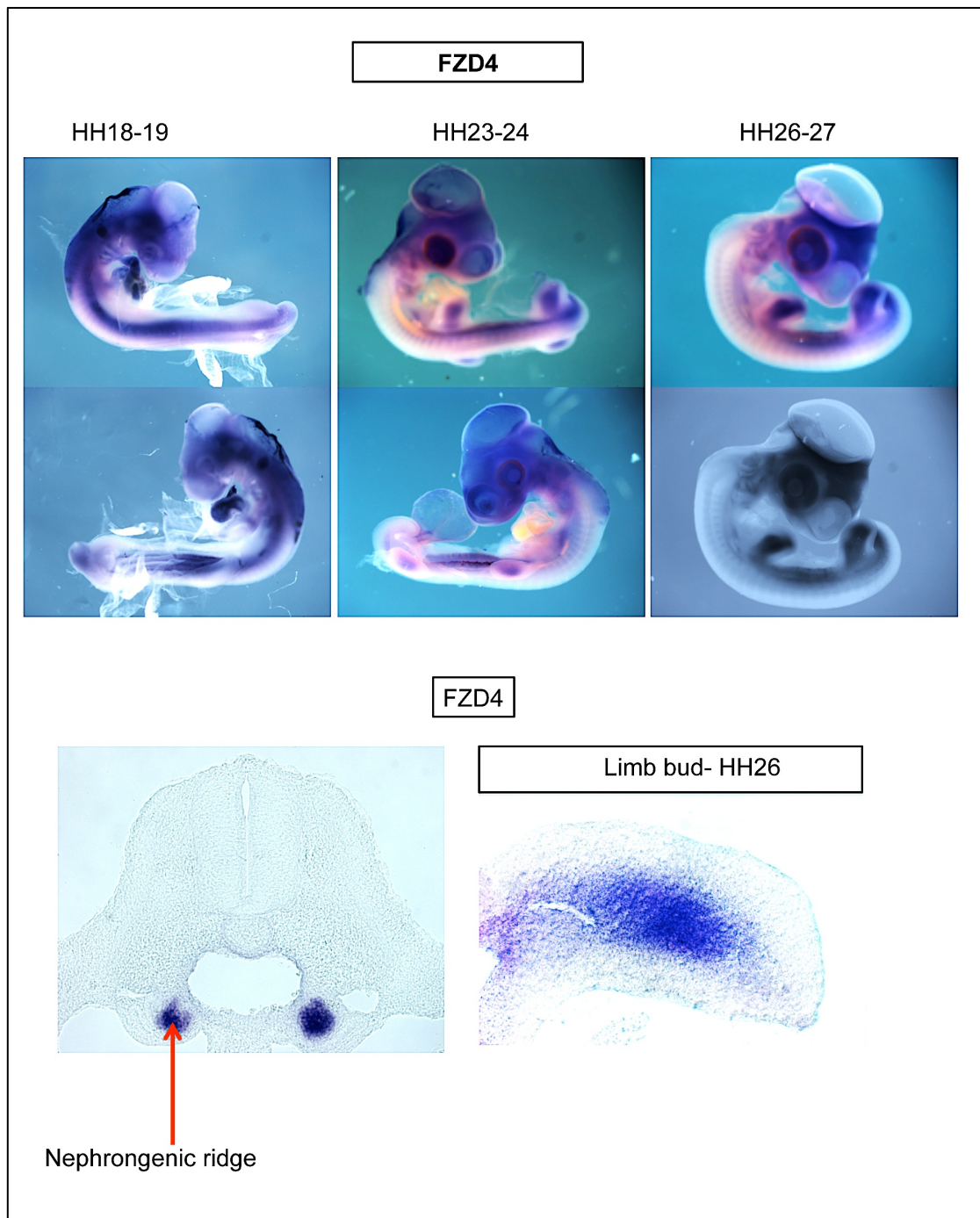


**Fig. 3.2 Whole mount in situ shows expression patterns of FZD4 at different stages.** FZD4 is expressed in head, limb bud and nephrogenic ridge. Cross sections show that FZD4 transcripts are found in nephrogenic ridge and limb bud.

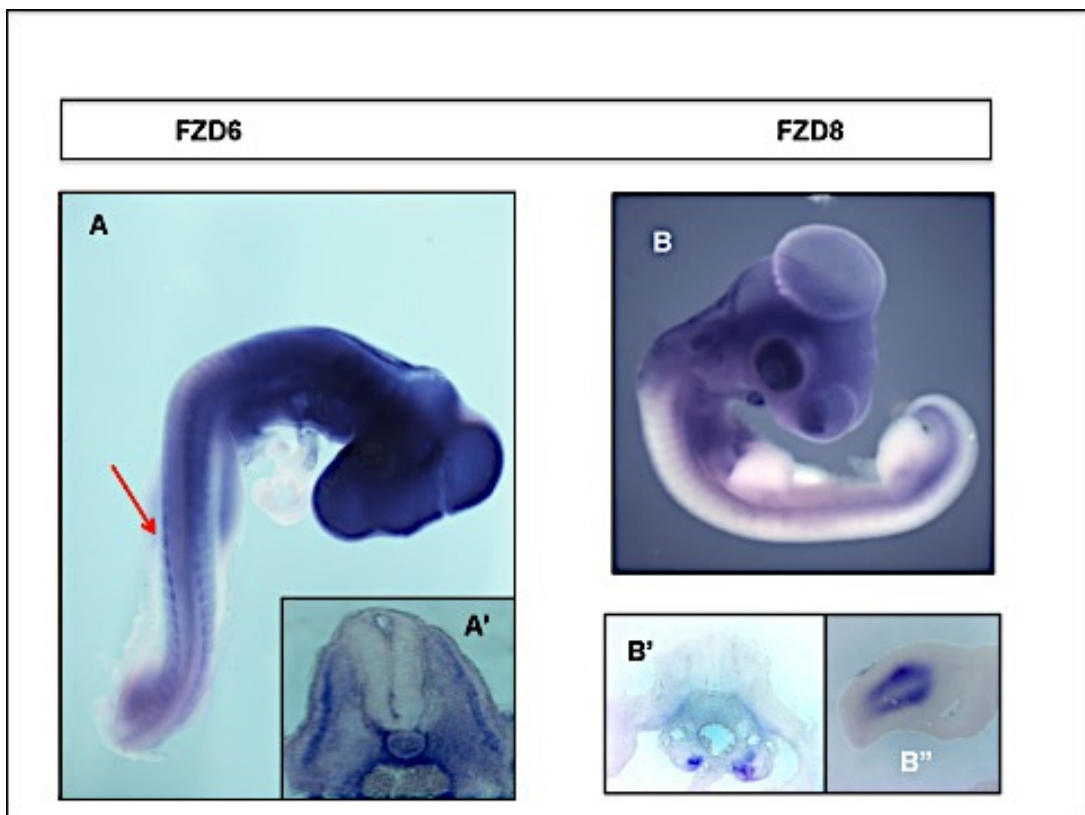


**Fig. 3.3 Whole mount in situ shows expression patterns of FZD6 and 8.** FZD6 was detected in somite. ridge. (A) FZD6 expression at stage HH18+. (A') FZD6 is expressed in developing somite. (B) FZD8 expression at stage HH24, it was found in the head and limb buds. (B') FZD8 was found nephrongenic ridge. (B'') cryosection shows that FZD8 transcripts were seen in limp bud.

### **3-3-FZD7 and FZD10 are expressed during spinal cord neurogenesis:**

FZD7 and FZD10 are expressed during early neural specification and their expression continues throughout embryogenesis (Chapman et al., 2004). We showed that they are strongly expressed in specific domains in the spinal cord at stage HH14-15 during the initiation of neurogenesis (Fig. 3.1HK).

It was reported that almost half of all neurons were generated after 4 days of development in chick spinal cord (HH24) (Le Dréau et al., 2012). Thus, we investigated the spatial and temporal expression of FZD7 and 10 in this stage of development (Fig. 3.4). FZD7 transcripts were found to be highly expressed in the intermediate and ventral spinal cord where the intermediate and ventral progenitors are located and its expression pattern correlated with Pax6 and Nkx2.2 expression (Fig. 3.4B,C,E). A strong signal for FZD10 expression was detected in the dorsal domains of neural progenitors and its expression correlated with Pax7 (Fig. 3.4A and F). Both, FZD7 and 10 expression seems to be restricted to the proliferative progenitors whilst neurogenesis takes place and their expression was not detected in differentiating neurons (Fig. 3.4D,E,F). Also, we studied their regulation by dorsal Wnts in the spinal cord (see Chapter 5). Also other FZDs such as FZD1 need to be investigated but because of time limitation it was not possible to do further analysis.

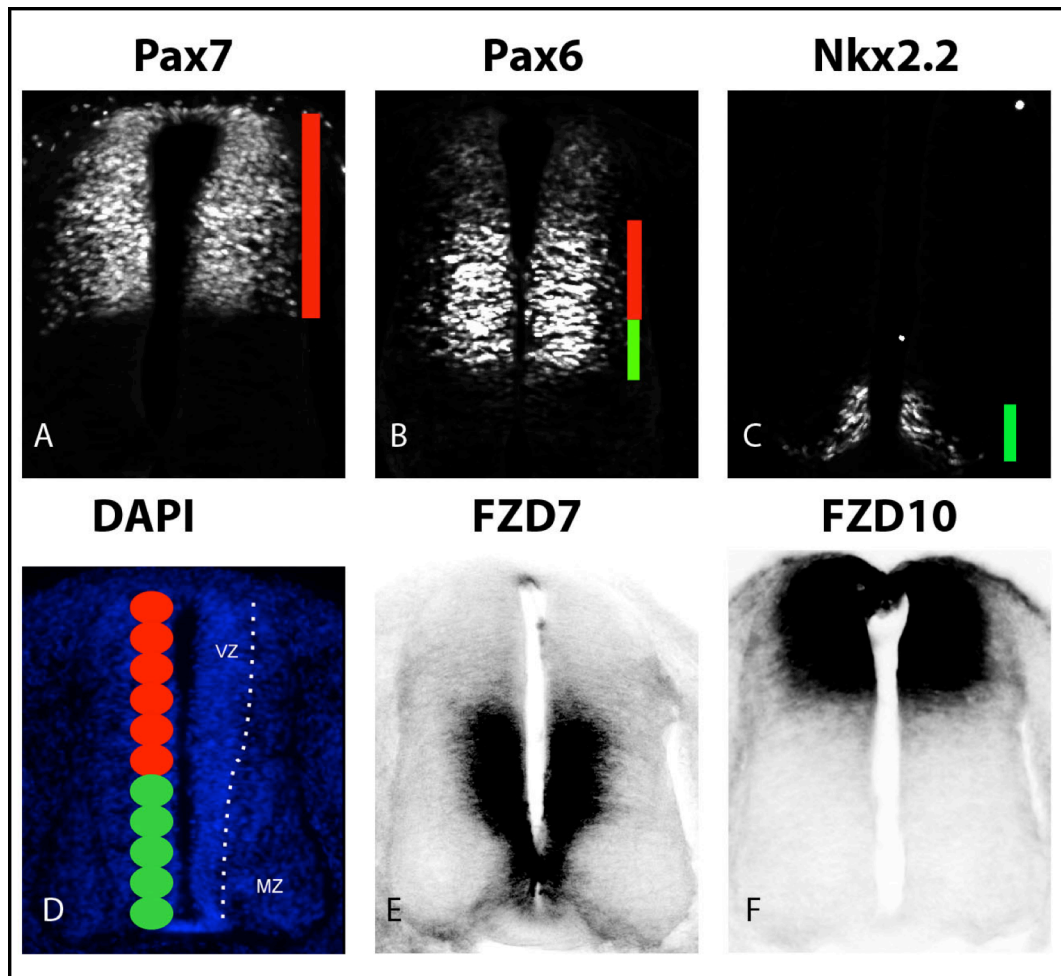


**Fig. 3.4** Expression patterns of FZD7 and FZD10 correlate with neural progenitors markers in the spinal cord at stage HH24. (A) Pax7 stained 6 dorsal progenitors. (B) Pax6 marked intermediate progenitors. (C) Nkx2.2 is a marker for p3 ventral progenitors. (D) Cross section of the developing spinal cord at stage HH24 stained with DAPI; red circles mark six dorsal progenitor domains while green circles represent five ventral progenitor domains. VZ, the ventricular zone; MZ, the mantle zone. (E) FZD7 expression in the intermediate ventral progenitors and excluded from MZ. (F) FZD10 expression in the dorsal domain of the spinal cord during neurogenesis.

### **3-4- summary:**

We established a complete expression profile of cFZD receptors in chick spinal cord and identified FZDs that could be involved in spinal cord development in either dorsal or ventral domains (Fig. 3.1 and Table. 3.1). By taking advantage of using in situ hybridization we observed that six out of ten FZDs are expressed in the spinal cord and showed specific and different expression patterns at stage HH14-15. FZD1 and FZD10 expression was found in the dorsal neural tube and FZD10 was strongly and specifically detected in the dorsal neural progenitor domains. Whereas FZD2 and FZD7 were expressed in the intermediate ventral spinal cord and their expression seems to be overlapping, but FZD7 showed stronger expression in the neural progenitors. FZD3 and FZD9 transcripts were found throughout the dorsal-ventral spinal cord. FZD3 expression was specific in the ventricular zone where proliferation occurs while FZD9 expression was ubiquitous. Also, we showed that FZD7 and FZD10 were expressed during spinal cord neurogenesis. The expression profile of cFZDs suggests potential roles for these receptors during spinal cord development. Also, it could be proposed that dorsal FZDs such as FZD10 may mediate signaling in response to Wnt ligands that are expressed in the dorsal spinal cord.

Frizzleds	FZD expression in the Spinal cord	
	Dorsal	Ventral
1	Yes	No
2	No	Yes
3	Yes	Yes
4	No	No
5	No	No
6	No	No
7	No	Yes
8	No	No
9	Yes	Yes
10	Yes	No

**Table. 3.1 Summary of FZD receptor expression in the spinal cord.** Red colour represents the dorsal FZDs whereas green colour represents ventral FZDs.

# Chapter 4

**Expression pattern of FZD10  
during spinal cord Development**

#### **4-1 introduction**

FZD10 is one of the FZD family receptors and it has been detected in different species including zebrafish, *Xenopus*, chick and mouse (Kawakami et al, 2000; Moriwaki et al., 2000; Wheeler and Hoppler, 1999; Nikaido et al., 2013; Yan et al., 2009). In zebrafish, FZD10 expression was found in neural plate at 1-somite stage, in the neural tube and in the tail bud (Nikaido et al., 2013). In *Xenopus*, FZD10 is expressed in the neural ectoderm and in the neural fold at early stages of development (Wheeler and Hoppler, 1999). FZD10 is detected in the central nervous system where it is strongly expressed in the midbrain and hindbrain and in the dorsal neural tube (Moriwaki et al., 2000; Wheeler and Hoppler, 1999). Using double in situ hybridization, it was reported that FZD10 expression is partially overlapping with neural markers such as Sox2 and N-CAM, while it shows strong co-localizations with the differentiated neuron marker N-tubulin (Garcia-Morales et al., 2009).

In chick, FZD10 is expressed at early stages of development as it was found in pre-streak stages and by stage 4 was detected in the posterior of the primitive streak (Chapman et al., 2004). FZD10 expression continues throughout embryonic development and it was detected by in situ hybridization in several developing tissues such as the central nervous system, limb bud and branchial arches (Kawakami et al, 2000). Chick FZD10 and human FZD10 have more than 85% identity in the amino acid sequence (Kawakami et al, 2000; Koike et al., 1999). Moreover, human FZD10 shares 65.7% amino-acid similarity with FZD9 (Koike et al., 1999).

In mouse, FZD10 expression is detected in the posterior epiblast at 7dpc and in the primitive streak at 7.5 dpc (Kemp et al., 2007). Also, it is strongly expressed in different parts of the developing central nervous system including midbrain, hindbrain and the

spinal cord (Kemp et al., 2007; Yan et al., 2009). FZD10 expression is also found in the limb bud and the tail bud during mouse development (Yan et al., 2009).

Furthermore, FZD10 was cloned and described in human, and expressed in multiple human tissues including brain, heart, lung, skeletal muscle, and fetal kidney (Koike et al., 1999). Also, It was reported that FZD10 is highly expressed in a variety of cancer tissues such as synovial sarcoma, colon and lung (Nagayama et al., 2009; Terasaki et al., 2002).

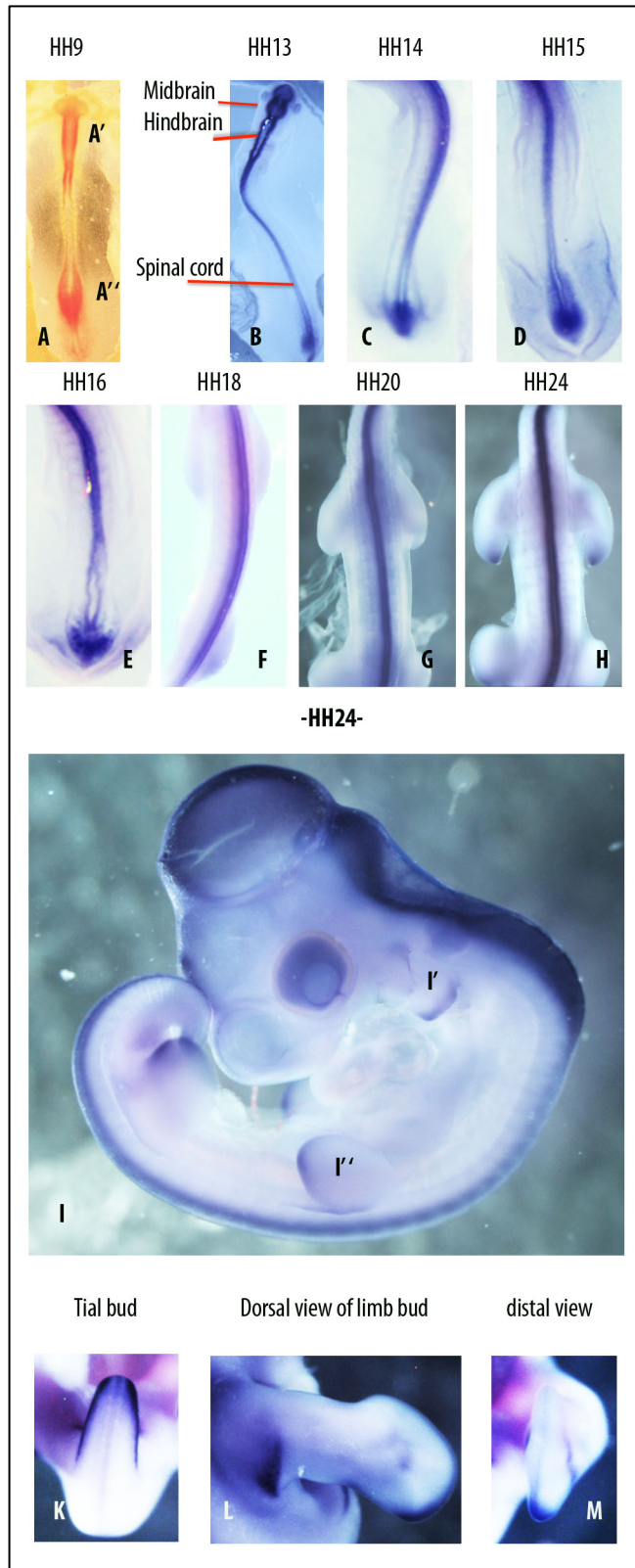
Chapter aims:

- To characterize FZD10 expression during chick embryo development.
- To follow FZD10 expression during spinal cord neurogenesis and compare it to neural marker gene expression.
- To compare Wnt1, Wnt3a and FZD10 expression in the developing spinal cord.

#### **4-2- FZD10 expression pattern during chick embryo development:**

To study when and where FZD10 is expressed during embryogenesis, we cloned full length of cFZD10 was cloned and antisense RNA probe was generated and then used for whole mount in situ hybridization. In this study, FZD10 expression was investigated from stage HH9 to HH24 (Fig. 4.1A). FZD10 transcripts were found in the developing midbrain and hindbrain during neural tube closure (Fig. 4.1A') as well as in the posterior region where secondary neurulation occurs (Fig. 4.1A''). By stage HH13, FZD10 expression was detected in the developing brain and spinal cord (Fig. 4.1B). Notably, FZD10 was strongly expressed in the spinal cord in all examined stages (Fig. 4.1C,D,E,F,G,H,I). Also, it was found in the tail bud throughout development (Fig. 4.1C,D,E,K). FZD10 expression was found in the branchial arch 1 and 2, and in the developing limb (Fig. 4.1',I). It was exclusively expressed in the dorsal posterior of the limb bud (Fig. 4.1,I''). By stage HH28, FZD10 expression was seen in different parts of the limb mesenchyme including in the proximal region (Fig. 4.1LM). Our data is consistent with previous study documented by Kawakami et al (2000a).

**Fig. 4.1 Whole mount in situ hybridization of FZD10 expression during chick embryo development in HH9-28 embryos.** (A-H) Dorsal views of different stages of development. (I) FZD10 expression in HH24; I', the branchial arch; I'', Limb bud. (K) Dorsal view of tail bud at HH28. (L) Dorsal view of the stage 28 hindlimb bud and distal view (M).



#### **4-3-FZD10 is expressed in the dorsal domain of the spinal cord during neurogenesis:**

It was previously shown that FZD10 is expressed in specific domains in the dorsal spinal cord at stage HH14-15 and HH24 (Chapter3). It has been shown that neurogenesis of dorsal neurons has begun at stage HH18 and half of neurons are formed by stage HH23 in the spinal cord (Le Dréau et al., 2012). Therefore, we followed FZD10 expression during neural tube development at different times; before the onset of neurogenesis, during neurogenesis initiation and during formation of dorsal neurons. Before the onset of neurogenesis FZD10 expression seems to be graded from dorsal to ventral as seen by stage HH12 (Fig. 4.2A). It continued to be expressed in the spinal cord but expression was more dorsally restricted during the initiation of neurogenesis (Fig. 4.2B,C,D). During neurogenesis, FZD10 was highly expressed in the dorsal half of the spinal cord while dorsal progenitors were being formed (Fig. 4.2D,E,F). Also, a high level of FZD10 expression was found in the ventricular zone where progenitors were still in proliferative mode and during neurogenesis. Because of time limitation, it was not possible to perform immunostaining (Pax7 or Lhx1/5) after FZD10 in situ at stage HH12 or HH24.

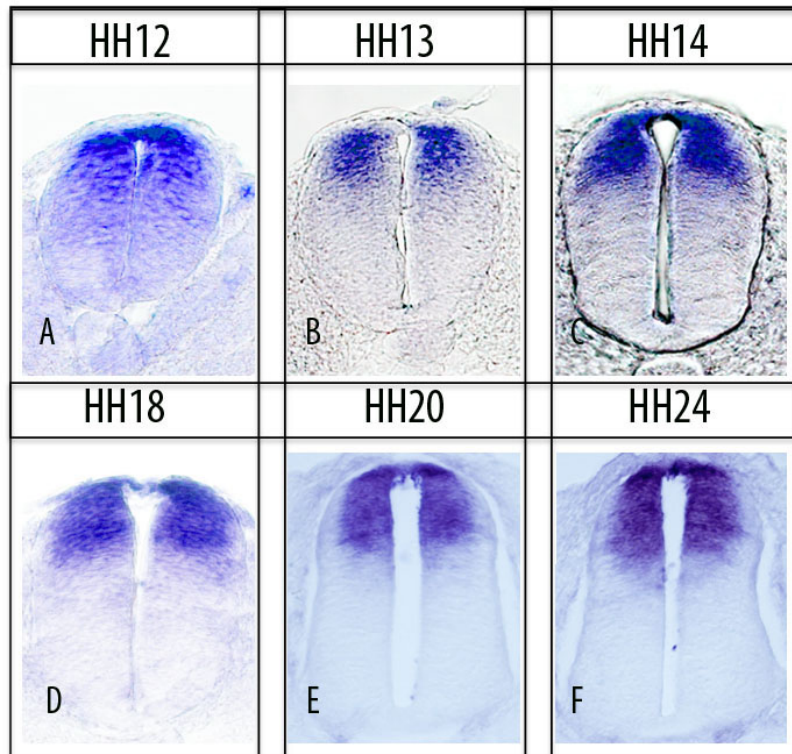
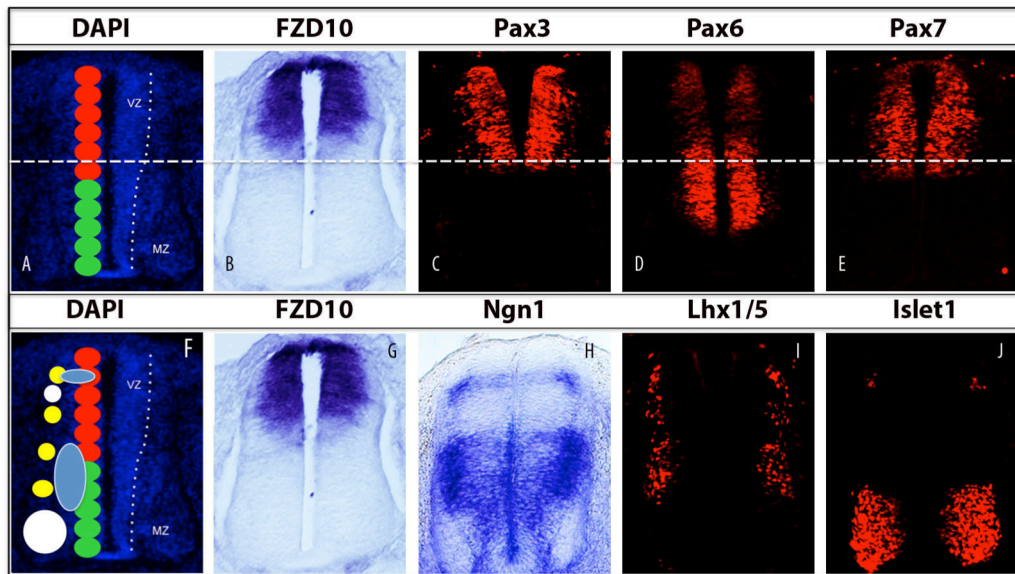


Fig. 4.2 **FZD10 expression in the dorsal spinal cord during dorsal neurogenesis.** Transverse sections of chick spinal cords at different stages HH12-24. (A-F) In situ hybridization shows the dorso-ventral extend of FZD10 expression.

#### **4-4-FZD10 expression overlaps with dorsal neural progenitors markers:**

The dorsal ventral axis of the spinal cord can be divided into eleven domains based on the expression of specific transcription factors (Le Dreau and Marti, 2012). For example, Pax3/7 expression marks six dorsal progenitors (dp1-6), whereas Pax6 is a marker for three dorsal progenitors (dp4-6) and one intermediate ventral progenitor (p0). Thus, as FZD10 is strongly expressed in dorsal domains of the spinal cord, the FZD10 expression pattern was compared to these well-characterized transcription factors during dorsal neurogenesis at stage HH24 (Fig. 4.3). To achieve this we used in situ hybridization and immunostaining in chick embryos as mentioned in Materials and Methods (Chapter2). FZD10 expression was found in 5 progenitor domains and showed a complete overlap with Pax3/7 expression (Fig. 4.3A,B,C,E). Also, FZD10 and Pax7 were expressed in the roof plate but Pax3 was not (Fig. 4.3B,C,E). FZD10 has some overlap with Pax6 expression in the dorsal domain where Pax6 was weakly expressed (Fig. 4.3A,B,D). FZD10 expression showed some overlap with Ngn1 expression in the dorsal progenitor 2 (Fig. 4.3G,H). Additionally, FZD10 expression was compared to dorsal differentiated neurons markers such as Lhx1/5 and Islet1, and FZD10 was expressed during the formation of dorsal interneurons (Fig. 4.3F,G,I,J). Therefore, FZD10 is specifically and strongly expressed in the dorsal domains of the spinal cord and overlaps with dorsal progenitors markers.



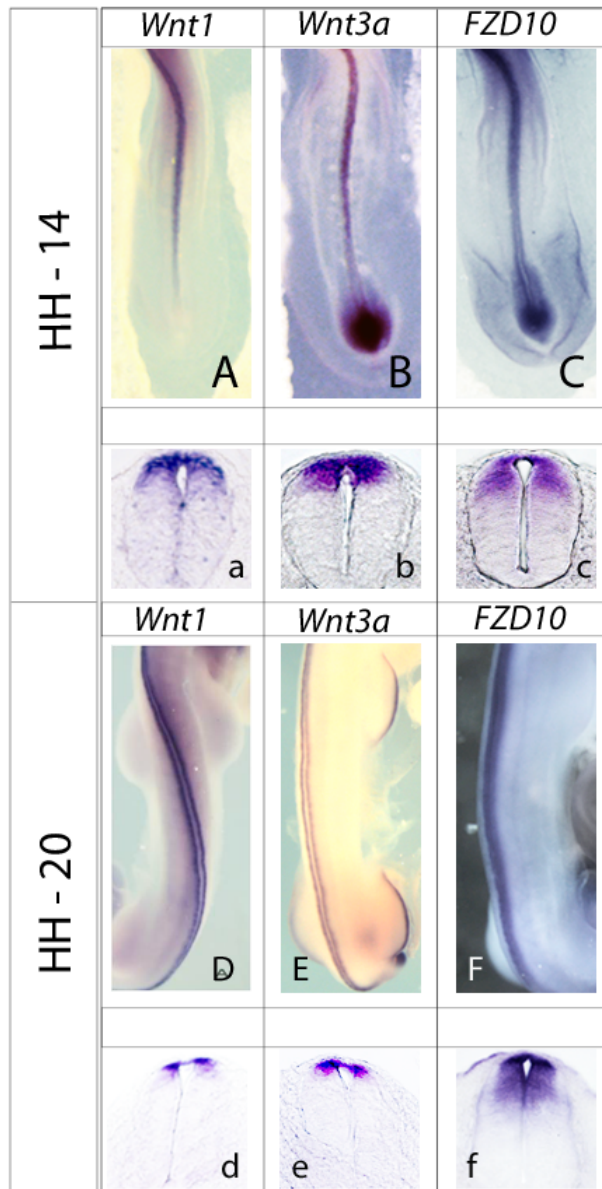
**Fig. 4.3 Comparison of the expression patterns of FZD10 and neural markers at stage 24HH:** (A) Dorsal–ventral sections of the developing spinal cord at stage HH24 stained with DAPI; red circles represent 6 dorsal progenitor domains (dp1-6) whereas green circles represents 5 ventral progenitor domains (p0-2, pMN, p3). (B and G) In situ section shows FZD10 expression. (C and E) Pax3/7 proteins are markers for all 6 dorsal progenitors (red colour in A). (D) Pax6 protein is weakly expressed in the dorsal domain, but the expression was stronger in the intermediate and it is a marker for dp4,5,6 and p0 (ventral progenitor). (F) Schematic representation of differentiated neurons markers expression at HH24; yellow circles (Lhx1/5); white colour (Islet-1). (H) Ngn1 is a proneural basic-helix–loop–helix factor, and a marker for dp2 and dp6-p2 (blue colour in F). (I) Lhx1/5 is a marker for differentiated interneurons dI2,4,6 and V1. (J) Islet-1 is a marker for dI3 in the dorsal spinal cord and it is also a marker for motoneurons (MN) in the ventral spinal cord (white colour in F).

#### **4-5- FZD10 expression overlaps with dorsal Wnts (Wnt1 and Wnt3a) in the spinal cord:**

FZD10 is expressed in the dorsal neural tube including the roof plate where some Wnts are expressed such as Wnt1 and Wnt3a (Fig. 4.4). Wnt1 and Wnt3a are co-expressed in developing spinal cord in chick and mouse, and they are involved in proliferation, neural specification and dorsal-ventral neural tube patterning (Alvarez-Medina et al., 2008; Megason et al., 2002; Muroyama et al., 2002). Here, we attempted to compare and contrast the expression patterns of Wnt1, Wnt3a and FZD10 in chick embryo and in the dorsal spinal cord. Accordingly, the Wnt1 and Wnt3a anti-sense probes were generated and labeled with DIG-UTP and whole mount in situ was performed as mentioned in materials and methods (Chapter2). Then, Wnt1 and Wnt3a expression patterns were analysed in chick embryos by completing an expression profile for each Wnt from stage HH14 to stage HH25 (Fig. 4.4 and appendix. B1,2,3). From whole mount in situ, FZD10 was co-expressed with Wnt1 and Wnt3a in the neural tube at stage HH14 and HH20 (Fig. 4.4A-F and appendix. B1). Also, Wnt3a expression was found in the limb bud and in the tail bud (Fig. 4.4B,C and appendix. B1.2). From whole mount in situ hybridization, it was difficult to observe expression patterns in the dorsal-ventral axis of the spinal cord so the embryos were sectioned using the cryostat and then the sections were mounted, imaged and analyzed (Fig 4.4 and appendix. B1,2,3). At stage HH14, FZD10 showed strong overlapping expression with Wnt1 and Wnt3a in the dorsal domain of the neural tube (Fig. 4.4a,b,c). By stage HH20, Wnt1 and Wnt3a expression patterns were dorsally restricted but FZD10 expression still covered the dorsal part of the spinal cord (Fig. 4.4d,e,f and appendix. B2,3). From the FZD10 expression profile, it is apparent that FZD10 overlaps with Wnt1 and Wnt3a. This data is consistent with a previous report, which was published while this study was under investigation (Galli et al., 2014).

**Fig. 4.4 Expression profile of Wnt1, Wnt3a and FZD10 in chick embryo at HH14 and HH20.**

(A to F) Dorsal views of whole mount embryos after in situ hybridization to show expression patterns of Wnt1, Wnt3a and FZD10 in chick at stage HH14 and HH20. (a-c) Transverse sections of chick neural tube showing Wnt1, Wnt3a and FZD10 expression in the dorsal part of the developing spinal cord at stage HH14 and HH20. (d-f) transverse sections of chick neural tube showing the expression patterns of Wnt1, Wnt3a and FZD10 at stage HH20.



#### **4-6 Summary:**

In this chapter, FZD10 expression was characterized during chick embryo development. At stage HH9, FZD10 is expressed in the midbrain while the neural tube is closing as well as in the posterior region during neurulation. FZD10 expression was found in the developing central nervous system; in the midbrain, the hindbrain and the spinal cord in all stages examined throughout development (Fig. 4.1). In addition, at stage HH24, FZD transcripts were found in the limb bud and the branchial arch 1 and 2. Also, it showed very strong expression in the tail bud throughout the developmental stages. We showed that FZD10 is expressed in the dorsal spinal cord and it continued to be expressed during different time of neurogenesis. FZD10 expression was detected in the dorsal spinal cord and overlapped with well known dorsal progenitor markers such as Pax3/7. FZD10 is also expressed during dorsal interneuron formation as shown by these markers; Islet1 and *lhx1/5*.

Importantly, we preformed a careful observation for the expression patterns of Wnt1, Wnt3a and FZD10 during spinal cord development. Results show that the expression profiles of Wnt1 and Wnt3a is similar. FZD10 expression overlapped with Wnt1 and Wnt3a in the dorsal spinal cord. These dorsal Wnts are required for spinal cord development (Alvarez-Medina et al., 2008; Megason et al., 2002; Muroyama et al., 2002). The expression profile of Wnt1, Wnt3a and FZD10 could suggest that FZD10 has a potential function and interaction with these ligands in the developing spinal cord.

# Chapter 5

**Canonical Wnt signalling regulates FZD10 expression  
during spinal cord development**

## 5-1 Introduction:

Wnt/FZD signalling is involved in embryonic development through regulating cell proliferation, cell polarity, cell differentiation and cell fate specification (Moon et al., 2004; Logan and Nusse, 2004). Canonical Wnt signalling members are required for several developing tissues during embryogenesis. For example, Wnt1 and Wnt3a can regulate induction of myogenesis in somites, neural crest formation, and spinal cord growth and patterning (Galli et al., 2004; Ikeya et al. 1997; Le Dréau and Martí, 2012; Münsterberg et al., 1995). Secreted Wnt1 and Wnt3a are supplied from roof plate and they are implicated in roof plate-dependent specification of interneurons (dII-3) as seen in Wnt1/Wnt3a double mutant mice (Le Dréau and Martí, 2012; Muroyama et al., 2002).

They are also required for neural tube development as seen from several studies; Megason and McMahon (2002), using *in ovo* chick electroporation approaches, reported a mitogenic effect of Wnt1 and Wnt3a on neural progenitors. Many other studies using gain or loss of function in chicken, mice, zebrafish and mice showed a proliferative role of Wnt1 and Wnt3a (Dickinson et al., 1994; Zechner et al., 2003; Chesnutt et al., 2004; Ille et al., 2007; Bonner et al., 2008). Additionally, they have a role in patterning as reported in chick, electroporation assays, co-overexpression of Wnt1 and Wnt3a resulted in the expansion of expression of dorsal genes, while ventrally expressed genes were repressed which indicates the involvement of these ligands in DV patterning (Alvarez-Medina et al., 2008). To date Wnt1 and Wnt3a receptors have not been studied *in vivo* to determine a specific receptor mediating their biological activities in the spinal cord. Therefore, Studying FZD receptors that are expressed in the dorsal neural tube and have a potential interaction with Wnt1 or/and Wnt3a, could lead to the identification of their receptors. This will then allow to

separate their functions and to investigate the mechanism behind their biological activities.

In this study, we examined Wnt1 and Wnt3a expression patterns during neural tube neurogenesis and we found that they are highly expressed during the initiation of neurogenesis in the dorsal neural tube and they have similar expression patterns (Appendix B).

We next analysed FZD10 expression in chick embryos by in situ hybridisation. FZD10 is expressed in the dorsal spinal cord, its expression appears to correlate with dp1-5 progenitor regions and overlaps with expression domains for progenitor markers including Pax3, Pax6 and Pax7. It overlaps with Wnt1 and Wnt3a expression patterns in the dorsal part of the early developing spinal cord. Moreover, it was previously shown that FZD10 acts through canonical Wnt signaling pathway and is required for sensory neuron formation in *Xenopus* (Garcia-Morales et al., 2009). Therefore, we investigated Wnt1/3a and FZD10 interactions in the chick spinal cord by performing *in ovo* electroporation experiments using microinjection of Wnt1/3a expression vectors into the neural tube.

Chapter aims:

-To investigate the effects of Wnt1/3a mis-expression on regulation of FZD7 and 10 in developing spinal cord.

-To study individual roles for Wnt1 and Wnt3a in patterning and in FZD10 regulation.

## **5-2 Wnt1 and Wnt3a regulate FZDs expression in the dorsal-ventral axis of the spinal cord:**

We showed previously FZD10 is expressed in the dorsal domain of the developing spinal cord and FZD7 expression is found in the intermediate-ventral domain (Chapter3). Here, we investigated how Wnt1 and Wnt3a regulate the expression of both FZDs in the developing spinal cord, thus we used in ovo electroporation, immunohistochemistry and in situ hybridization as explained in Methods and Materials (chapter2). Electroporation allowed us to overexpress Wnt1 and Wnt3a ectopically, along the dorsal-ventral axis of the chick spinal cord. We electroporated Wnt1 or Wnt3a construct individually (chapter2) in chick neural tube at stage HH11-12. Embryos were dissected after 24 hours post electroporation and then screened for GFP, with GFP expressed from the same plasmid. Both constructs resulted in GFP expression after electroporation as seen in dorsal view of whole mount pictures of injected embryos (Fig. 5.1A,B). Then, we co-electroporated Wnt1 and Wnt3a in chick neural tube at stage HH11-12. After 24 hours embryos were dissected, fixed and cryosectioned to visualize GFP in transfected side of the neural tube before immunostaining (Fig. 5.1C).

To analyse the effects of Wnt1/3a co-overexpression in neural tube we used neural markers such as Pax7 and Nkx2.2. Pax7 is a marker for six dorsal progenitors and it was ventrally expanded on the transfected side after Wnt1/3a misexpression compared to the control side (Fig. 5.1C). Nkx2.2 is expressed in the ventral neural tube and it was severely repressed in the transfected side compared to control side (Fig. 5.1C). These results are consistent with a previous report showing that Wnt1 and Wnt3a co-electroporation in neural tube affect neural progenitors patterning (Alvarez-Medina et al., 2008).

We next investigated FZD10 and 7 expression following Wnt1/3a overexpression; embryos showed strong GFP expression after co-electroporation were proceeded for whole mount in situ to analyse changes in the expression patterns. We found that FZD10 expression was strongly upregulated and ventrally expanded on the electroporated side of neural tube (Fig. 5.1D). Suggesting that dorsal Wnts activate expression of FZDs such as FZD10 in the dorsal spinal cord. Conversely, FZD7 expression was lost in the intermediate domain and ventrally restricted on the electroporated side of neural tube compared to the control side (Fig. 5.1E). This indicates that expression of ventrally expressed FZDs (FZD7) is repressed by dorsally expressed Wnts (Wnt1/3a) in the developing spinal cord.

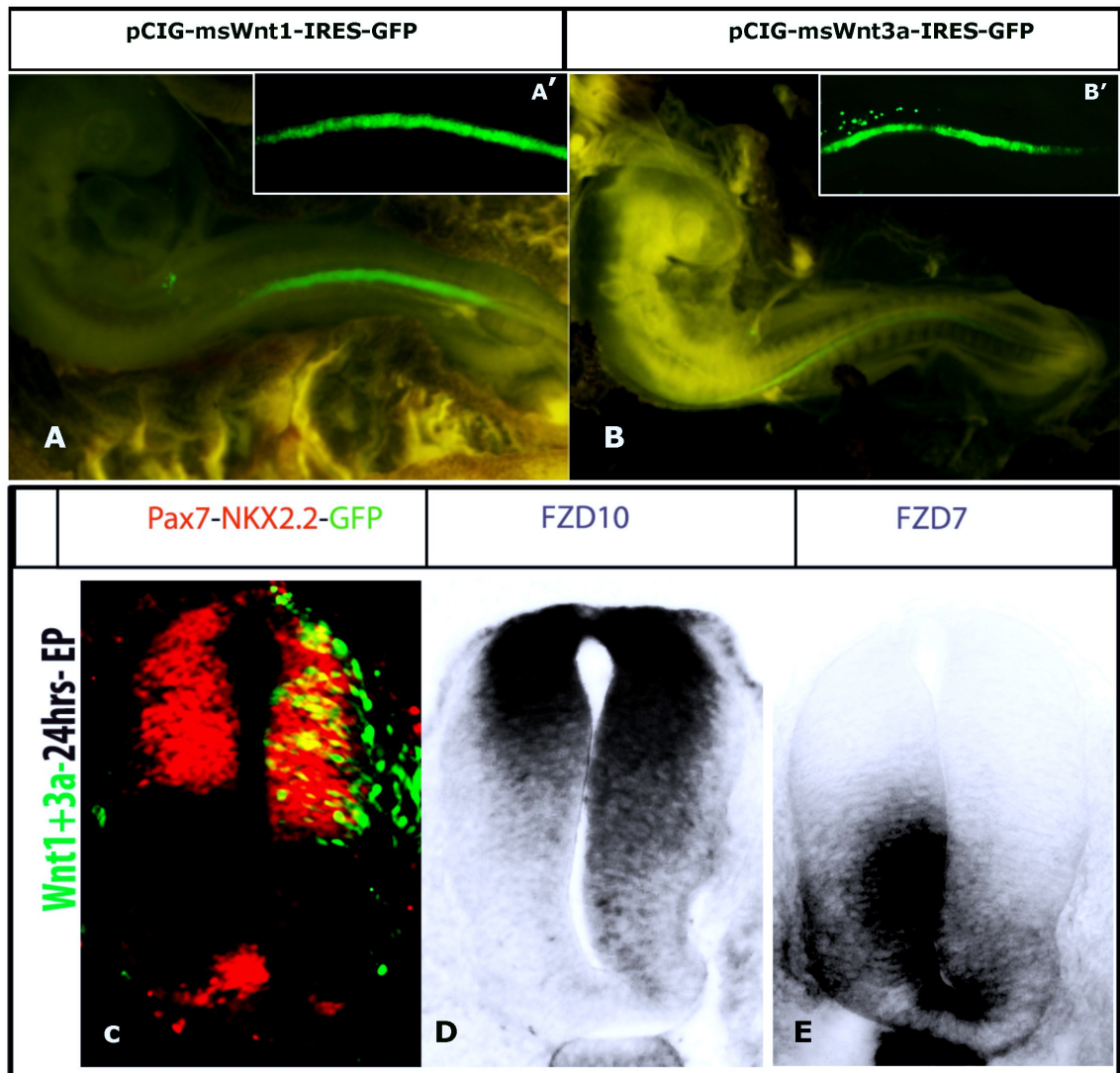


**Fig. 5.1 Wnt1 and Wn3a affect FZD10 and 7 expression in chick spinal cord (24hours PE).** (A,B) Dorsal views of whole mount pictures of electroporated embryos show GFP expression in chick neural tube. (A',B') Green colour shows GFP expression after Wnt1 and Wnt3a electroporation indicating successful transfection. (C) Cross section of the neural tube shows GFP expression (green) in the electroporated side, Pax7 expression is ventrally expanded (red), Nkx2.2 expression was repressed in the ventral (red) (n;). (D) FZD10 expression is ventrally expanded. (D) FZD7 expression is lost in the intermediate region and repressed in the ventral neural tube. GFP staining after FZD7/10 in Situ was performed, but GFP antibody did not work, it may be important to be repeated in the future.

Embryos number, (C, n=8/9), (D, n=13/15), (E. n=12/15). EP side will always be shown on the right in this experiment.

### **5-3 Wnt1 and Wnt3a affect spinal cord patterning and Wnt1 overexpression up-regulates FZD10 expression:**

We found that FZD10 is expressed during spinal cord neurogenesis and its expression overlaps with Wnt1 and Wnt3a (Chapter 4). It has been shown that Wnt1 and Wnt3a are required for proper development of spinal cord (Le Dréau and Martí, 2012). Here, we examined the role for each individual Wnt in patterning and in FZD10 regulation. To do this, we electroporated Wnt1 and Wnt3a individually in chick neural tube at stage HH11-12 and then re-incubated the embryos for 48 hours. The embryos were screened for GFP, fixed and cryosectioned (Fig. 5.2A,B,C).

GFP was visualised in all sections before staining, and we observed that electroporated side of spinal cord was bigger than control side in Wnt1 or Wnt3a electroporated embryos (Fig. 5.2D,E,G). This could be a result of high rate of proliferation on the electroporated side as shown in a previous report (Megason and McMahon, 2002). Then, we used immunohistochemistry to analyze the effects of Wnt1 and Wnt3a misexpression in patterning and neurogenesis. We found that ectopic expression of Wnt1 or Wnt3a led to expansion of dorsal progenitor cell domains. This was evidenced by the expression domains of Pax6 and Pax7, which were ventrally extended on the transfected side when compared to the control side (Fig. 5.3A,B and Fig. 5.4A,B). Conversely, the Nkx2.2 expression domain was repressed and restricted to the ventral part of the spinal cord (Fig. 5.3C and Fig. 5.4C). These results demonstrate that both Wnts produce same phenotype which affect neural progenitor patterning in the spinal cord.

We next investigated the effect of Wnt1 or Wnt3a misexpression on formation of dorsal interneurons. Therefore, we analyzed the expression pattern of Islet-1, a marker for dorsal interneurons 3 (chapter 4). We found that Islet-1 expression domain was broader

on the transfected side, indicating that more differentiated neurons were being generated after Wnt1 or Wnt3a electroporation (Fig. 5.3D and Fig. 5.4D). This suggests that Wnt1 and Wnt3a promoted neurogenesis of dorsal interneurons 3.

Then, we analyzed the effect of dominant-negative (dn) Wnt3a electroporation in spinal cord. We previously generated chicken dnWnt3a by deleting C-terminal and subcloned it into IRES-GFP expression vector (Yue et al., 2008). Dominant-negative Wnts are presumed to function extracellularly and to block Wnt signaling through preventing Wnts from binding to their receptors and/or directly inhibit wild-type Wnt ligands (Hoppler et al., 1996). Therefore, we examined whether dnWnt3a electroporation in the neural tube would affect proliferation and patterning. dnWnt3a was electroporated into neural tube at HH11-12 and the embryos were dissected after 48 hours to analyze the phenotype. The embryos had strong GFP expression were fixed and cryosectioned (Appendix B. Fig. 1A,B). We found that the size of the spinal cord was severely reduced on the electroporated side, suggesting that rate of cell proliferation was reduced (Appendix B. Fig. 1C). To investigate the effect of dnWnt3a on patterning, immunohistochemistry for Pax7 was used. We observed that Pax7 expression was repressed and its domain was reduced (Appendix B. 1C,D). Because of time limitations the dnWnt phenotype was not characterized further.

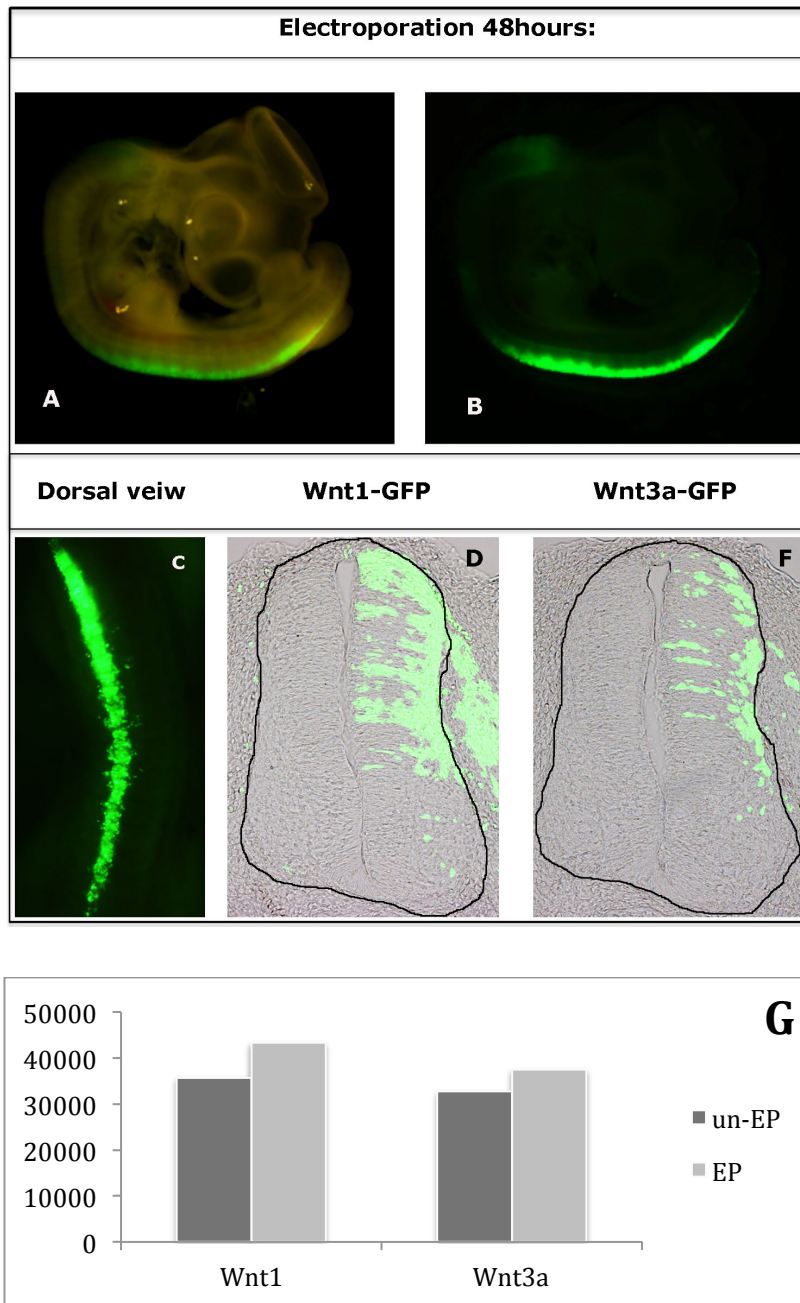


**Fig. 5.2 Wnt1 and Wn3a electroporation in chick spinal cord after 48hours.** (A,B) Whole mount picture of electroporated embryo showing GFP expression after Wnt1 or Wnt3a electroporation in spinal cord. (C) A dorsal view of electroporated embryo. (D,E) Cross section of transfected spinal cord with Wnt1 or Wnt3a plasmid. Embryos number, (D, n=5), (E, n=4). (G) Measurement of un-electroporated and electroporated half side of neural tubes after Wnt1 or Wnt3a transfection.

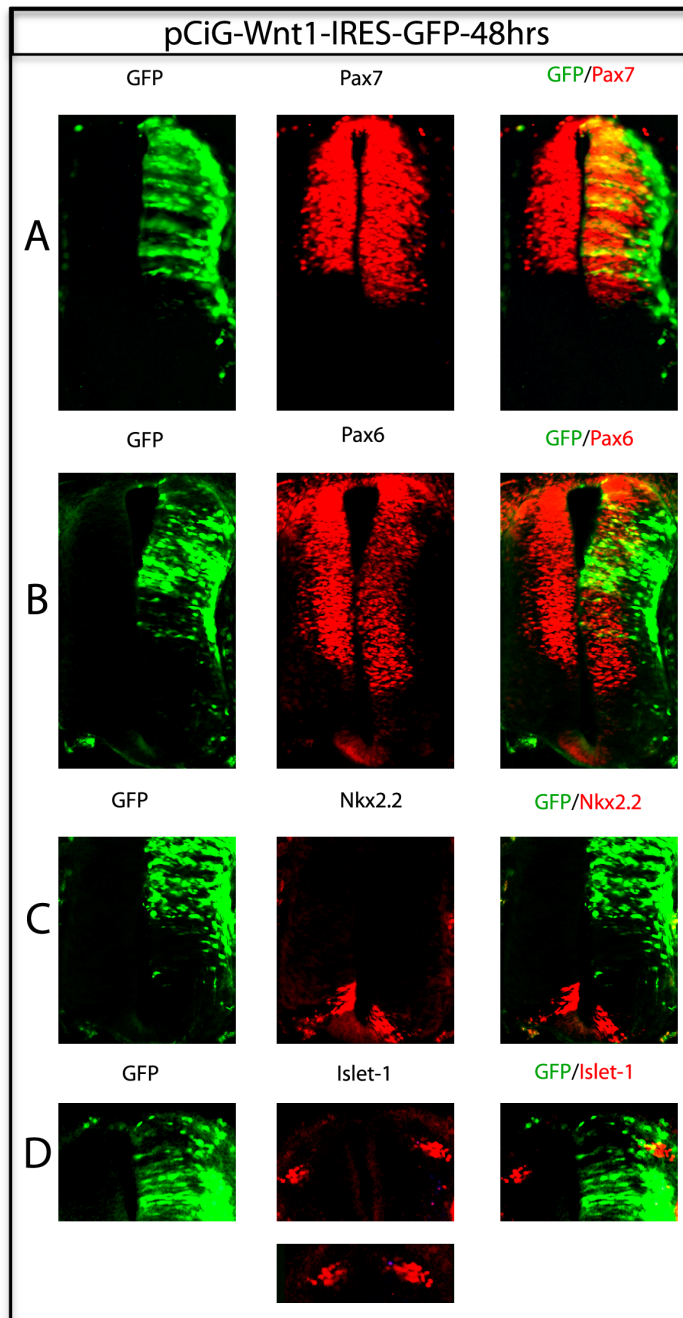


**Fig. 5.3 Analysis of protein expression patterns after Wnt1 misexpression in spinal cord.** (A) Shows GFP expression in the transfected side (green), Pax7 expression and its expansion in experimental side of the spinal cord. (B) Pax6 is ventrally extended in the transfected side following ectopic expression of Wnt1 as marked by GFP. (c) Nkx2.2 is ventrally shifted and repressed. (D) Islet-1 expression domain is increased in the transfected side. Embryos number was 12/14.

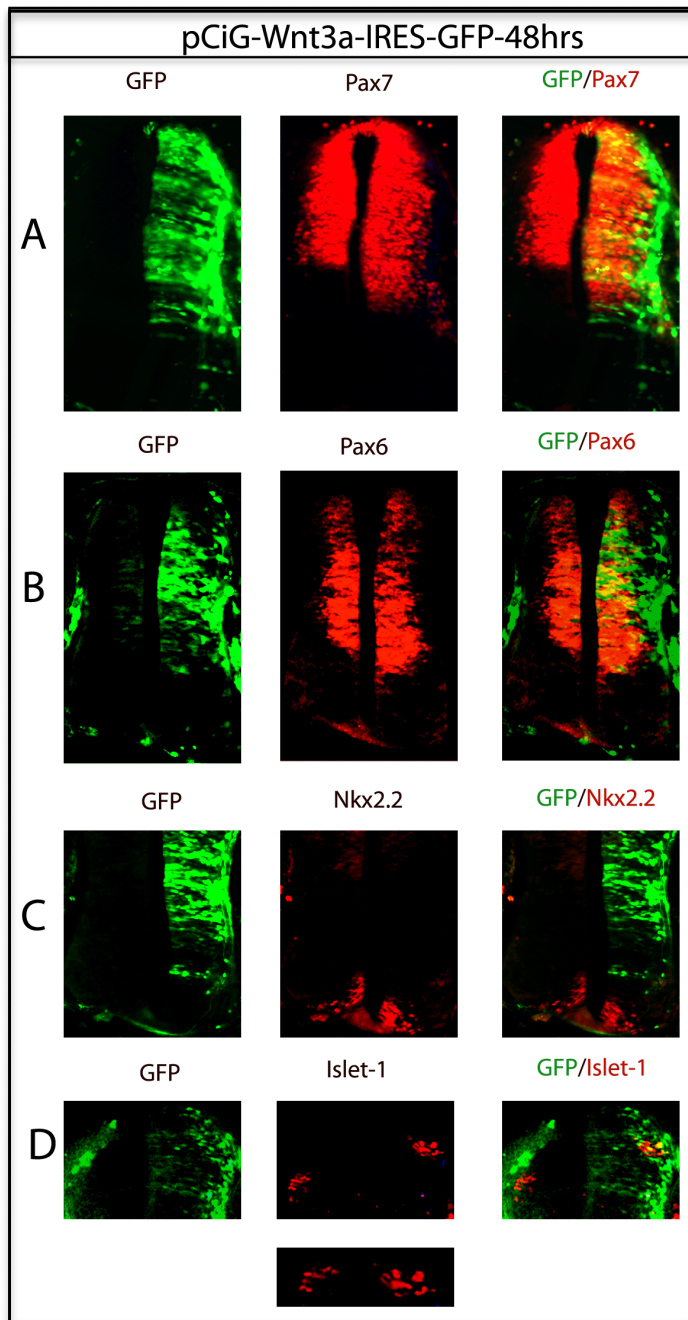


**Fig. 5.4 Analysis of protein expression patterns after Wnt3a misexpression in spinal cord.** (A) Shows GFP expression in the electroporated side (green), Pax7 expression is expanded following ectopic expression of Wnt3a. (B) Pax6 is ventrally extended in the transfected side. (c) Nkx2.2 is ventrally shifted and repressed. (D) Islet-1 expression domain is increased in the transfected side when compared to the control. Embryos number was 11/14.

-As FZD10 is expressed in dorsal spinal cord and its expression was strongly expanded ventrally after Wnt1/3a co-electroporation. To determine the individual effects of Wnt1 and Wnt3a electroporation on FZD10 expression, the neural tube was electroporated at stage HH11-12 and the embryos were re-incubated for 48hours. The embryos were dissected and screened for GFP and only strongly transfected embryos were hybridised with FZD10 probe to assess potential changes in expression pattern. We observed that FZD10 expression was broader and extended ventrally after Wnt1 overexpression on the electroporated side when compared to non-electroporated side (Fig. 5.5A,B). Also, we noticed that FZD10 expression was strongly increased in the roof plate (Fig. 5.5B). Interestingly, FZD10 expression was not affected after Wnt3a electroporation (Fig. 5.5C,D). These data suggest that Wnt1 overexpression led to up-regulation of FZD10 expression in the dorsal neural tube.

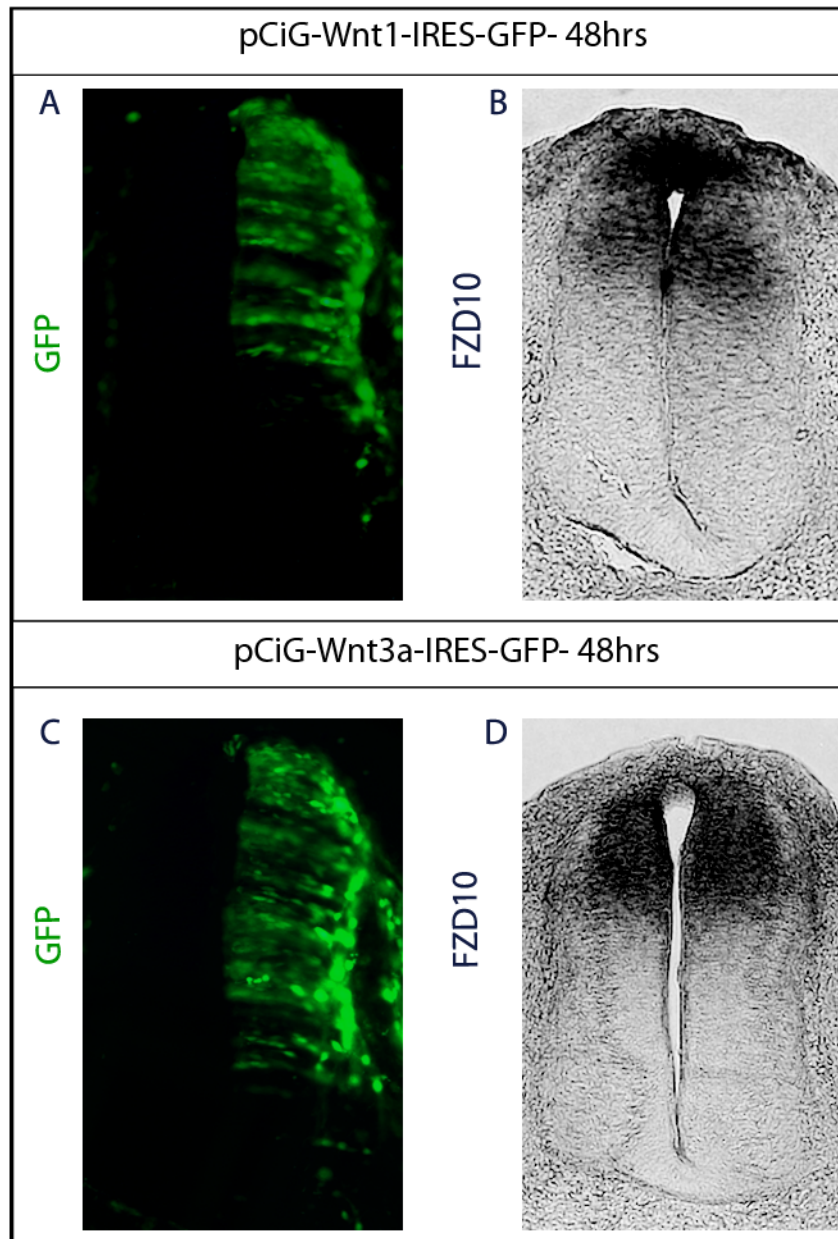


**Fig. 5.5 FZD10 expression is up-regulated following Wn1 misexpression.** (A) GFP expression in the electroporated side indicating Wnt1 is ectopically expressed. (B) FZD10 expression is ventrally expanded and increased in the roof plate region. (c) GFP expression shows Wnt3a misexpression along the dorsal-ventral axis of the spinal cord. (D) FZD10 expression was not changed after Wnt3a misexpression. (B,D) Green arrows points to a curve in the ventral spinal cord that always presents following Wnt1 or Wnt3a electroporation as result of overgrowth. Embryos number, (B, n=13/15), (D, n=12/15).

#### **5-4 Summary:**

In this chapter, we investigated the effects of dorsally expressed Wnts on patterning and on FZDs regulation in spinal cord. We found that co-misexpression of Wnt1 and Wnt3a led to expansion of dorsal genes as shown by Pax7 immunostaining (Fig. 5.1C). By contrast, the ventrally expressed gene Nkx2.2 was repressed (Fig. 5.1C). These data are in agreement with other studies, which reported the same observations (Alvarez-Medina et al., 2008). We also showed that FZD10 expression was expanded to the ventral spinal cord following Wnt1/3a co-electroporation, indicating that FZD10 expression is positively regulated by canonical Wnt signaling. Conversely, FZD7 expression was lost in the intermediate-ventral spinal cord. This suggests that the expression of FZD7 and potentially other ventrally expressed FZD receptors is inhibited by secreted Wnts from the dorsal spinal cord.

It has been shown that electroporation of Wnt1 or Wnt3a increases proliferation in spinal cord through controlling cell cycle regulators (Megason and McMahon, 2002). Also, Wnt1/3a co-electroporation affects patterning by antagonizing Shh activity through controlling Gli3 transcription (Alvarez-Medina et al., 2008). Here, we electroporated Wnt1 and Wnt3a individually into the neural tube and we found that both Wnt1 and Wnt3a are able to regulate patterning of neural progenitors along dorsal-ventral axis and stimulate neurogenesis of dorsal interneurons 3 (Fig. 5.3 and Fig. 5.4).

Moreover, we attempted to determine which Wnt affects FZD10 regulation; embryos were electroporated with Wnt1 and Wnt3a individually. We found that FZD10 expression was upregulated and ventrally extended after Wnt1 overexpression but its expression pattern was not affected following Wnt3a overexpression. This suggests that the FZD10 promoter may react to a Wnt1 signal and may indicate that this receptor

mediates Wnt1 function in the dorsal spinal cord, potentially creating positive feed-back interaction. Also, FZD10 promoter regions could be analysed using bioinformatics tools to identify cis-elements, such as transcription factor binding sites. These data encouraged us to examine Fzd10 function and interactions during spinal cord development (Chapter6). Wnt3a may activate the expression of other different FZD receptors in the spinal cord such as FZD1 and FZD3. For example, it has been shown that Wnt3a can mediate canonical Wnt signaling through FZD1 in hippocampal neurons and PC12 cells (Chacon et al., 2008).

# Chapter 6

**Investigating FZD10 function and its interactions  
with Wnt1 and Lrp6 during spinal cord  
development**

## 6-1 Introduction

FZD10 is expressed in the neural tube in many species, including *Xenopus* and chicks (Galli et al., 2014; Garcia-Morales et al., 2009; Wheeler and Hoppler, 1999; Kawakami et al., 2000a). FZD10 expression has been found in the limb buds of chick embryos (Chapter 4; Kawakami et al., 2000a). It appears to interact with Wnt7a and overlaps with Shh expression in the dorsal-posterior-distal mesenchyme in the limb bud, where it was also shown that Shh and Wnt7a induce and maintain FZD10 expression. These results suggest that FZD10 interacts with Wnt7a and plays a positive role in limb bud development. Furthermore, in *Xenopus* animal cap assays, FZD10 synergises with Wnt7a but not with Wnt3a and induces Wnt-target genes, such as Siamios (Kawakami et al., 2000b).

Furthermore, Nikaido et al. (2013) found that FZD10, FZD7a and FZD7b are involved in the regulation of epiboly movements and mesoderm differentiation in zebrafish.

Work from the Wheeler lab on *Xenopus*, showed that FZD10 is expressed in the dorsal neural ectoderm and neural folds in the region where primary sensory neurons develop (Garcia-Morales et al., 2009). Their investigation into loss of function in *Xenopus* showed that FZD10 is required for the formation of sensory neurons. Furthermore, in mouse P19 cells, retinoic acid was used to induce neural differentiation; overexpression of *Xenopus* FZD10 leads to an increase in the number of neurons generated, while siRNA knockdown of endogenous mouse FZD10 inhibits neurogenesis. FZD10 injection results in partial axis formation and interacts with Wnt1 and Wnt8 but not with Wnt3a, as shown in synergy assays. Clearly, these data indicate that FZD10 functions through canonical Wnt signalling and is a potential receptor for Wnt1. They, therefore, indicate that FZD10 mediates canonical Wnt signalling to determine sensory neural

differentiation in *Xenopus* and neuron development in mouse P19 cells (Garcia-Morales et al., 2009).

In the present study, we found that Wnt1 overexpression up-regulated FZD10 expression in the spinal cord (Chapter 5). Therefore, we investigated FZD10 function in dorsal-ventral patterning of the spinal cord as well as its interactions in vivo with Wnt1/3a and Lrp6; using loss and gain of function experiments in chick neural tubes.

Chapter aims:

- To study the role of FZD10 during spinal cord development by using loss and gain of function approaches.
- To examine the requirement of FZD10 for Wnt1 and/or Wnt3a in the spinal cord in vivo using rescue experiments.
- To investigate Lrp6 function and potential interaction with FZD10 and Wnt1 in the spinal cord using gain of function studies.

## **6-2 Knockdown of FZD10 led to a decrease in cell proliferation in the spinal cord**

To study the function of FZD10 in spinal cord development, we obtained three short-hairpin vectors (sh-RNA) that were specifically designed against chick FZD10 (Chapter 2). FZD10 sh-RNA plasmids (pRFP-C-RS) were electroporated into chick neural tubes at stage HH11-12. After 48 hours following electroporation, embryos were screened for RFP expression and processed for in situ hybridization in order to assess FZD10 knockdown. Each sh-RNA vector was electroporated individually. Electroporation of FZD10 sh-RNA vectors B and C resulted in a strong reduction in FZD10 expression on the electroporated side of the spinal cord when compared to the unelectroporated side (Fig. 6.1 D, E, F). This indicates that endogenous FZD10 transcripts were knocked down. Also, RT-PCR or qRT-PCR could be useful to detect FZD10 knockdown, and rescue FZD10 knockdown with mouse or *Xenopus* FZD10 in the future. Electroporation of the scrambled sh-RNA vector did not affect FZD10 expression, so it was used as a negative control (Fig. 6.1 A, B, C).

Next, we analysed the effects of FZD10 knockdown on the spinal cord. We observed that the electroporated side of the spinal cord was often smaller and thinner following knockdown of FZD10 by sh-RNA (Fig. 6.2 D, E). This suggested that proliferation could be affected in the ventricular zone where neural progenitors are located. Therefore, we used immunostaining for phosphor-histone H3 (pH3), which is a marker for mitotic cells, to assess proliferation along the dorso-ventral axis of the spinal cord after FZD10 knockdown. The number of pH3 positive cells in the spinal cord was counted on the experimental and control sides of embryos electroporated with FZD10 sh-RNAs or scrambled sh-RNA, and statistical analysis was performed using Excel and

a Student's t-test (paired). The statistical analysis showed that the number of mitotic cells was significantly decreased 1.42-fold ( $p < 0.01$ , Student's t-test) on the experimental side of the spinal cord (Fig. 6.2 F). Conversely, scrambled sh-RNA electroporation did not lead to a significant change in the number of pH3 positive cells on either side of the spinal cord (Fig. 6.2 C). Thus, FZD10 knockdown led to a reduction in cell proliferation in the ventricular zone of the spinal cord.

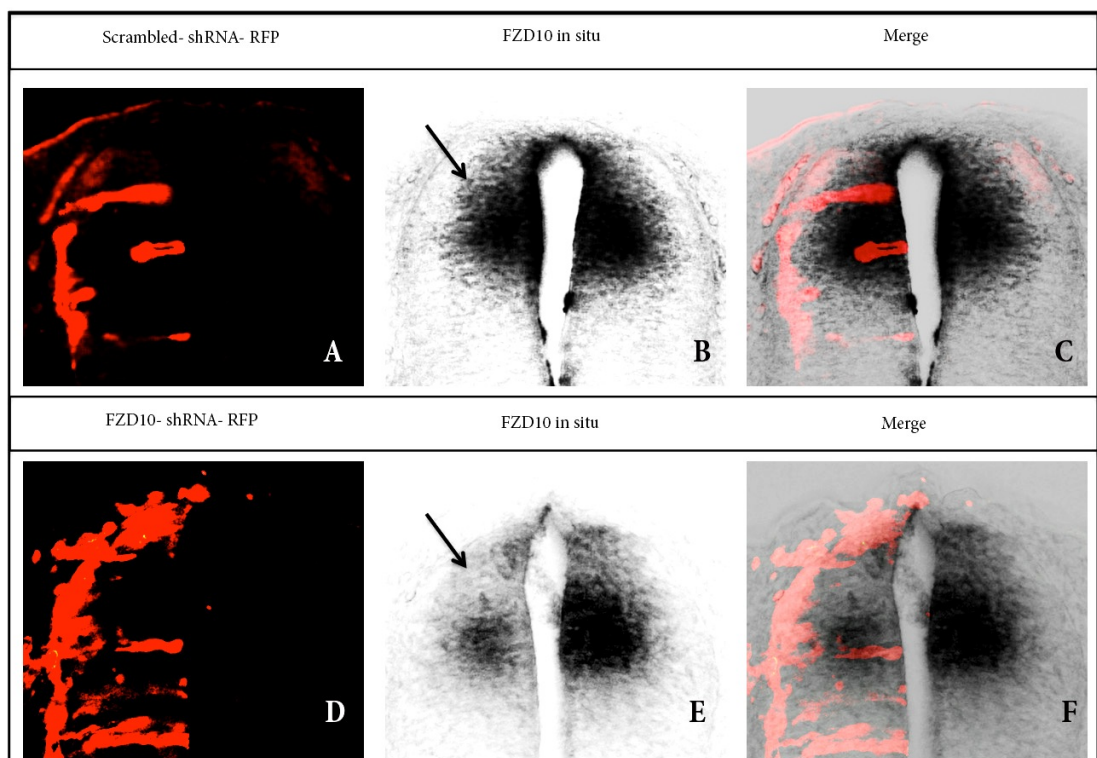


**Fig. 6-1 FZD10 was knocked down after electroporating FZD10 sh-RNA vectors in the spinal cord.** (A) RFP expression in the electroporated side of the spinal cord. (B, C) FZD10 expression was not affected after scrambled sh-RNA electroporation. (D) RFP expression after electroporating FZD10 sh-RNA vectors. (E, F) FZD10 expression was strongly inhibited on the experimental side of the spinal cord in electroporated embryos. RFP was detected by RFP antibody in cryosections after in situ hybridization.

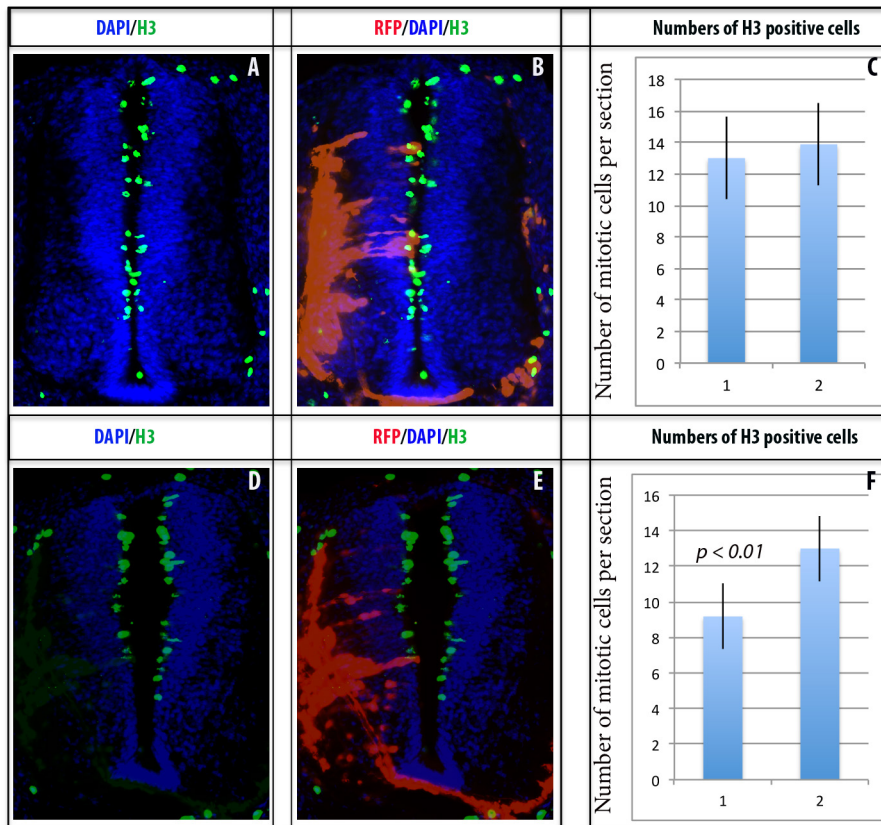


**Fig. 6-2 Knockdown of FZD10 led to a reduction in spinal cord size and a decrease in proliferative cells.** (A, B) Cross sections of spinal cord stained with DAPI and phosphor-histone H3, showing that the sizes of the experimental and control sides of the spinal cord were not affected after electroporating scrambled sh-RNA vector, as shown by RFP expression. (D, E) the size of the electroporated half of the spinal cord was smaller than the control, as shown by DAPI staining in the spinal cord electroporated with FZD10 sh-RNA vector: blue, DAPI; green, pH3; red, RFP.

Proliferative cells were stained with pH3 and counted in the experimental and control sides of the spinal cord electroporated with scrambled sh-RNA or FZD10 sh-RNA. Statistical analysis was performed using Excel and a Student's t-test. (C) The average number of pH3 positive cells per section on both sides of the spinal cord electroporated with scrambled sh-RNA; there was no significant difference between the experimental (column 1) and control (column 2) sides of the spinal cord. There were 5 embryos and 32 sections were analysed. (F) The average number of pH3 positive cells per section in the spinal cord electroporated with FZD10 sh-RNA vector; enumeration of the pH3 positive cells showed a statistically significant decrease in proliferative cells on the electroporated side (column 1) when compared to the control side (column 2) of the spinal cord after FZD10 knockdown. 7 embryos and 53 sections were analysed.

### **6-3 Knockdown of FZD10 affected neurogenesis in the spinal cord**

Next, we investigated the effect of FZD10 knockdown on the dorsal-ventral patterning and neurogenesis in the spinal cord by using neural markers that overlap with FZD10 expression (Chapter 4). To achieve this, FZD10 sh-RNA vectors were introduced by *in vivo* electroporation in the neural tubes at HH11-12, and the electroporated embryos were cryosectioned at 24 or 48 hours. The sections were screened for RFP expression and then the phenotypes were assessed by immunohistochemistry for Pax6 and Pax7. After 24 hours PE, we observed that the Pax7 expression domain had shifted slightly dorsally in the experimental side of the embryos transfected with FZD10 sh-RNA vector, whereas it was not affected in the control side (Fig. 6.3E). Scrambled sh-RNA electroporation did not exhibit any effect on Pax7 expression in either side of the spinal cord (Fig. 6.3B).

After 48 hours Post-electroporation of FZD10-shRNA, we did not observe a consistent effect on the expression domains of Pax6 and Pax7 following FZD10 knockdown (Fig. 6.4A-D'). However, we noticed that the expression domains of Pax6 and Pax7 were smaller in the electroporated side as compared to the control side (Fig. 6.4A-D'). This could be a result of a reduction in proliferation, as previously shown.

Subsequently, we assessed whether FZD10 knockdown would affect neurogenesis in the spinal cord. To investigate the effect of FZD10 on neurogenesis, embryos were electroporated into neural tubes at stage HH11-12 with a vector encoding sh-RNA against cFZD10 and expressing RFP as a reporter. The embryos were analysed after 48 hours and immunostained for Lhx1/5 and Tuj-1, markers for differentiated neurons. Lhx1/5 expression was strongly reduced on the electroporated side of the spinal cord compared to the control (Fig. 6.4F,F').

After 24 hours, Tuj-1 expression was reduced along the dorsal-ventral sides of the spinal cord in the embryos electroporated with FZD10 sh-RNA (Fig. 6.3H). After 48 hours post-electroporation, we still observed a reduction in Tuj-1 expression on the electroporated side of spinal cord especially in the dorsal domain when compared with the control (Fig. 6.4H,H'). In contrast, scrambled sh-RNA electroporation did not affect expression of any neural markers used (Fig. 6.4). Therefore, knockdown of FZD10 inhibited neurogenesis in the spinal cord.

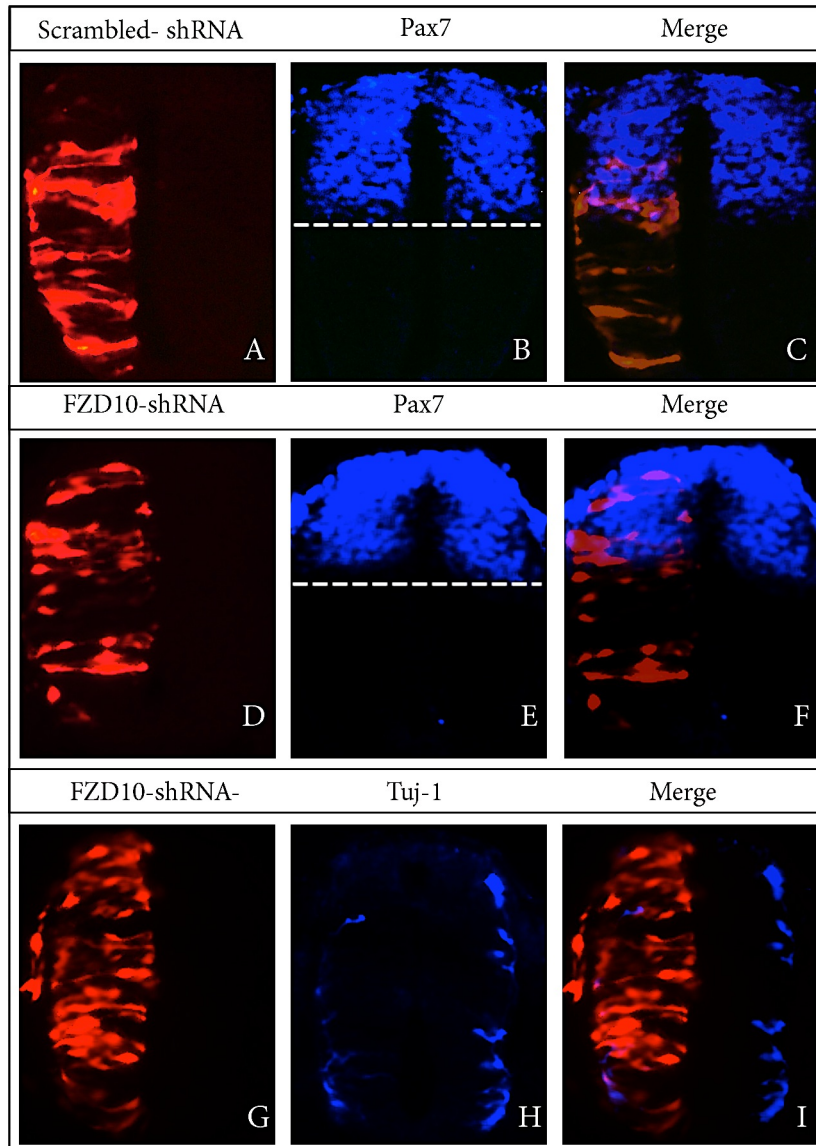


**Fig. 6.3 FZD10 knockdown affects neural markers in spinal cord (24hours PE).** Scrambled sh-RNA vector was introduced into neural tubes at stage 11-12 and the effect was analysed after 24 hours using dorsal marker; Pax7, (A-C) shows that the expression domain of Pax7 was not affected in either side of the spinal cord. (D-F) Pax7 expression was slightly reduced in the experimental half of spinal cord eletroporated with FZD10 sh-RNA vector. (G-I) Tuj-1 expression was severely repressed in the experimental half of spinal cord, suggesting that FZD10 is required for the differentiation of interneurons in chick. Number of embryos was 3 and more than 10 sections were analysed for each markers.

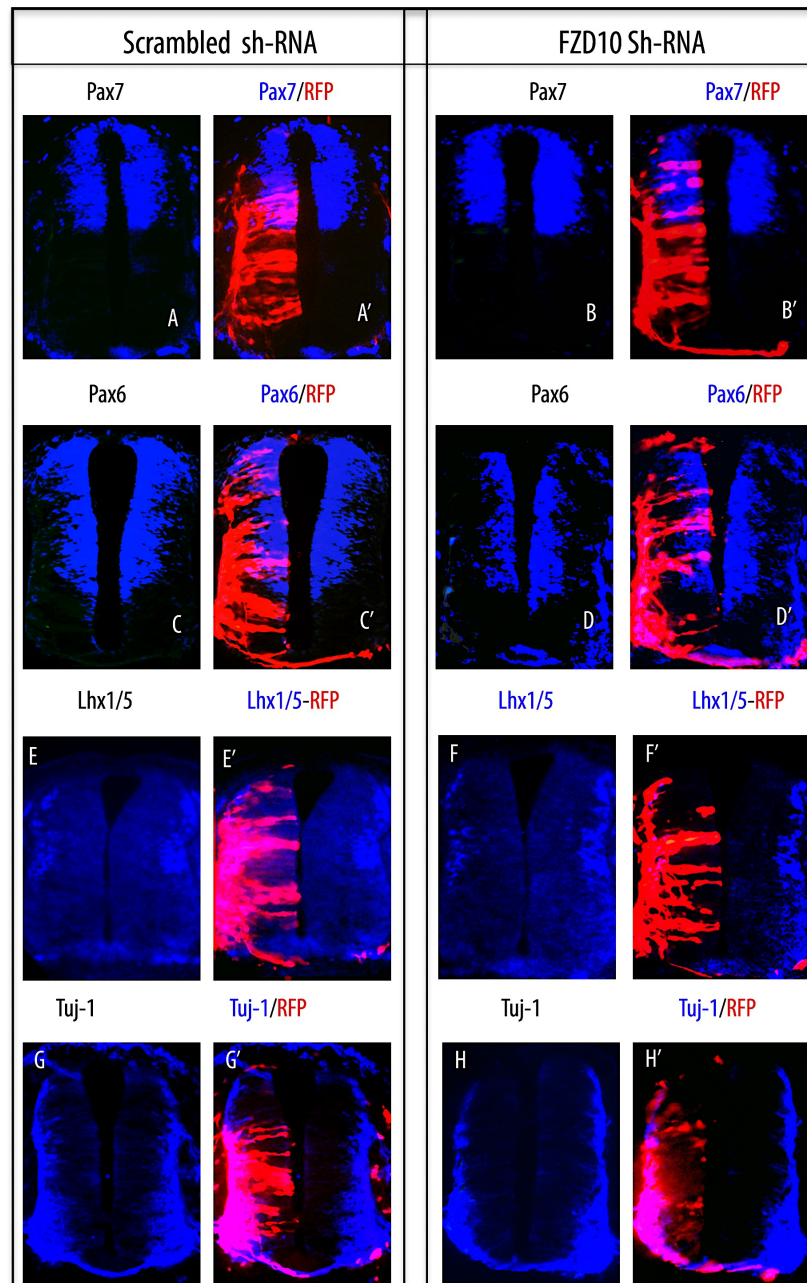


**Fig. 6.4 Effects of FZD10 knockdown on neural marker expression after 48hours post-electroporation.** Scrambled and FZD10 sh-RNA vectors were electroporated into neural tubes and these vectors expressed RFP as reporter for successful transfection. (A,A') Pax7 expression after Scrambled shRNA-vector electroporation. (B,B') Pax7 expression domain was moderately reduced on the electroporated side of the spinal cord. (C,C') Pax6 expression was not affected after scrambled sh-RNA, but it was slightly shifted dorsally on the electroporated side of the spinal cord after electroporation with the FZD10 shRNA-vector. (E,E') Lhx1/5 expression in embryos electroporated with scrambled shRNA. (F,F') Lhx1/5 expression was repressed after FZD shRNA-vector electroporation. (G,G') Tuj-1 expression. (H,H') Tuj-1 was inhibited in the dorsal domain of spinal cord electroporated with FZD10 shRNA-vector. Embryos number (N) (Pax6/7=12/13) (Lhx1/5 and Tuj-1=7/8). If time had allowed, these sections would have been analysed by ImageJ software to count cells or measure area.

#### **6-4 Knockdown of FZD10 rescued the Wnt1 overexpression phenotype:**

FZD10 was shown to function through canonical Wnt signalling as injection of *Xenopus* FZD10 into the ventral marginal zone (VMZ) results in partial axis formation in early *Xenopus* embryos and the phenotype of FZD10 knockdown can be rescued by  $\beta$ -catenin in *Xenopus* embryos (Garcia-Morales et al., 2009). Therefore, we further investigated FZD10 integration in canonical Wnt signalling and its involvement in spinal cord development, we tested the requirement of FZD10 for Wnt1 and/or Wnt3a in the spinal cord using in vivo electroporation. We performed rescue experiments by co-electroporating Wnt1 or Wnt3a with shRNA vectors (scrambled shRNA or FZD10 shRNA) in neural tubes at stage HH11-12 (Fig. 6.5). The embryos were analysed after 48 hours and neural markers (Pax6/7) that are regulated by canonical Wnt signalling were used to assess the phenotypes (Fig. 6.6). Co-electroporation of scrambled shRNA with Wnt1 did not result in any change in the Wnt1-induced phenotype; Pax6 and Pax7 were ventrally expanded as before (Fig. 6.6 A, C and Fig. 5.3). In contrast, co-electroporation of FZD10 shRNA with Wnt1 attenuated the effect of Wnt1 overexpression; expression domains of Pax6 and Pax7 on the electroporated side were comparable to the control side in the spinal cord (Fig. 6.6 B, D). Also counting cells would be good but the time had not allowed. Moreover, the Wnt1 phenotype was rescued from the majority of embryos (80%) (Fig. 6.8). These data suggest that FZD10 knockdown rescues the Wnt1-induced phenotype and that the Wnt1 signal is mediated through FZD10 in the spinal cord.

We next examined whether FZD10 knockdown would affect the phenotype induced by Wnt3a overexpression. We applied the same experimental conditions used with Wnt1 to remain consistent and to avoid variability due to differences in the approach (Fig. 6.5).

We found that the co-electroporation of scrambled shRNA or FZD10 shRNA with Wnt3a did not seem to affect the phenotype of Wnt3a overexpression as the expression domains of Pax6 and Pax7 were ventrally expanded in both experiments (Fig. 6.7 A, B, C, D). In addition, Wnt3a-induced phenotype was not affected in a majority of the embryos examined (81%) after FZD10 knockdown (Fig. 6.8). These results indicate that FZD10 knockdown did not interfere with the Wnt3a-induced phenotype and that Wnt3a may function through different FZD receptors, such as FZD1 and FZD3, in the spinal cord. Consistent with this hypothesis, Wnt3a is capable of activating canonical Wnt signalling through FZD1 in P12 cells (Chacon et al., 2008).

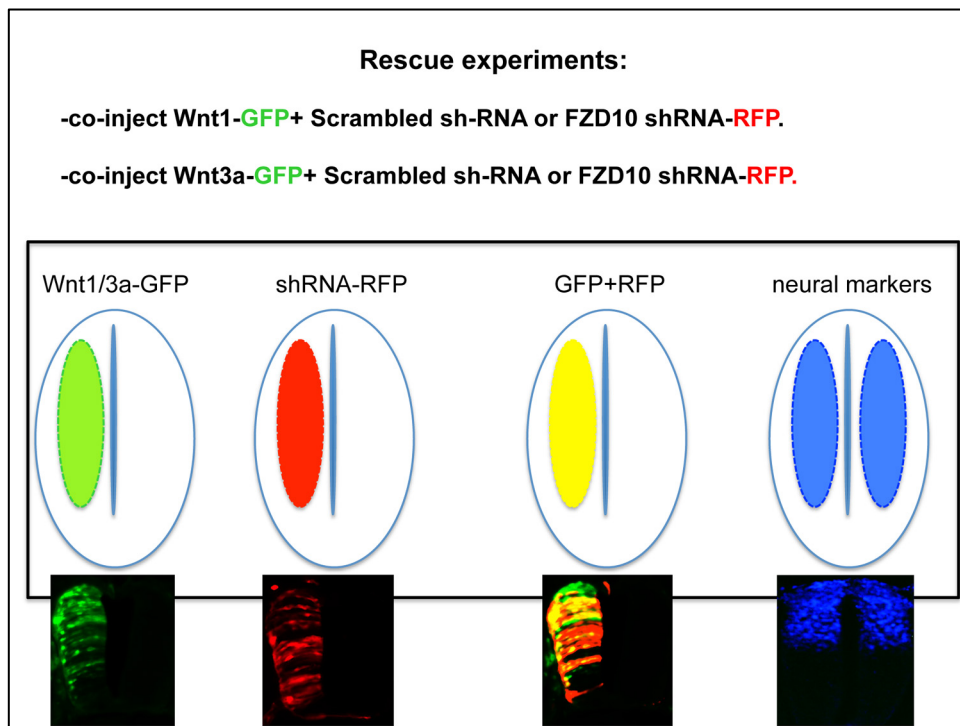


**Fig. 6-5 Schematic illustration of rescue experiments in the spinal cord.** To investigate the requirement of FZD10 for Wnt1 biological activity, embryos were electroporated with pCiG-Wnt1-IRES-GFP/ pCiG-Wnt3a-IRES-GFP on their own or with and shRNA- RFP vectors (scrambled shRNA or FZD10 shRNA) at HH11-12. Embryos were analysed and cryosectioned after 48 hours. Then, neural markers were used to assess the effects on the expression patterns of the neural markers, Pax6 and Pax7. We ensured the consistency of experimental conditions in all experiments. Therefore, experiments were preformed in parallel on the same days.

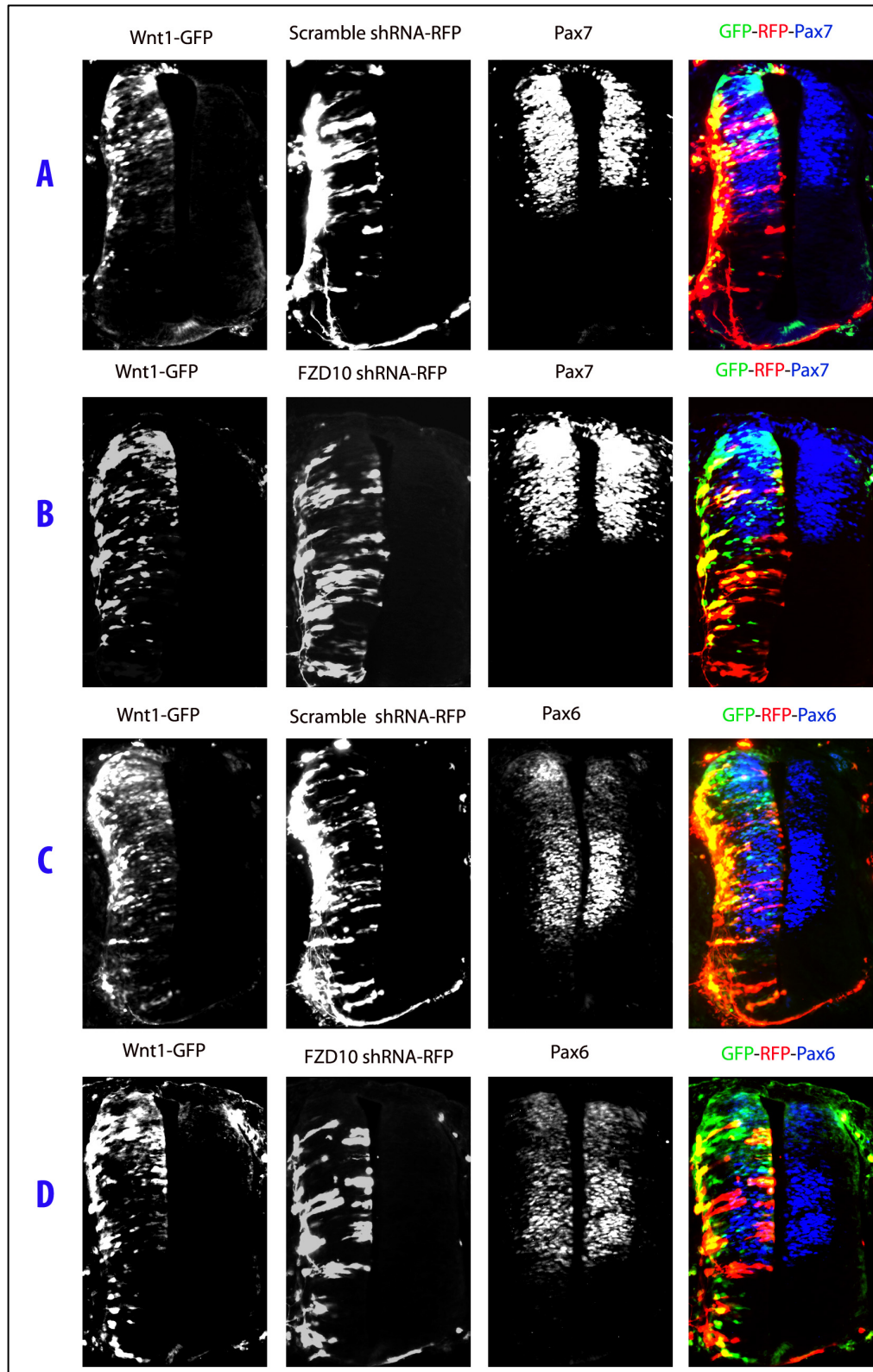


**Fig.**

**Fig. 6.6 FZD10 knockdown by shRNA rescues the Wnt1-induced phenotype.** Scrambled shRNA electroporation with Wnt1 did not affect the phenotype; Pax6 and Pax7 were ventrally expanded (A, C), whereas FZD10 sh-RNA electroporation with Wnt1 inhibited the Wnt1-induced phenotype and prevented (B) or reduced (D) the ventral expansion of the expression domains of Pax6 and Pax7 in the electroporated side of the spinal cord (B, D).

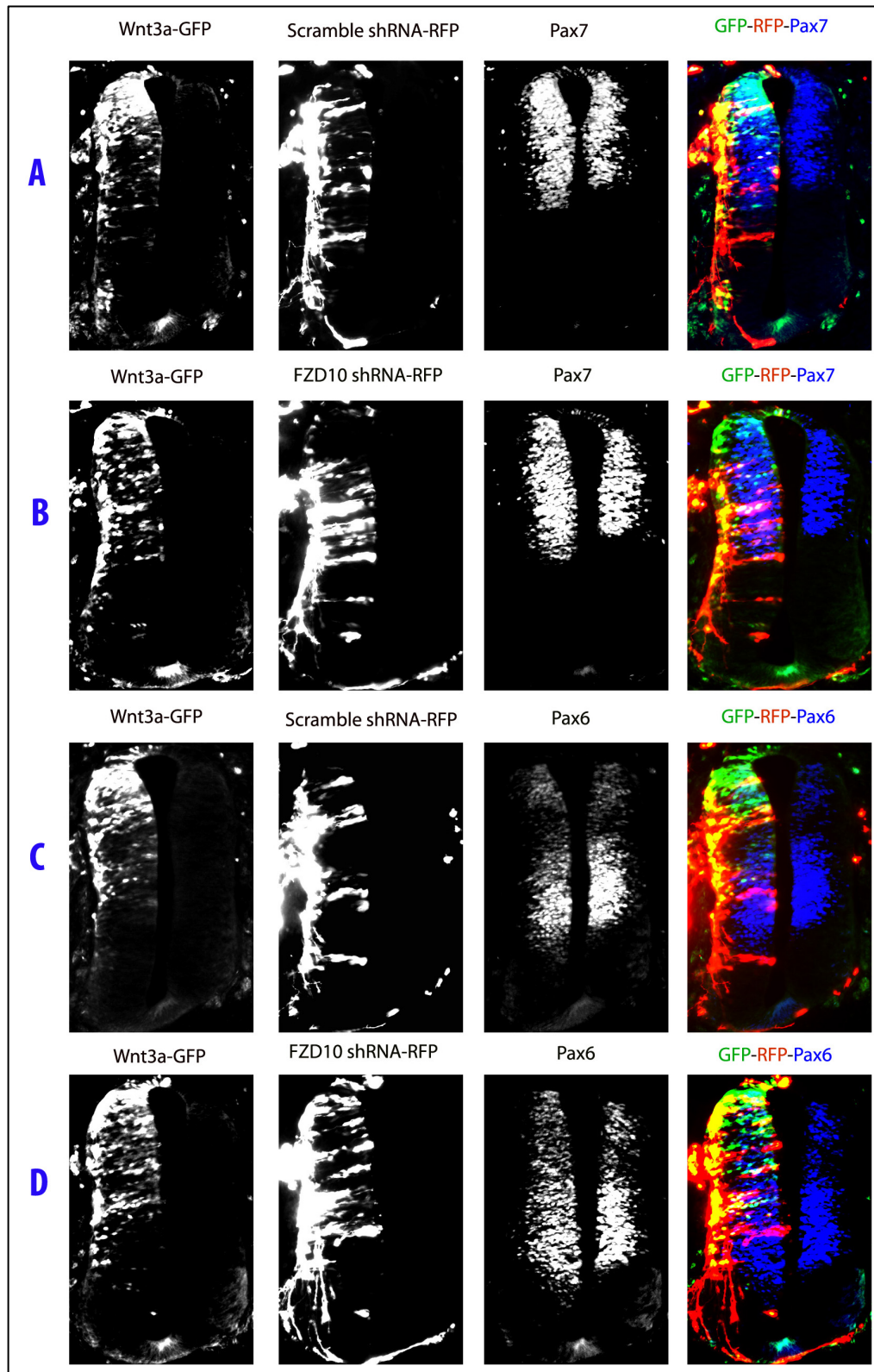


**Fig. 6-7 Knockdown of FZD10 did not affect the phenotype of Wnt3a overexpression.** Scrambled shRNA or FZD10 shRNA co-electroporation with Wnt3a did not affect the ventral expansion of Pax6 or Pax7 on the electroporated side of the spinal cord (A-D).

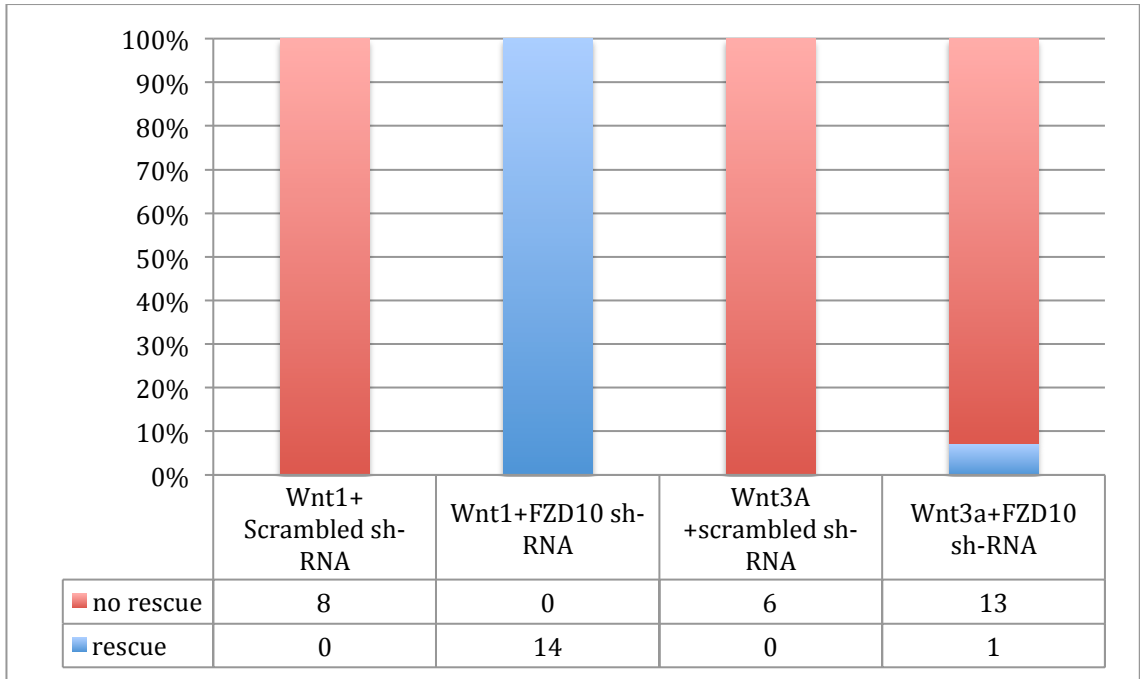


**Fig. 6.8 Summary of rescue experiments that shows numbers of embryos and their phenotypes.**

### **6-5 Overexpression of FZD10 affected the patterning of neural progenitors and inhibited neurogenesis**

To further study FZD10 function, we cloned full-length chick FZD10 and subcloned it into expression vector pCAB-IRES-GFP (Chapter 2). FZD10 was introduced into the chick neural tube at stage HH11-12 by *in vivo* electroporation. Embryos were analysed after 48 hours and screened for GFP expression (Fig. 6.8 A, B). They were subsequently hybridized with an FZD10 probe to ensure that FZD10 was ectopically expressed along the DV axis of the electroporated half of the spinal cord (Fig. 6.8 C). Indeed, cryosections revealed that FZD10 transcripts were misexpressed on the experimental side of the electroporated embryos, suggesting that FZD10 was successfully overexpressed in the spinal cord (Fig. 6.8 D). Interestingly, we observed that the electroporated side was smaller in size (Fig. 6.8 D).

We next examined whether FZD10 misexpression would affect neural progenitor patterning. We assessed the expression domains of Pax6, Pax7 and Nkx2.2 after 48 hours post-electroporation. FZD10 overexpression affected patterning cell-autonomously; the expression domains of Pax6 and Pax7 were shifted to the dorsal domain of the spinal cord in the electroporated embryos, whereas the Nkx2.2 domain in the ventral part of the spinal cord was broader in the electroporated half compared to the control half of the spinal cord (Fig. 6.9 B, E, H). This suggests that dorsal progenitor domains were reduced whilst ventral progenitors were expanded dorsally.

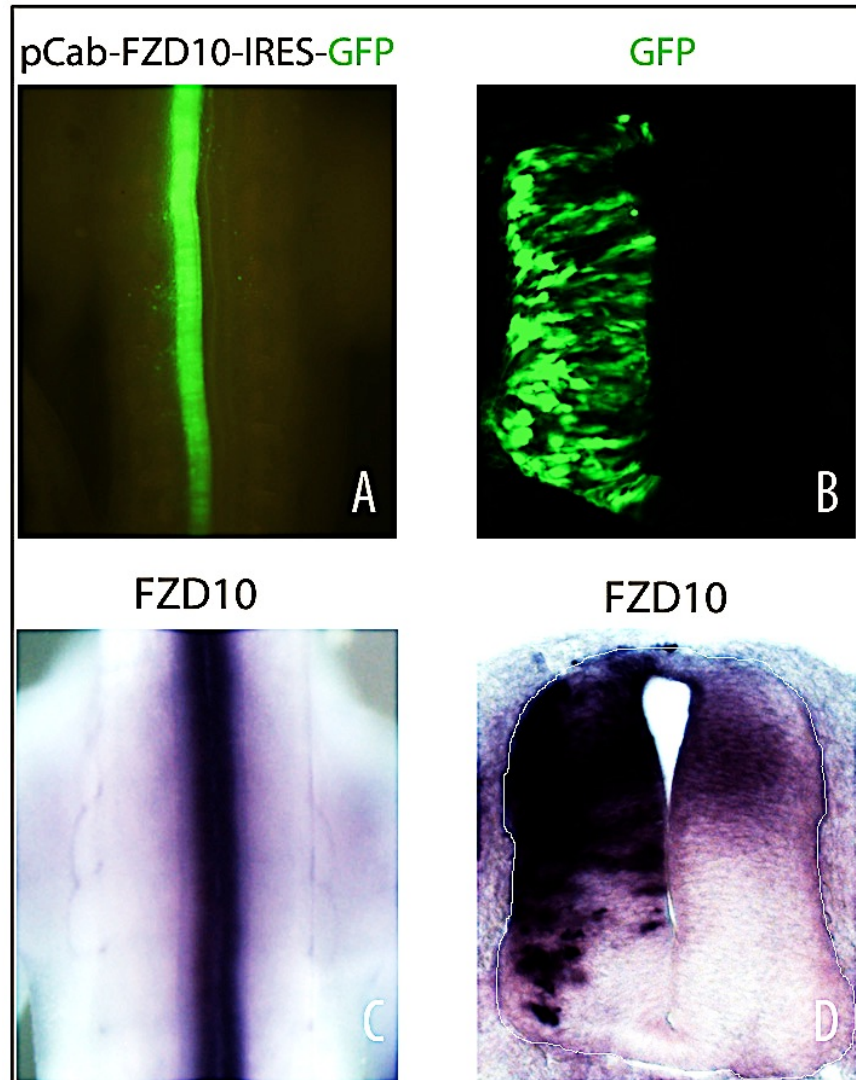


**Fig. 6-8 Ectopic expression of FZD10 is detected in the spinal cord after electroporation.** (A) A dorsal view of an embryo electroporated with an expression construct encoding full-length cFZD10 and GFP from the same vector backbone. (B) Cross section of a spinal cord showing GFP expression in the electroporated embryos. (C) Dorsal view of an embryo hybridized with a FZD10 probe. (D) Ectopic FZD10 expression along the dorsal-ventral axis of the spinal cord was detected by in situ hybridization after electroporation. N=3/3.

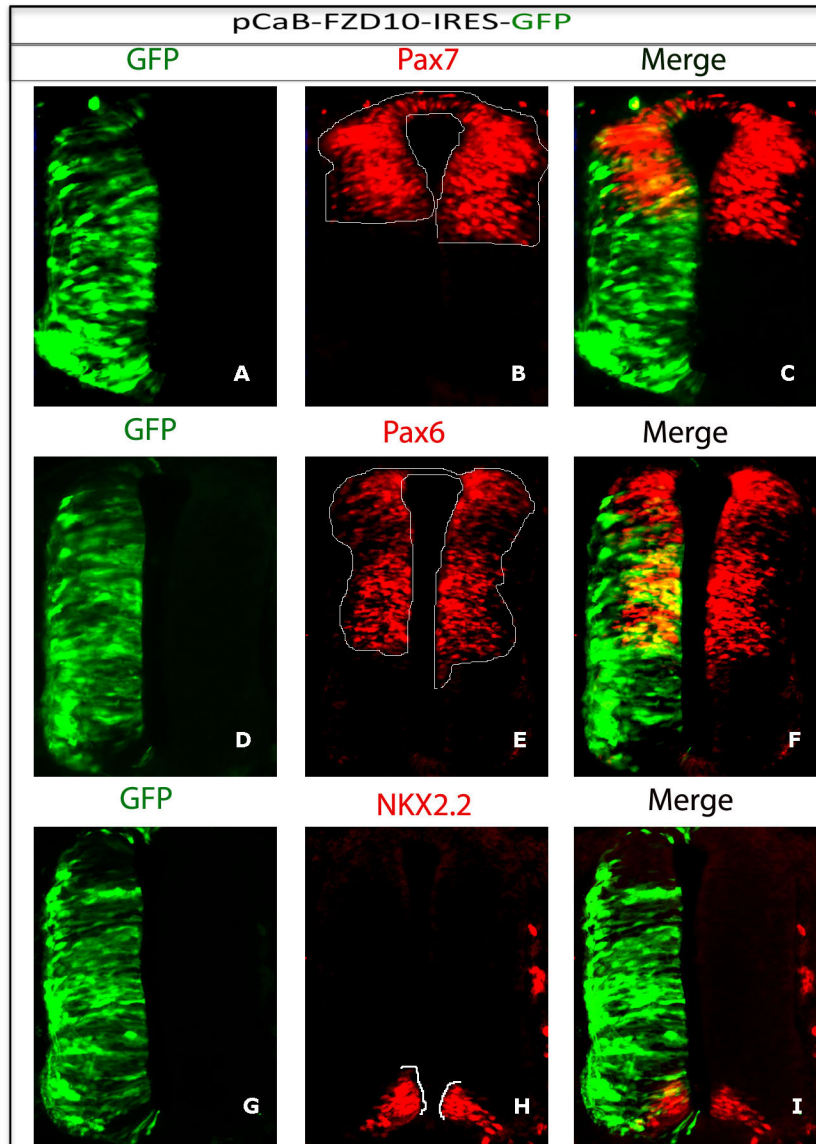


**Fig. 6.9 FZD10 overexpression affects neural progenitor patterning the in D-V axis of the spinal cord.** (A, D, G) The green colour represents GFP expression on the transfected side of the spinal cord, indicating that FZD10 is ectopically expressed. (B, C) The Pax7 expression domain is more dorsally restricted on the electroporated side. (E, F) The Pax6 expression domain is dorsally shifted. (H, I) The Nkx2.2 expression domain is dorsally expanded on the electroporated side of the spinal cord. N=11/13.

We further investigated the effect of FZD10 overexpression on neurogenesis of the DV of the spinal cord. Neural markers, such as Lhx1/5, Islet-1 and Tuj-1, were used to assess their expression in electroporated embryos (48 hours post-electroporation). Lhx1/5 expression was repressed along the dorsal half of the electroporated spinal cord and it was missed in the interneuron V1 region (Fig. 6.10 A, B, C). Islet-1 positive cells were reduced in the dorsal interneuron 3 region on the electroporated half of the spinal cord compared to the control (Fig. 6.10 D, E, F). Tuj-1 is a marker for differentiated neurons along the DV spinal cord and its expression was moderately affected in the dorsal domain after 48 hours post-electroporation (Fig. 6.10 G, H, I). We also analysed the effect of FZD10 overexpression after 72 hours of electroporation; the phenotype was weaker compared to the phenotype after 48 hours. However, we observed that the electroporated side was still smaller when compared with the control side of spinal cord electroporated with full-length FZD10 (Fig. 6.11). Boundaries between the interneurons (dI2, dI4, dI6, V0 and V1) were reduced on the experimental side of spinal cord, as seen by Lhx1/5 staining (Fig. 6.11 A, B). Fewer differentiated neurons were noted in the dI3 domain as marked by Islet-1, whereas the motoneurons were not affected, as assessed by the Islet-1 expression in the ventral spinal cord (Fig. 6.11 C, D). Tuj-1 expression was more repressed in the experimental side of the spinal cord in electroporated embryos (Fig. 6.11 E, F). Interestingly, we observed that most GFP positive cells accumulated along the DV spinal cord in the MZ where the differentiated neurons were located (Fig. 6.11 B, D, F). These findings indicate that FZD10 is involved in spinal cord development and that it regulates neurogenesis.

These results also demonstrate inhibitory effects for FZD10 overexpression in neural progenitors and in neurogenesis in the spinal cord. It is not clear how FZD10 causes these effects, but there are a number of possibilities; full length FZD10 may act in a dominant negative fashion by sequestering (other) Wnt ligands and preventing them from binding to their receptors in the spinal cord (see summary 6). Alternatively, overexpressed FZD10 may disrupt non-canonical Wnt signalling by depleting co-factors (see 6-6), or FZD10 may require the Lrp6 co-receptor to activate canonical Wnt signalling (Wnt1). Availability of Lrp6 may be rate-limiting and therefore FZD10 overexpression impairs rather than activates the pathway (see also 6-7).

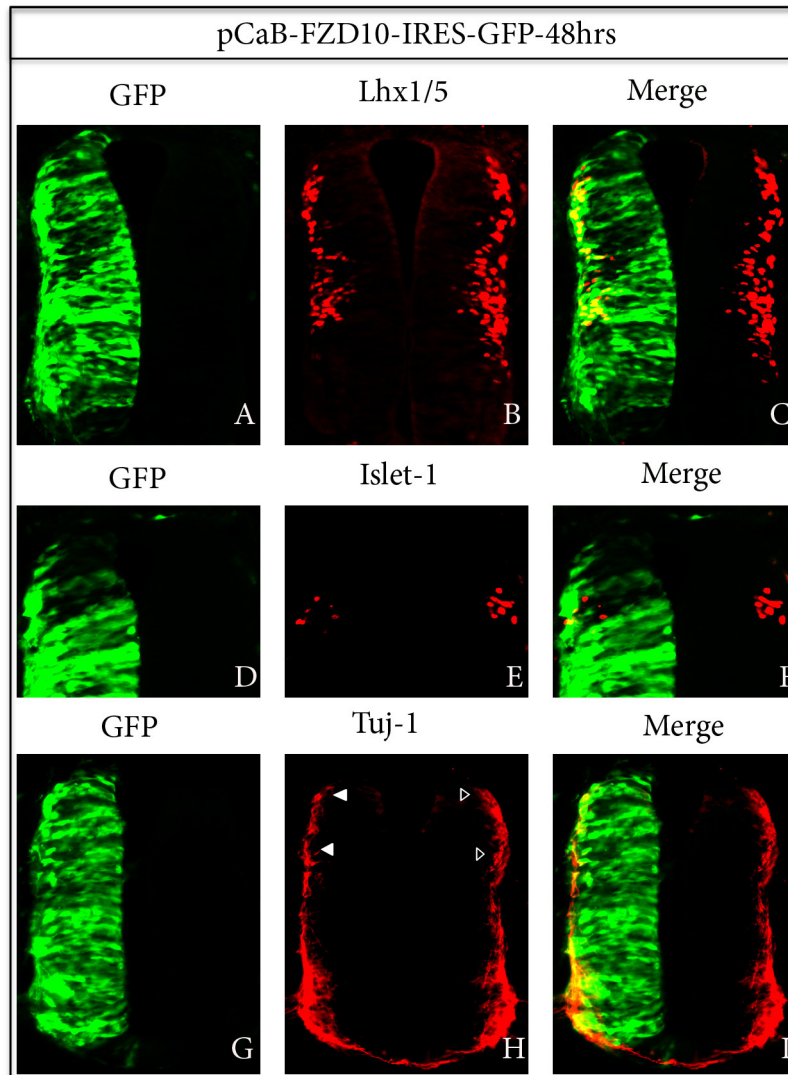


**Fig. 6.10 FZD10 overexpression leads to inhibition of neurogenesis of the spinal cord 48 hours post-electroporation.** (A, D, G) The green colour represents GFP expression on the electroporated side of the spinal cord, indicating that FZD10 is ectopically expressed along the DV axis of the spinal cord. Expression of differentiated neuron markers was inhibited in the electroporated half of the spinal cord, (B, C) Lhx1/5 expression (E, F) Islet-1 expression, (H, I) Tuj-1 expression. N=11/13.

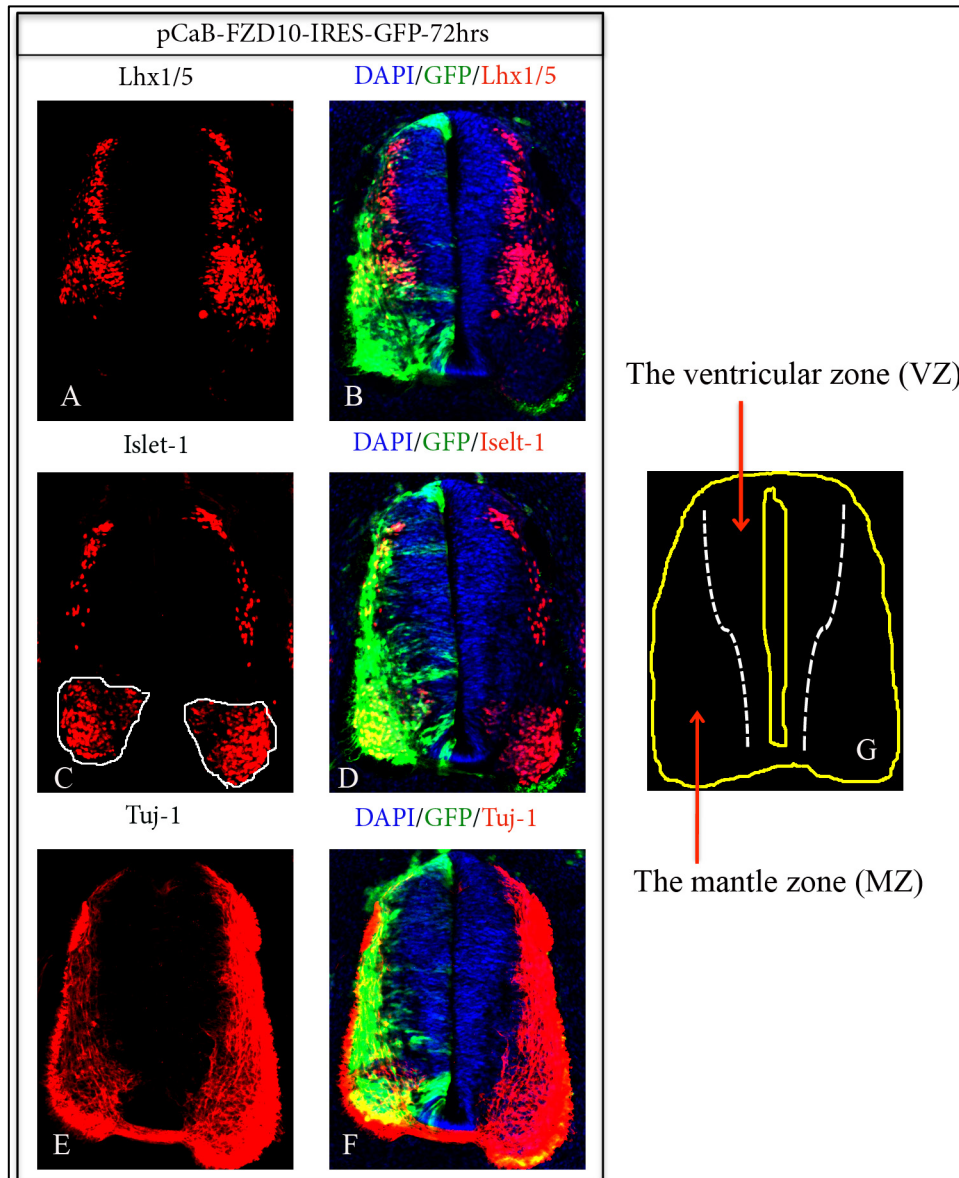


**Fig. 6.11 FZD10 overexpression reduces neurogenesis of the spinal cord 72 hours post-electroporation.** Markers for differentiated neurons were inhibited in the electroporated half of the spinal cord, (A) Lhx1/5 expression, (C) Islet-1 expression, whereas Islet-1 expression in motor neurons was not affected, (E) Tuj-1 expression. (B, D, F) Most of GFP positive cells were present along the DV axis of the spinal cord in the mantle zone (MZ) (G), where differentiated neurons are formed. Embryos number was 2/2 and multiple sections were analysed for each marker.

## **6-6 Overexpressed FZD10 affected the actin cytoskeleton on the apical side of the spinal cord**

FZD receptors are involved in cell polarity and tissue closure. For example, FZD1 and/or FZD2 mutations lead to defects in neural tube closure in mice (Yu et al., 2010). Also, FZD3<sup>-/-</sup>; FZD6<sup>-/-</sup> mutations result in neural tube defects, which is a failure of neural tube closure along the anterior-posterior axis (Wang et al., 2006). FZD7 regulates convergent extension movements in *Xenopus* embryos (Djiane et al., 2000). All these effects have been linked to a disruption in non-canonical Wnt signalling (PCP). Recently, it has been shown that FZD10 affects convergent extension in the mesoderm of zebrafish embryos (Nikaido et al., 2013).

Therefore, we examined here whether overexpressed FZD10 would affect cell polarity in the DV spinal cord. To test this hypothesis, we used phalloidin to stain filamentous actin (F-actin) in the spinal cord after cryosectioning embryos electroporated with FZD10. We observed that phalloidin staining was reduced in the injected half of the spinal cord (Fig. 6.11 C, D). Moreover, phalloidin staining was also disrupted in the apical surface of the lumen following FZD10 overexpression, suggesting that F-actin failed to accumulate on the cells' apical side (Fig. 6.11 D').

We also used Laminin antibody to assess the effect of FZD10 overexpression on the cells' basal side. We found that Laminin staining was not affected in the electroporated side of the spinal cord and it was comparable to the control (Fig. 6.11 E, F, G). These data indicate that overexpressed FZD10 affected the polarity of cells in the spinal cord, particularly their apical side. This might also suggest that overexpressed FZD10 may disrupt non-canonical Wnt signalling. Consistent with this, FZD10 has been shown to activate the JNK pathway and regulate RhoA activity in different cell lines (Fukukawa

et al., 2009).

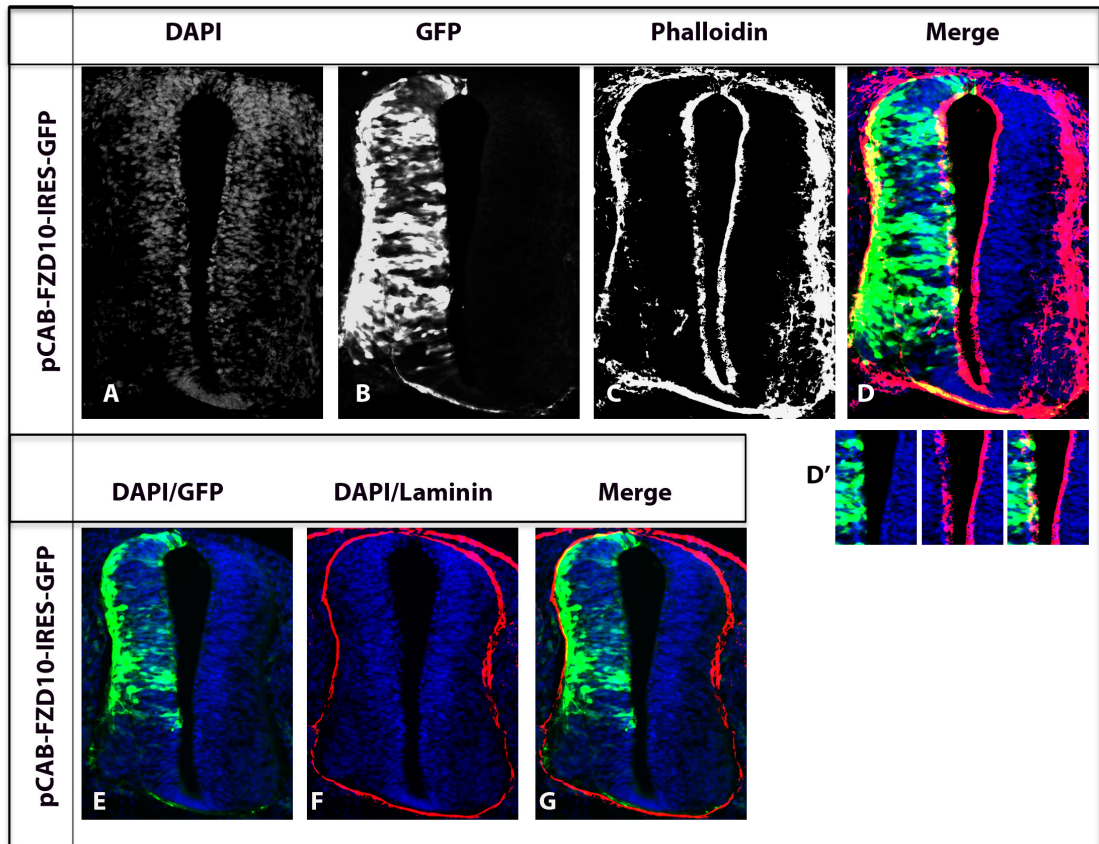


**Fig. 6.12 FZD10 affected the actin cytoskeleton on the apical surface of the spinal cord 48 hours post-electroporation.** (A) DAPI stained nuclei in a cross section of the spinal cord. (B, E) GFP expression in the transfected side of the spinal cord. (C, D) Phalloidin stained F-actin; its accumulation was reduced in the electroporated side of the spinal cord, indicating that the structure of the cytoskeleton was disrupted. (D') Phalloidin staining was inhibited and disrupted in the apical cells in the luminal face of the spinal cord. (F, G) Cross section of spinal cord stained with DAPI and Laminin; Laminin-stained basal cells in the spinal cord. N=4/5.

### **6-7 Co-overexpression of Lrp6 and FZD10 enhanced the Wnt1-induced phenotype, leading to overgrowth and dorsalization in the spinal cord**

Next, we wanted to test whether FZD10 overexpression caused inhibition of canonical Wnt signalling potentially due to a ‘dominant-negative’ sequestration of important co-factors with limited availability. In particular, we examined the requirement of Lrp6 for the function of Wnt1 and FZD10 in vivo in the spinal cord. Lrp6 is a FZD co-receptor; it binds Wnt1 and is necessary for the activation of Wnt signalling (He et al., 2004; MacDonald and He et al., 2012; Tamai et al., 2000). Importantly, it is expressed in neural tube and its mutations result in neural tube defects including a failure of neural tube closure and disruption in cell polarity (Allache et al., 2014; Gray et al., 2013; Houston and Wylie, 2002). We blasted human Lrp6 sequences against the chick genome and found that the predicted chick Lrp6 protein shares more than 92% identity in its amino acid sequence with hLrp6 protein (Appendix C).

Therefore, we co-electroporated human Lrp6 (pCS2-hLrp6) with pCiG (pCiG-IRES-GFP) as a tracer into neural tubes at HH11-12 and analysed the embryos after 48 hours. To assess the effect on dorso-ventral patterning, Pax3 and Pax7 antibodies were used. The Pax3/Pax7 expression domains did not appear to be affected in the experimental side of the spinal cord in embryos electroporated with hLrp6+pCiG or with empty pCiG alone (Fig. 6.12). These data suggest that hLrp6 on its own did not affect the dorso-ventral patterning of the spinal cord, and it may require the formation of active complexes bound by Wnt ligand to be activated. In agreement with our findings, it has been shown in a study in mice that dorsal-ventral patterning is not affected in Lrp6 gain of function ( $Lrp6^{Cd/Cd}$ ) (Gray et al., 2013).

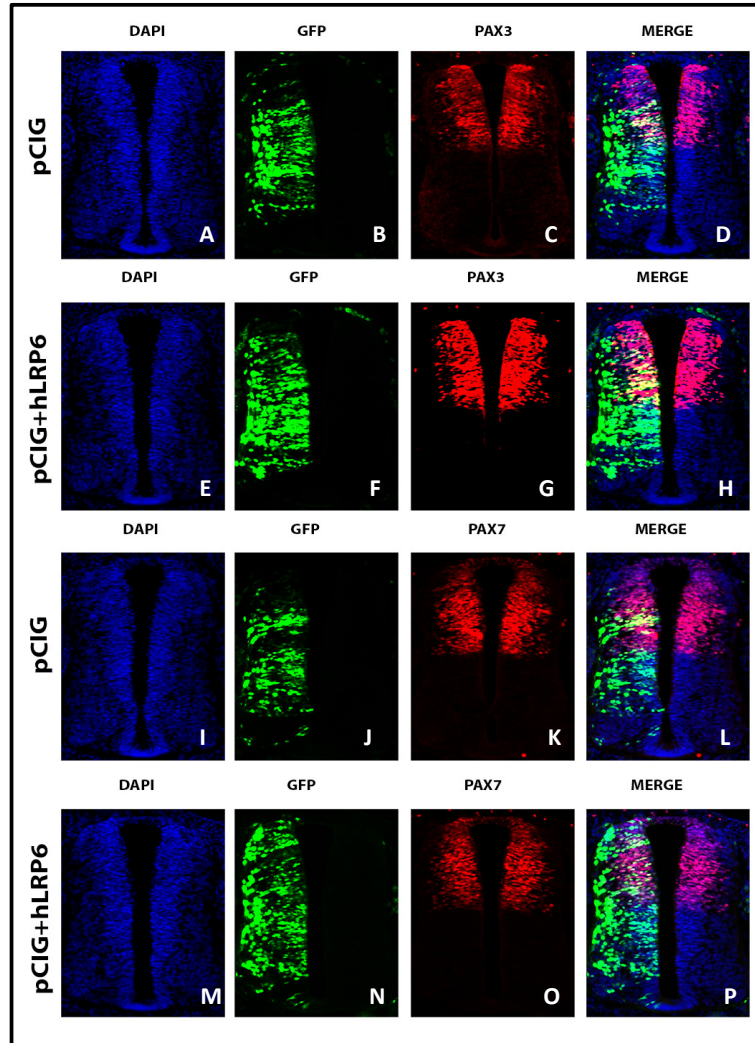


**Fig. 6.13 LRP6 misexpression does not affect dorsal progenitor patterning in the spinal cord.** Pax3 (A-D) and Pax7 (I-L) expression domains are not affected after electroporation of the empty pCIG vector alone (N=3). Pax3 (E-H) and Pax7 (M-P) expression patterns were not altered in either side of spinal cords co-electroporated with pCIG and the hLRP6 vector (N=6/6).

Next, we tested the interactions between Wnt1, hLrp6 and FZD10 in the spinal cord. First, hLrp6 was co-electroporated with FZD10 into the neural tube at HH11-12 and the phenotype was examined using the dorsal marker Pax7. We found that in the presence of hLRP6 the more dorsal restriction of dorsal markers observed after electroporation of FZD10 alone (see 6-5) was reverted and the dorso-ventral expanse of Pax7 expression was rescued (Fig. 6.14 A-D). This suggests an interaction between FZD10 and Lrp6, but may indicate limited availability of the relevant ligand. Interestingly, we also found that FZD10 electroporation together with Wnt1 seemed to inhibit the Wnt1-induced phenotype. Assessment of dorso-ventral patterning showed that the ventral expansion of Pax7 was reduced compared to what had been seen following Wnt1 electroporation alone (see for example Fig. 6.5). In addition, the kink-related to Wnt1 overexpression in the ventral part of the spinal cord was missed (Fig. 6.14 E-H). Finally, the effects of FZD10, hLrp6 and Wnt1 co-electroporation into the spinal cord were investigated. The embryos were dissected after 48 hours post-electroporation to be cryosectioned and analysed. We found that Pax7 expression was expanded ventrally on the electroporated side of the spinal cord (Fig. 6.14 I-L). This expansion was more dramatic than what had been observed after electroporation of Wnt1 or Wnt3a alone (see chapter5; Fig.5.3 and Fig.5.4). Furthermore, the experimental side was larger than the control, possibly due to overgrowth although we have not directly measured the number of proliferating cells in this scenario (Fig. 6.14 I). We found that the ventral expansion of Pax7 expression doubled in size and significantly increased 1.9-fold after Wnt1 co-electroporation with FZD10 and Lrp6 compared to Wnt1 electroporation alone (Fig. 6.15). These findings are consistent with the idea that FZD10 interacts with Lrp6 to transduce a Wnt1 signal in vivo in the spinal cord.

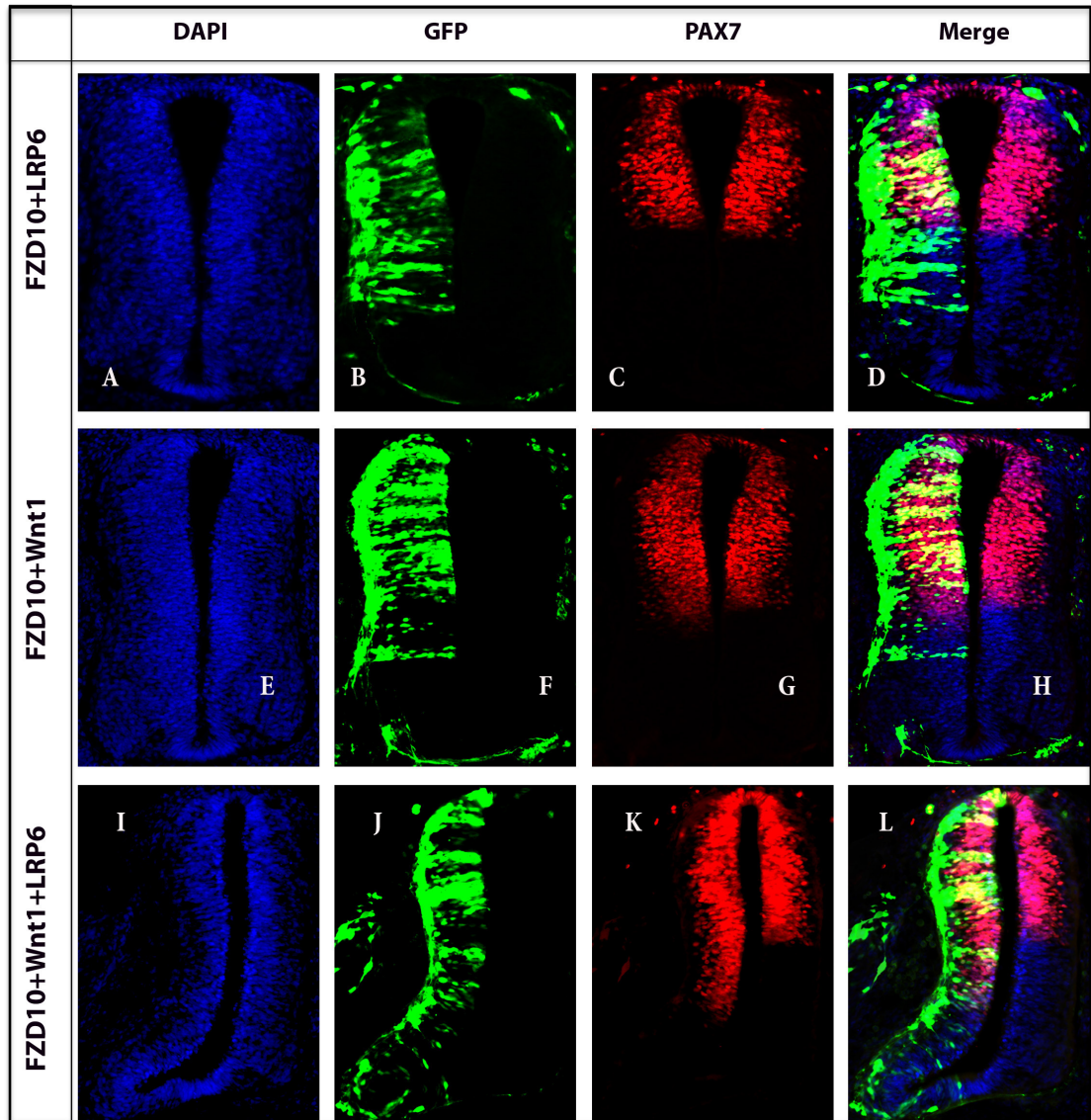


**Fig. 6.14 FZD10 interacts with Lrp6 to mediate Wnt1 activity in vivo in the spinal cord.** (A, E, I) DAPI staining. (B, F, J) GFP expression in the electroporated side of the spinal cord as a reporter for ectopically expressed FZD10, Lrp6 and Wnt1. (C, D) The Pax7 expression domain is almost restored to wild type expression after Lrp6 co-electroporation with FZD10 (N=8/10). (G, H) FZD10 co-electroporation with Wnt1 attenuates the phenotype of Wnt1 overexpression; the kink in the ventral spinal cord was missed and ventral Pax7 expansion was reduced (N=4/5). However, there is a slight enlargement restricted to the dorsal domain of the spinal cord where endogenous and ectopic FZD10 are expressed. (I-L) Electroporation of FZD10, Lrp6 and Wnt1 in combination results in overgrowth of the electroporated side of the spinal cord (I, J) and a dramatic ventral expansion of the Pax7 expression domain (K, L) (N=5/5).

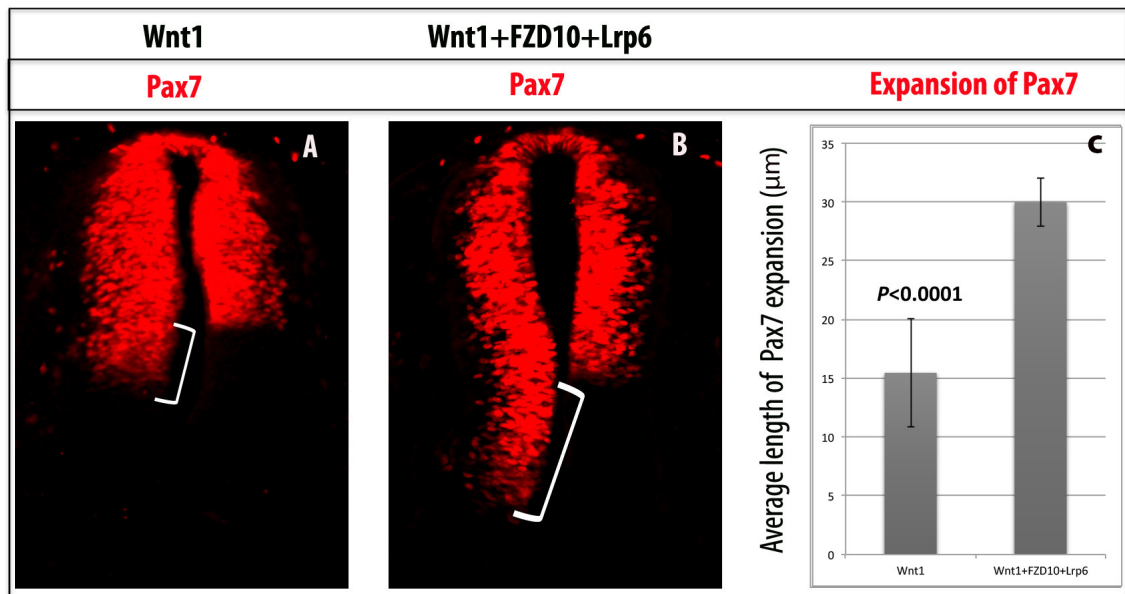


**Fig. 6.15** The degree of ventral expansion of Pax7 48 hours after electroporation of Wnt1 alone compared to Wnt1, FZD10 and Lrp6. (A) Pax7 expression after Wnt1 electroporation. (B) Pax7 expression after co-electroporation of Wnt1 with FZD10 and Lrp6. The white bracket in A, B indicates the ventral expansion that was measured. (C) The average length of Pax7 expansion in both experiments; ventral expansion of Pax7 was strongly enhanced after introducing both FZD10 and Lrp6 together with Wnt1 into the spinal cord, indicating that the dorsal domains of the six neural progenitors were expanded along the DV spinal cord and these receptors mediates Wnt1 activity in vivo.

The measurement was done using AxioVision (Rel.4.8.2) software and the measurement unit was micron ( $\mu\text{m}$ ). Statistical analysis was performed using Excel and a Student's t-test. 4 embryos and 20 sections were analysed for each experiment.

## 6-8 Summary

To study how FZD10 is involved in spinal cord development and in Wnt signal transduction, different approaches were applied using in vivo loss- and gain-of-function and rescue experiments. Targeting FZD10 by sh-RNA results in a reduction in the size of the spinal cord due to the significant decrease in proliferative cells in the ventricular zone (Fig. 6.1 and Fig. 6.2). In addition, the dorsal progenitor domains were slightly affected after FZD10 knockdown. Neurogenesis was affected as the expression of Lhx1/5 and Tuj-1 was reduced (Fig. 6.3).

We next investigated the requirement of FZD10 for Wnt1 and/or Wnt3a activity in the spinal cord. We previously showed that Wnt1 overexpression up-regulated FZD10 expression (Chapter 5). Here we found that FZD10 is required for the biological activity of Wnt1 as FZD10 knockdown by sh-RNA rescued the Wnt1-induced phenotype whereas the Wnt3a-induced phenotype was not affected (Fig. 6.5 and Fig. 6.6).

Overexpression of FZD10 led to inhibitory effects in neural progenitors and neurogenesis. The expression domains of Pax6 and Pax7 were reduced and dorsally shifted and neurogenesis was inhibited as differentiated neuron markers, Lhx1/5, Islet-1 and Tuj-1, were repressed (Fig. 6.9, Fig. 6.10 and Fig. 6.11). These results could suggest that full-length FZD10 may act in a dominant negative fashion and inhibit proliferation and differentiation in the spinal cord. This is supported by a study reporting that misexpression of full-length cFZD1 or cFZD7 mimics the effect of misexpression of putative dominant negative forms of these two FZDs, which results in a severe reduction in the size of the cartilage element in the developing chick wing (Hartmann and Tabin, 2000). This study has suggested that changing FZDs levels may

disturb Wnt signalling that may need balanced levels of FZDs.

We also found that FZD10 overexpression led to reduced phalloidin staining, which was evident on the apical side of cells, abutting the lumen of the spinal cord. In contrast, expression of laminin was not altered in basal cells (Fig. 6.12). This could suggest that overexpressed FZD10 may affect microfilament movement and neural cell division.

We also showed that misexpression of hLRP6 on its own did not seem to affect patterning in the spinal cord (Fig. 6.13). On the other hand, we found that co-electroporation of hLRP6 with Wnt1 and FZD10 resulted in a striking expansion of the dorsal neural progenitor domains and that the spinal cord was dorsalized (Fig. 6.14 and Fig. 6.15).

# Chapter 7

## **Discussion**

## **7-1 Introduction**

The canonical Wnt ligands belong to a family of secreted glycoproteins that bind to the N-terminal extracellular cysteine-rich domain of the frizzled (FZD) receptor family of seven-pass transmembrane proteins and activate  $\beta$ -catenin/TCF (Komiya and Habas, 2008; Logan and Nusse, 2004; MacDonald et al., 2009). Canonical Wnt signalling is also called Wnt/ $\beta$ -catenin signalling because  $\beta$ -catenin is a major player in this pathway (Komiya and Habas, 2008).

Wnt signalling controls several developmental processes in both invertebrates and vertebrates, from fruit flies to humans. Wnt signalling has been shown to be involved in the regulation of a wide variety of biological processes, such as cell proliferation, cell polarity, cell differentiation and cell fate specification (Moon et al., 2004; Logan and Nusse, 2004). It also plays several roles in the development of the central nervous system (CNS), such as in neural induction, neurulation, patterning, neuronal differentiation in the spinal cord, neural stem cells, axon guidance and synaptogenesis (Yoshikawa et al., 1997; Pöpperl et al., 1997; Davidson et al., 2002; Muroyama et al., 2004; Muroyama et al., 2002; Chenn and Walsh, 2003; Lyuksyutova et al., 2003; Hall et al., 2000).

## **7-2 Wnt1 and Wnt3a expression and function during spinal cord development**

Canonical Wnt signalling has been shown to be involved in dorsal-ventral patterning of the spinal cord, including cell proliferation and specification (Le Dréau and Martí, 2012; Ulloa and Martí, 2010). Elevating  $\beta$ -catenin levels by electroporating a constitutively active form of  $\beta$ -catenin cell autonomously accelerates cell proliferation and activates dorsal genes in chick spinal cords, whereas reducing  $\beta$ -catenin activity by

introducing dominant-negative forms of Tcfs results in a reduction in cell proliferation and dorsal genes were repressed (Alvarez-Medina et al., 2008; Megason and McMahon, 2002). Consistent with this, we also found that blocking canonical Wnt signalling using a dominant-negative form of Wnt3a resulted in a marked reduction in spinal cord size and that dorsal marker (Pax7) was inhibited (Appendix B. Fig. B.1). This indicates that canonical Wnt signalling is required for spinal cord development.

Some Wnt genes are expressed in the neural tube including Wnt1 and Wnt3a (Alvarez-Medina et al., 2008; Galli et al., 2014; Megason and McMahon, 2002; Parr et al., 1993). Wnt1 and Wnt3a are known to function through canonical Wnt signalling and they are implicated in neural tube development (Dickinson et al., 1994; Megason and McMahon, 2002; Muroyama et al., 2002; Alvarez-Medina et al., 2008). Wnt1 and Wnt3a control cell cycle regulators and promote cell proliferation in the spinal cord (Megason and McMahon, 2002). They also regulate neural specification through patterning of the spinal cord along the dorsal ventral axis (Muroyama et al., 2002; Alvarez-Medina et al., 2008).

Here, we followed Wnt1 and Wnt3a expression patterns during chick embryo development using in situ hybridization to observe any changes in their expression. We performed careful analysis of their expression patterns from HH14 to HH25; overlapping expression was shown throughout the chick dorsal neural tube (Appendix A. 1, 2, 3). Moreover, it was apparent that Wnt1 and Wnt3a are highly expressed during the initiation of neurogenesis of the dorsal neural tube, but their expression was restricted to the dorsal midline after neurogenesis (Appendix A. 2, 3). Our results confirmed that Wnt1 and Wnt3a expression was restricted to the domain surrounding the roof plate at all stages examined. Wnt1 and Wnt3a function is required for dorsal

neural tube development, as seen from several studies. We here questioned whether Wnt1 and Wnt3a have the same capacity to regulate patterning in the spinal cord. Therefore, we individually electroporated Wnt1 and Wnt3a in the neural tube and the effects were assessed using DV neural markers (Chapter 5). We found that both Wnts were able to activate Pax6 and Pax7 expression more ventrally within the dorsal domain, whereas Nkx2.2 was more restricted to the ventral domain of the spinal cord (Chapter 5). Both Wnts also promoted neurogenesis of dorsal interneuron 3, as Islet-1 expression was increased (Chapter 5). These results indicate that Wnt1 and Wnt3a have the same biological activities in chick spinal cord even though they only share 43% amino acid identity (Chapter 5; Alvarez-Medina et al., 2008; Megason and McMahon, 2002). In addition their functions have been studied in mice, their mutations result in different phenotypes because they are expressed in different tissues. In Wnt1 knockout mice, the midbrain was lost and the hindbrain was affected, whereas in Wnt3a knockout mice, the anterior-posterior axis was truncated, there were defects in somitogenesis and the hippocampus was lost (reviewed in Amerongen and Berns, 2006). In Wnt1<sup>-/-</sup>; Wnt3a<sup>-/-</sup> double mutant mice, dorsal neural specification and neural crest expansion were affected (Ikeya et al., 1997; Muroyama et al., 2002).

In this study, we also sought to explain how Wnt1 and/or Wnt3a initiate canonical Wnt signalling in the chick spinal cord and through which receptors. Thus, we performed expression analysis for all known FZDs in order to identify which FZDs are expressed in the spinal cord.

### **7-3 FZDs are expressed during spinal cord development**

FZD receptors are involved in neural tube development. For example, neural tube closure was affected in FZD1 and/or FZD2 knockout mice (Yu et al., 2010). Also, the neural tube failed to close along the anterior-posterior axis in FZD3<sup>-/-</sup>; FZD6<sup>-/-</sup> double mutants (Wang et al., 2006). FZD3 knockout mice show severe defects in axon development in the central nervous system (Hua et al., 2013; Wang et al., 2001; Wang et al., 2006). In addition, some neurons fail to migrate and cluster in the midline of the spinal cord of this mutant (Wang et al., 2006).

In chicks, all FZDs are expressed during the early stage of development and they are detected in different tissues, including the developing brain (Chapman et al., 2004; Fuhrmann et al., 2003; Stark et al., 2000; Quinlan et al., 2009; Theodosiou and Tabin, 2003). Here, we were particularly interested in FZD expression patterns during chick spinal cord development. We established a complete expression profile of cFZD receptors in chick spinal cord and identified FZDs that could be involved in the dorsal-ventral patterning of the spinal cord (Fig. 3.1 and Table. 3.1). Through in situ hybridization, we identified that six out of ten FZDs were expressed in the spinal cord and showed specific and different expression patterns at stage HH14-15. FZD1 and FZD10 expression was seen in the dorsal neural tube and FZD10 was strongly and specifically detected in the dorsal part of the neural tube (Chapter 3). Whereas FZD2 and FZD7 were found in the intermediate ventral spinal cord and their expression patterns seemed to overlap, FZD7 showed stronger expression in the neural progenitors. FZD3 and FZD9 transcripts were found throughout the dorsal ventral spinal cord. FZD3 expression was specific in the ventricular zone where proliferation occurs, while FZD9 expression was ubiquitous. We also observed that FZD7 and FZD10 were expressed

during spinal cord neurogenesis (Chapter 3). The expression profile of cFZDs could suggest potential interactions of these receptors with Wnt ligands that are expressed during spinal cord development. Moreover, it could be proposed that dorsal FZDs, such as FZD10, may mediate signalling that is activated by Wnt ligands expressed in the dorsal spinal cord, whereas ventral FZDs may transduce the signals of Wnt ligands in the ventral spinal cord.

#### **7-4 FZD10 expression during spinal cord neurogenesis**

FZD10 is one of the FZD family receptors that has been detected in different species, including zebrafish, *Xenopus*, chick and mouse (Galli et al., 2014; Kawakami et al., 2000a; Moriwaki et al., 2000; Wheeler and Hoppler, 1999; Nikaido et al., 2013; Yan et al., 2009). In chicks, FZD10 is expressed at the early stage of development as it is found in the pre-streak stages, and by stage 4, is detected in the posterior of the primitive streak (Chapman et al., 2004). FZD10 expression continues throughout embryonic development and it has been detected by in situ hybridization in several developing tissues, such as the central nervous system, limb buds and branchial arches (Kawakami et al., 2000a).

In this report, full-length cFZD10 was cloned and its expression profile was established during chick embryo development as well as in the spinal cord using an in situ hybridization approach (Chapter 4). At stage HH9, FZD10 was expressed in the midbrain and in the posterior region during secondary neurulation. FZD10 expression was found in the developing central nervous system, in the midbrain, the hindbrain and the spinal cord in all stages examined throughout development (Fig. 4.1). In addition, at

stage HH24, FZD transcripts were found in the limb bud and the branchial arches. FZD10 also showed very strong expression in the tail bud throughout the developmental stages.

We followed FZD10 expression during spinal cord development from HH14 to HH24 and it was apparent that FZD10 is expressed in the dorsal spinal cord and continues to be expressed at different times during neurogenesis. FZD10 expression was detected in the region of neural progenitors and overlapped with well-known dorsal progenitor markers, such as Pax3/6/7 and Ngn1. FZD10 is also expressed during dorsal interneuron formation as shown by the differentiated neural markers; Islet-1 and Lhx1/5 (Chapter 4).

Importantly, we conducted a careful analysis for the expression patterns of Wnt1, Wnt3a and FZD10 during spinal cord development (Chapter 4 and Appendix A). As seen in the expression profiles, Wnt1, Wnt3a and FZD10 are expressed in the spinal cord and their expression overlapped (Chapter 4; Galli et al., 2014). FZD10 expression was detected in the entire dorsal domain of the spinal cord and may interact with dorsal Wnts including Wnt1 and Wnt3a. Wnt1 and Wnt3a are required for spinal cord development (Alvarez-Medina et al., 2008; Megason and McMahon, 2002; Muroyama et al., 2002).

#### **7-5 Dorsally expressed Wnts (Wnt1/Wnt3a) regulate the expression of FZD7 and FZD10 in the spinal cord**

Wnt1 and Wnt3a are expressed in the dorsal spinal cord, function through canonical Wnt signalling and play important roles during development. We previously showed

that FZD7 is expressed in the intermediate-ventral spinal cord, whereas FZD10 expression is detected in the dorsal spinal cord (Chapter 4). Here, we investigated whether dorsally expressed Wnts regulate the expression of FZDs in the spinal cord. Therefore, Wnt1 and Wnt3a were co-electroporated in chick neural tubes and the embryos were analysed after 24 hours. The transfected embryos were hybridized with probes detecting FZDs. In situ hybridization followed by cryosections revealed that FZD10 expression was ventrally expanded on the experimental side of the spinal cord in electroporated embryos. This indicates that FZD10 expression is up-regulated by canonical Wnt signalling (Wnt1/3a) potentially enhancing the ability of cells to respond in a positive feed-back loop. This result might also suggest that FZD10 may be involved in mediating canonical Wnt signalling in the chick spinal cord.

Conversely, FZD7 expression was lost in the intermediate-ventral spinal cord on the transfected side of the spinal cord after Wnt1 and Wnt3a co-electroporation. This suggests that ventrally expressed FZDs are negatively regulated by secreted Wnts from the dorsal spinal cord.

Wnt/FZD interactions and selectivity are not fully understood and this is a current topic of interest, especially in some aspects of pharmacology and pathophysiology. For example, Wnt–FZD selectivity, receptor complex stoichiometry and signal initiation still need to be studied at the molecular level (Schulte, 2015). Recently, Wnts have shown selective binding to FZDs and Wnt-FZD pairs drive different biological outcomes in different cell lines (Dijksterhuis et al., 2014). We here introduced the chick spinal cord as a tool to dissect Wnt-FZD interaction and selectivity *in vivo*.

## 7-6 Wnt1 up-regulates FZD10 expression in the spinal cord

Recently, it was shown that FZD10 seems to interact with Wnt1 and Wnt3a in vitro as demonstrated by an in situ proximity ligation assay (Galli et al., 2014). We also found that FZD10 expression was strongly up-regulated and ventrally expanded in spinal cords co-electroporated with Wnt1 and Wnt3a. Thus, we attempted to determine which Wnts affect FZD10 expression in vivo; embryos were electroporated with Wnt1 and Wnt3a individually. We found that FZD10 expression was upregulated and ventrally extended after Wnt1 overexpression but it was not affected following Wnt3a overexpression (Chapter 5). This demonstrates that FZD10 expression in the dorsal spinal cord responds exclusively to Wnt1 and thus FZD10 may mediate Wnt1 function in vivo in this context. These data encouraged us to examine FZD10 function and interactions during spinal cord development (see 7-7). Many in vivo and in vitro studies have found no interaction between Wnt3a and FZD10; FZD10 did not seem to synergise with Wnt3a in the *Xenopus* animal cap assays (Kawakami et al., 2000b). Research from the Wheeler lab showed that FZD10 synergises with Wnt1 and Wnt8 (but not with Wnt3a) and induces axis duplication in *Xenopus* embryos (Garcia-Morales et al., 2009). In addition, FZD10-CRD was not able to interact with Wnt3a, as shown by a co-immunoprecipitation experiment (Carmon and Loose, 2010). Thus, our findings as well as those of others suggest that FZD10 does not seem to bind Wnt3a. Therefore, Wnt3a may activate different FZDs, such as FZD1 and FZD3, in the spinal cord. Due to time limitations, we were unable to conduct any further experimentation to test this, however, it has been shown that Wnt3a can mediate canonical Wnt signalling through FZD1 in hippocampal neurons and PC12 cells (Chacon et al., 2008).

## **7-7 FZD10 function during spinal cord neurogenesis**

FZD10 has the ability to function through canonical Wnt signalling as injection of human or *Xenopus* FZD10 into the ventral marginal zone (VMZ) results in partial axis formation in early *Xenopus* embryos (Garcia-Morales et al., 2009; Terasaki et al., 2002). Also FZD10 can interact with Wnt1 and the phenotype of FZD10 knockdown can be rescued by  $\beta$ -catenin in *Xenopus* embryos (Garcia-Morales et al., 2009). Additionally, we showed that FZD10 expression is up-regulated by Wnt1 in chick spinal cord (Chapter 5).

Loss of function in *Xenopus* shows that FZD10 is required for generation of sensory neurons (Garcia-Morales et al., 2009). Furthermore, in mouse P19 cells, in which neural differentiation is induced by retinoic acid, overexpression of *Xenopus* FZD10 results in an increase in the number of neurons generated, while siRNA knockdown of endogenous mouse FZD10 inhibits neurogenesis (Garcia-Morales et al., 2009). Here, we further investigated FZD10 function in the dorsal ventral patterning of the spinal cord in vivo.

### **7-7-1 FZD10 knockdown reduces cell proliferation and inhibits neurogenesis in spinal cord**

Different approaches, such as loss and gain of function experiments and rescue experiments, were applied in vivo in order to study how FZD10 is involved in spinal cord development and in Wnt signal transduction (Chapter 6). shRNA was used to knock-down FZD10 in the spinal cord. Chick neural tubes were electroporated with FZD10 shRNA vectors and then they were assessed. We found that targeting FZD10 by

shRNA vectors reduced FZD10 expression. Furthermore, the electroporated side of the spinal cord was smaller compared to the control. We found that the reduction in the size of the spinal cord was a consequence of a significant decrease in the number of proliferative cells in the ventricular zone, demonstrated by pH3 staining and cell counting (Fig. 6.1 and Fig. 6.2). This is consistent with the role of canonical Wnt in cell proliferation. In addition, domains of dorsal progenitors were slightly affected after FZD10 knockdown as judged by Pax6 and Pax7 expression. Neurogenesis was affected as Lhx1/5 and Tuj-1 expressions were reduced (Fig. 6.3). Our results demonstrate that FZD10 knockdown inhibits proliferation of neural progenitors, which results in a reduction in interneuron differentiation.

#### **7-7-2 FZD10 knockdown rescues the Wnt1-induced phenotype**

We previously found that Wnt1 overexpression up-regulated FZD10 expression but it was not affected by Wnt3a overexpression (Chapter 5). We further investigated FZD10 requirements for Wnt1 and/or Wnt3a activity in the spinal cord. Therefore, we performed rescue experiments by electroporating Wnt1 or Wnt3a with FZD10 shRNA in neural tubes. Then, the embryos were analysed using neural markers Pax6 and Pax7. We found that FZD10 is required for Wnt1-induced dorsalisation of the neural tube as FZD10 knockdown by shRNA rescued the Wnt1 overexpression phenotype. In this experiment, the ventral expansion of the expression domains of Pax6 and Pax7 was reduced in the electroporated half of the spinal cord. Moreover, a vast majority of the embryos (80%) were rescued by FZD10 shRNA electroporation. In contrast, the Wnt3a overexpression phenotype was not affected, as ventral expansion of dorsal genes Pax6 and Pax7 was not altered after FZD10 knockdown (Fig. 6.5 and Fig. 6.6). These results

showed that FZD10 mediates Wnt1 signalling in vivo in the spinal cord. They also confirmed our previous observations that demonstrate that FZD10 only interacted with Wnt1 in the spinal cord, but it does not seem to interact with Wnt3a in vivo (Fig. 7.1).

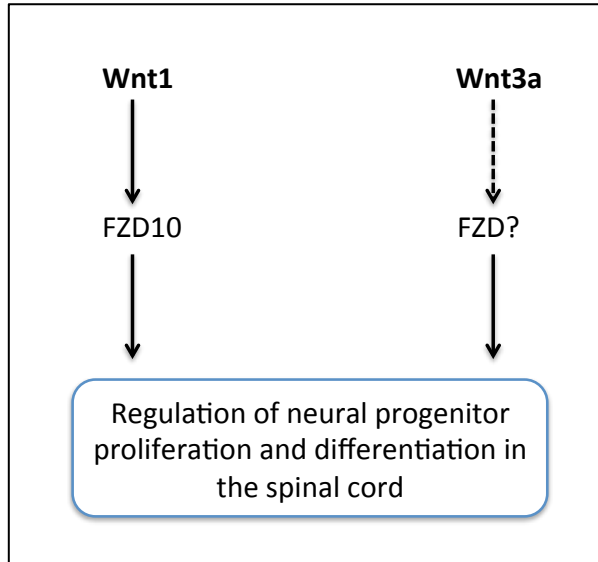


**Fig. 7.1** proposed model for Wnt1 and Wnt3a signalling in the spinal cord.

### **7-7-3 FZD10 overexpression affects neural progenitors and neural differentiation markers**

To further investigate the role of FZD10 in spinal cord development, a full-length cDNA of FZD10 was subcloned into expression vector (pCAB-IRES-GFP) and was introduced into chick neural tubes by in vivo electroporation. Embryos were analysed after 48 or 72 hours post-electroporation (Chapter 6). The effects were assessed using neural markers for different neural cells. Overexpression of FZD10 led to cell-autonomous inhibitory effects in neural progenitors and neurogenesis. The expression domains of Pax6 and Pax7 were reduced and dorsally shifted on the experimental side of the spinal cord as compared to the control (Fig. 6.9). This suggests that the size of the

dorsal progenitor domain was reduced. In contrast, the Nkx2.2 expression domain (a ventral marker) was moderately expanded on the electroporated half of the spinal cord (Fig. 6.9).

We also found that neurogenesis was inhibited as differentiated neuron markers were repressed (Fig. 6.10 and Fig. 6.11). Lhx1/5 expression was severely reduced and it was lost in the ventral interneurons. There were fewer Islet-1 positive cells on the electroporated side of spinal cord, but motoneurons were not affected in the ventral spinal cord. In addition, Tuj-1 expression was repressed along the dorsal-ventral spinal cord in embryos electroporated with FZD10.

These results show inhibitory effect after FZD10 overexpression, it was anticipated that if FZD10 activated canonical Wnt signalling, its overexpression would promote proliferation and neurogenesis in the dorsal spinal cord. However, it has been shown that Wg signalling was attenuated by dFZD3 up-regulation in *Drosophila* (Sato et al., 1999) and this is similar to our observation. Thus, our results may suggest that full-length cFZD10 interferes in a dominant negative manner, leading to inhibition of the pathway and inhibition of proliferation and differentiation in the spinal cord. This is supported by a study reporting that overexpression of full-length cFZD1 or cFZD7 mimics the effect of overexpression of putative dominant-negative forms of these two FZDs, which results in a severe reduction in the size of the cartilage element in the developing chick wing (Hartmann and Tabin, 2000). Other possibilities are that overexpressed FZD10 may interfere with non-canonical Wnt or that FZD10 requires co-receptors to activate canonical Wnt signaling effectively (see 7-7-3 and 7-7-4).

### **7-7-3 FZD10 overexpression severely affects the actin cytoskeleton in the spinal cord**

We sought to further explore FZD10 function in the cell structure cytoskeleton of the spinal cord and to explain inhibitory effects of FZD10 overexpression in vivo (Chapter 6). Therefore, FZD10 was electroporated in chick neural tubes and markers for apical and basal cell surfaces were used. We found that FZD10 overexpression led to a reduction in phalloidin staining, which was severely disrupted on the apical lumen of the spinal cord. Interestingly, Laminin expression was not altered on the basal side of the spinal cords in embryos electroporated with FZD10 (Fig. 6.12). It was clear that phalloidin staining was disrupted in the apical surface of the lumen in the spinal cord following FZD10 overexpression, suggesting that F-actin failed to accumulate on the apical side. These data indicate that overexpressed FZD10 could affect the polarity of cells in the spinal cord. This might also suggest that overexpressed FZD10 may disrupt non-canonical Wnt signalling, in particular the PCP pathway. Consistent with our data, Fukukawa and colleagues (2009) showed that overexpressed FZD10 severely disrupts the assembly of actin stress fibres in HuBM-Bmi1-hT-immortalized mesenchymal stem cells and in 1273/99 cells. Furthermore, it inhibits RhoA activity in a synovial sarcoma cell line (SYO-1 cells), enhances the phosphorylation of Dvl2 and Dvl3 and activates the Rac1–JNK pathway (Fukukawa et al., 2009). These researchers proposed that overexpressed FZD10 affects the actin cytoskeleton as a result of its interference with non-canonical Wnt signalling and by regulating RhoA activity. Therefore, our data and that of others suggest that FZD10 can also function through non-canonical Wnt signalling. FZDs are known to signal through multiple Wnt pathways including Wnt/ $\beta$ -catenin and Wnt/PCP signalling. For example, FZD1, 2 and 7 are shown to be involved in both types of Wnt signalling (Gros et al., 2009; Linker et al., 2003; Medina et al.,

2000; Sumanas et al., 2000; Yu et al., 2010).

#### **7-7-4 FZD10 interacts with Lrp6 to mediate Wnt1 activity in vivo in the spinal cord**

Lrp6 is a FZD co-receptor, binds Wnt1 and is necessary for the activation of Wnt signalling (He et al., 2004; MacDonald and He et al, 2012; Tamai et al., 2000). Importantly, it is expressed in neural tube and its mutations result in neural tube defects including effects in patterning, failure of neural tube closure and disruption in cell polarity (Allache et al., 2014; Gray et al., 2013; Houston and Wylie, 2002; Pinson et al., 2000). Therefore, we studied the function of Lrp6 and tested its requirement for FZD10 and Wnt1-induced patterning defects in chick spinal cords (Chapter 6). We found that hLrp6 misexpression did not have any pronounced effects on Pax3 and Pax7 expression domains, which are dorsal markers and are activated by canonical Wnt in the spinal cord (Fig. 6.13). This could suggest that hLrp6 gain of function did not seem to affect patterning on its own in chick spinal cord. This is consistent with experiments performed on mice in which the hLrp6 gain of function did not seem to regulate neural specification, whereas hLrp6 loss of function resulted in a reduction in neural fold size and affected the Pax6 expression domain (Gray et al., 2013). However, we observed that hLrp6 co-electroporation with FZD10 resulted in a positive effect on Pax7 expression, suggesting that hLrp6 partially rescues the inhibitory effects of FZD10 overexpression. We also found that FZD10 co-electroporation with Wnt1 led to a reduction in the Wnt1 phenotype, but when hLrp6 was co-electroporated with Wnt1 and FZD10 there was a striking ventral expansion of the dorsal neural progenitor domains and the spinal cord was strongly dorsalized (Fig. 6.14 and Fig. 6.15). Moreover, the overall size of the spinal cord was much larger and the overgrowth was apparent on the electroporated side of the spinal cord in the electroporated embryos. We also compared

the ventral expansion of Pax7 expression in spinal cords electroporated with Wnt1 alone to spinal cords co-electroporated with Wnt1, FZD10 and hLrp6. We found that the expansion of Pax7 expression doubled in size and increased 1.9-fold in the spinal cords that were co-electroporated with Wnt1 and both receptors (FZD10/Lrp6) (Chapter 6; Fig. 6.14). These results indicate that Lrp6 is required for FZD10 to mediate Wnt1 biological activity in vivo in the spinal cord. This also suggests the mechanism by which Wnt1 regulates proliferation and patterning in the spinal cord involves an interaction with both FZD10 and Lrp6 (Fig. 7.2). It would be good to investigate this mechanism more by performing luciferase assay experiments (Wnt signalling reporter; Top-flash) in the neural tube in the future as shown in Alvarez-Medina et al., 2008.

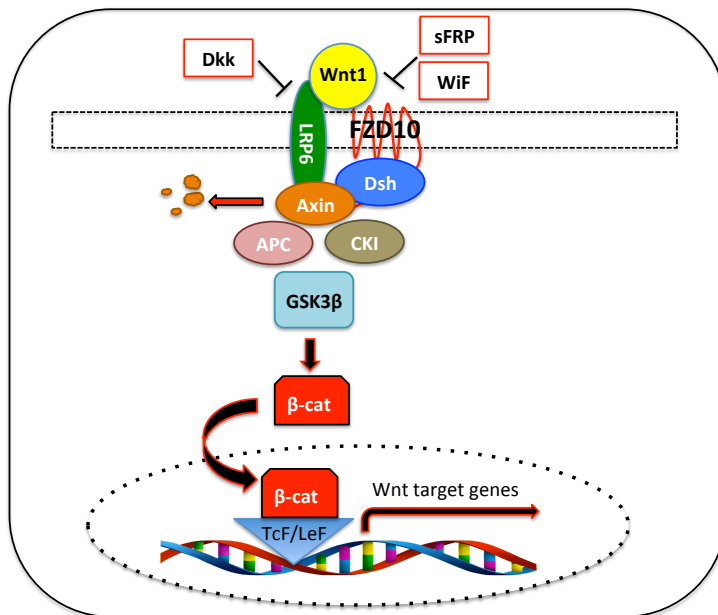


**Fig. 7.2 Schematic representation of Wnt1/FZD10/Lrp6 signalling model.** Wnt1 binds to FZD10 and Lrp6 which then activate a downstream pathway (canonical Wnt signalling) to regulate proliferation, patterning and neural differentiation in chick spinal cords.

## **7-8 Conclusion**

We established a complete expression profile for all chick FZDs in the spinal cord and identified six FZDs that are expressed in the spinal cord (Chapter 3). FZD10 expression was established in the dorsal domain of the spinal cord (Chapter 4). Wnt1 and Wnt3a activate dorsal genes, including FZD10, whereas they inhibit ventral FZD (FZD7) (Chapter 5). Wnt1 overexpression up-regulates FZD10 expression in the dorsal spinal cord. FZD10 knockdown significantly decreases cell proliferation and neurogenesis as well as rescues the Wnt1-induced phenotype (Chapter 6). Interestingly, FZD10 overexpression results in cell-autonomous effects in the spinal cord, leading to a reduction in the dorsal progenitor domains in the dorsal spinal cord. It also inhibits the differentiation of interneurons and disrupts the actin cytoskeleton of the spinal cord (Chapter 6). We uncovered a potential role for FZD10 in non-canonical Wnt signalling, as its overexpression affects F-actin accumulation in the apical surface of the spinal cord. We also demonstrated *in vivo* that Wnt1 mediated effects on dorso-ventral neural tube patterning involves FZD10 and Lrp6, which then activate a downstream pathway (canonical Wnt signalling) to regulate proliferation, patterning and neural differentiation in chick spinal cords (Fig. 7.2).

## References:

- Abu-Elmagd, M., C. Garcia-Morales and G. N. Wheeler (2006). "Frizzled7 mediates canonical Wnt signaling in neural crest induction." Developmental biology **298**(1): 285-298.
- Adler, P. N. and H. Lee (2001). "Frizzled signaling and cell–cell interactions in planar polarity." Current opinion in cell biology **13**(5): 635-640.
- Allache, R., S. Lachance, M. C. Guyot, P. De Marco, E. Merello, M. J. Justice, V. Capra and Z. Kibar (2014). "Novel mutations in Lrp6 orthologs in mouse and human neural tube defects affect a highly dosage-sensitive Wnt non-canonical planar cell polarity pathway." Human molecular genetics **23**(7): 1687-1699.
- Alvarez, A. R., J. A. Godoy, K. Mullendorff, G. H. Olivares, M. Bronfman and N. C. Inestrosa (2004). "Wnt-3a overcomes  $\beta$ -amyloid toxicity in rat hippocampal neurons." Experimental cell research **297**(1): 186-196.
- Alvarez-Medina, R., J. Cayuso, T. Okubo, S. Takada and E. Martí (2008). "Wnt canonical pathway restricts graded Shh/Gli patterning activity through the regulation of Gli3 expression." Development **135**(2): 237-247.
- Avilés, E. C. and E. T. Stoeckli (2015). "Canonical Wnt signaling is required for commissural axon guidance." Developmental neurobiology.
- Baker, J. C., R. S. Beddington and R. M. Harland (1999). "Wnt signaling in *Xenopus* embryos inhibits bmp4 expression and activates neural development." Genes & development **13**(23): 3149-3159.
- Barnes, M. R., D. M. Duckworth and L. J. Beeley (1998). "Frizzled proteins constitute a novel family of G protein-coupled receptors, most closely related to the secretin family." Trends in pharmacological sciences **19**(10): 399-400.
- Becker, C. G. and R. D. del Corral (2015). "Neural development and regeneration: it's all in your spinal cord." Development **142**(5): 811-816.
- Bertrand, V., C. Hudson, D. Caillol, C. Popovici and P. Lemaire (2003). "Neural tissue in ascidian embryos is induced by FGF9/16/20, acting via a combination of maternal GATA and Ets transcription factors." Cell **115**(5): 615-627.
- Bhanot, P., M. Brink, C. H. Samos, J.-C. Hsieh, Y. Wang, J. P. Macke, D. Andrew, J. Nathans and R. Nusse (1996). "A new member of the frizzled family from *Drosophila* functions as a Wingless receptor."
- Bhanot, P., M. Fish, J. A. Jemison, R. Nusse, J. Nathans and K. M. Cadigan (1999). "Frizzled and Dfrizzled-2 function as redundant receptors for Wingless during *Drosophila* embryonic development." Development **126**(18): 4175-4186.
- Bhat, K. M. (1998). "frizzled and frizzled 2 play a partially redundant role in wingless signaling and have similar requirements to wingless in neurogenesis." Cell **95**(7): 1027-1036.

- Bhat, R. A., B. Stauffer, B. S. Komm and P. V. Bodine (2007). "Structure–Function analysis of secreted frizzled–related protein–1 for its Wnt antagonist function." Journal of cellular biochemistry **102**(6): 1519-1528.
- Blumberg, B., J. Bolado, T. A. Moreno, C. Kintner, R. M. Evans and N. Papalopulu (1997). "An essential role for retinoid signaling in anteroposterior neural patterning." Development **124**(2): 373-379.
- Bonner, J., S. L. Gribble, E. S. Veien, O. B. Nikolaus, G. Weidinger and R. I. Dorsky (2008). "Proliferation and patterning are mediated independently in the dorsal spinal cord downstream of canonical Wnt signaling." Developmental biology **313**(1): 398-407.
- Borello, U., V. Buffa, C. Sonnino, R. Melchionna, E. Vivarelli and G. Cossu (1999). "Differential expression of the Wnt putative receptors Frizzled during mouse somitogenesis." Mechanisms of development **89**(1): 173-177.
- Bravo, D. T., Y.-L. Yang, K. Kuchenbecker, M.-S. Hung, Z. Xu, D. M. Jablons and L. You (2013). "Frizzled-8 receptor is activated by the Wnt-2 ligand in non-small cell lung cancer." BMC cancer **13**(1): 316.
- Briscoe, J., A. Pierani, T. M. Jessell and J. Ericson (2000). "A homeodomain protein code specifies progenitor cell identity and neuronal fate in the ventral neural tube." Cell **101**(4): 435-445.
- Cadigan, K. M., M. P. Fish, E. J. Rulifson and R. Nusse (1998). "Wingless repression of Drosophila frizzled 2 expression shapes the Wingless morphogen gradient in the wing." Cell **93**(5): 767-777.
- Cadigan, K. M. and Y. I. Liu (2006). "Wnt signaling: complexity at the surface." Journal of cell science **119**(3): 395-402.
- Cadigan, K. M. and R. Nusse (1997). "Wnt signaling: a common theme in animal development." Genes & development **11**(24): 3286-3305.
- Caricasole, A., A. Copani, F. Caraci, E. Aronica, A. J. Rozemuller, A. Caruso, M. Storto, G. Gaviraghi, G. C. Terstappen and F. Nicoletti (2004). "Induction of Dickkopf-1, a negative modulator of the Wnt pathway, is associated with neuronal degeneration in Alzheimer's brain." The Journal of neuroscience **24**(26): 6021-6027.
- Carmon, K. S. and D. S. Loose (2010). "Development of a bioassay for detection of Wnt-binding affinities for individual frizzled receptors." Analytical biochemistry **401**(2): 288-294.
- Chacon, M. A., L. Varela–Nallar and N. C. Inestrosa (2008). "Frizzled–1 is involved in the neuroprotective effect of Wnt3a against A $\beta$  oligomers." Journal of cellular physiology **217**(1): 215-227.
- Chapman, S. C., R. Brown, L. Lees, G. C. Schoenwolf and A. Lumsden (2004). "Expression analysis of chick Wnt and frizzled genes and selected inhibitors in early chick patterning." Developmental dynamics **229**(3): 668-676.

Chen, C. and G. Struhl (1999). "Wingless transduction by the Frizzled and Frizzled2 proteins of *Drosophila*." Development **126**(23): 5441-5452.

Chenn, A. and C. A. Walsh (2003). "Increased neuronal production, enlarged forebrains and cytoarchitectural distortions in  $\beta$ -catenin overexpressing transgenic mice." Cerebral Cortex **13**(6): 599-606.

Chesnutt, C., L. W. Burrus, A. M. Brown and L. Niswander (2004). "Coordinate regulation of neural tube patterning and proliferation by TGF $\beta$  and WNT activity." Developmental biology **274**(2): 334-347.

Clevers, H. (2006). "Wnt/ $\beta$ -catenin signaling in development and disease." Cell **127**(3): 469-480.

Colas, J. F. and G. C. Schoenwolf (2001). "Towards a cellular and molecular understanding of neurulation." Developmental dynamics **221**(2): 117-145.

Curtin, J. A., E. Quint, V. Tsipouri, R. M. Arkell, B. Cattanach, A. J. Copp, D. J. Henderson, N. Spurr, P. Stanier and E. M. Fisher (2003). "Mutation of *Celsr1* disrupts planar polarity of inner ear hair cells and causes severe neural tube defects in the mouse." Current Biology **13**(13): 1129-1133.

Dann, C. E., J.-C. Hsieh, A. Rattner, D. Sharma, J. Nathans and D. J. Leahy (2001). "Insights into Wnt binding and signalling from the structures of two Frizzled cysteine-rich domains." Nature **412**(6842): 86-90.

Davidson, G., B. Mao, I. del Barco Barrantes and C. Niehrs (2002). "Kremen proteins interact with *Dickkopf1* to regulate anteroposterior CNS patterning." Development **129**(24): 5587-5596.

Davis, E. K., Y. Zou and A. Ghosh (2008). "Wnts acting through canonical and noncanonical signaling pathways exert opposite effects on hippocampal synapse formation." Neural development **3**(1): 32.

De Calisto, J., C. Araya, L. Marchant, C. F. Riaz and R. Mayor (2005). "Essential role of non-canonical Wnt signalling in neural crest migration." Development **132**(11): 2587-2597.

De Ferrari, G., M. Chacon, M. Barria, J. Garrido, J. Godoy, G. Olivares, A. Reyes, A. Alvarez, M. Bronfman and N. Inestrosa (2003). "Activation of Wnt signaling rescues neurodegeneration and behavioral impairments induced by  $\beta$ -amyloid fibrils." Molecular psychiatry **8**(2): 195-208.

De Robertis, E., J. Larrain, M. Oelgeschläger and O. Wessely (2000). "The establishment of Spemann's organizer and patterning of the vertebrate embryo." Nature Reviews Genetics **1**(3): 171-181.

De Robertis, E. M. and H. Kuroda (2004). "Dorsal-ventral patterning and neural induction in *Xenopus* embryos." Annual review of cell and developmental biology **20**: 285.

De Robertis, E. M. and Y. Sasai (2000). "A common plan for dorsoventral patterning in Bilateria." Shaking the Tree: Readings from Nature in the History of Life: 89.

- Deardorff, M. A. and P. S. Klein (1999). "Xenopus frizzled-2 is expressed highly in the developing eye, otic vesicle and somites." Mechanisms of development **87**(1): 229-233.
- Deardorff, M. A., C. Tan, L. J. Conrad and P. S. Klein (1998). "Frizzled-8 is expressed in the Spemann organizer and plays a role in early morphogenesis." Development **125**(14): 2687-2700.
- Deardorff, M. A., C. Tan, J.-P. Saint-Jeannet and P. S. Klein (2001). "A role for frizzled 3 in neural crest development." Development **128**(19): 3655-3663.
- Dessaud, E., A. P. McMahon and J. Briscoe (2008). "Pattern formation in the vertebrate neural tube: a sonic hedgehog morphogen-regulated transcriptional network." Development **135**(15): 2489-2503.
- Dickinson, M. E., R. Krumlauf and A. P. McMahon (1994). "Evidence for a mitogenic effect of Wnt-1 in the developing mammalian central nervous system." Development **120**(6): 1453-1471.
- Dijksterhuis, J. P., B. Baljinnyam, K. Stanger, H. O. Sercan, Y. Ji, O. Andres, J. S. Rubin, R. N. Hannoush and G. Schulte (2015). "Systematic Mapping of WNT-FZD Protein Interactions Reveals Functional Selectivity by Distinct WNT-FZD Pairs." Journal of Biological Chemistry **290**(11): 6789-6798.
- Domingos, P. M., N. Itasaki, C. M. Jones, S. Mercurio, M. G. Sargent, J. C. Smith and R. Krumlauf (2001). "The Wnt/ $\beta$ -catenin pathway posteriorizes neural tissue in *Xenopus* by an indirect mechanism requiring FGF signalling." Developmental biology **239**(1): 148-160.
- Dorsky, R. I., R. T. Moon and D. W. Raible (1998). "Control of neural crest cell fate by the Wnt signalling pathway." Nature **396**(6709): 370-373.
- Dos Santos, M. A. and M. P. Smidt (2011). "En1 and Wnt signaling in midbrain dopaminergic neuronal development." Neural Dev. **6**: 23.
- Du, S. J., S. M. Purcell, J. L. Christian, L. L. McGrew and R. T. Moon (1995). "Identification of distinct classes and functional domains of Wnts through expression of wild-type and chimeric proteins in *Xenopus* embryos." Molecular and Cellular Biology **15**(5): 2625-2634.
- Fuhrmann, S., M. R. Stark and S. Heller (2003). "Expression of Frizzled genes in the developing chick eye." Gene expression patterns **3**(5): 659-662.
- Fukukawa, C., H. Hanaoka, S. Nagayama, T. Tsunoda, J. Toguchida, K. Endo, Y. Nakamura and T. Katagiri (2008). "Radioimmunotherapy of human synovial sarcoma using a monoclonal antibody against FZD10." Cancer science **99**(2): 432-440.
- Fukukawa, C., S. Nagayama, T. Tsunoda, J. Toguchida, Y. Nakamura and T. Katagiri (2009). "Activation of the non-canonical Dvl–Rac1–JNK pathway by Frizzled homologue 10 in human synovial sarcoma." Oncogene **28**(8): 1110-1120.
- Galli, L. M., R. N. Munji, S. C. Chapman, A. Easton, L. Li, O. Onguka, J. S. Ramahi, R.

Suriben, L. A. Szabo and C. Teng (2014). "Frizzled10 mediates WNT1 and WNT3A signaling in the dorsal spinal cord of the developing chick embryo." Developmental Dynamics **243**(6): 833-843.

Galli, L. M., K. Willert, R. Nusse, Z. Yablonka-Reuveni, T. Nohno, W. Denetclaw and L. W. Burrus (2004). "A proliferative role for Wnt-3a in chick somites." Developmental biology **269**(2): 489-504.

Galli, S., D. M. Lopes, R. Ammari, J. Kopra, S. E. Millar, A. Gibb and P. C. Salinas (2014). "Deficient Wnt signalling triggers striatal synaptic degeneration and impaired motor behaviour in adult mice." Nature communications **5**.

Gamse, J. and H. Sive (2000). "Vertebrate anteroposterior patterning: the *Xenopus* neurectoderm as a paradigm." BioEssays **22**(11): 976-986.

Garcia-Morales, C., C.-H. Liu, M. Abu-Elmagd, M. K. Hajihosseini and G. N. Wheeler (2009). "Frizzled-10 promotes sensory neuron development in *Xenopus* embryos." Developmental biology **335**(1): 143-155.

Gilbert, S. F. (2010). Developmental biology. Sunderland, Mass., Sinauer Associates Publishers.

Gordon, M. D. and R. Nusse (2006). "Wnt signaling: multiple pathways, multiple receptors, and multiple transcription factors." Journal of Biological Chemistry **281**(32): 22429-22433.

Gray, J. D., S. Kholmanskikh, B. S. Castaldo, A. Hansler, H. Chung, B. Klotz, S. Singh, A. M. Brown and M. E. Ross (2013). "LRP6 exerts non-canonical effects on Wnt signaling during neural tube closure." Human molecular genetics **22**(21): 4267-4281.

Greene, N. D. and A. J. Copp (2009). "Development of the vertebrate central nervous system: formation of the neural tube." Prenatal diagnosis **29**(4): 303-311.

Gros, J., O. Serralbo and C. Marcelle (2009). "WNT11 acts as a directional cue to organize the elongation of early muscle fibres." Nature **457**(7229): 589-593.

Gubb, D. and A. García-Bellido (1982). "A genetic analysis of the determination of cuticular polarity during development in *Drosophila melanogaster*." Journal of embryology and experimental morphology **68**(1): 37-57.

Guo, N., C. Hawkins and J. Nathans (2004). "Frizzled6 controls hair patterning in mice." Proceedings of the National Academy of Sciences of the United States of America **101**(25): 9277-9281.

Gurney, A., F. Axelrod, C. J. Bond, J. Cain, C. Chartier, L. Donigan, M. Fischer, A. Chaudhari, M. Ji and A. M. Kapoun (2012). "Wnt pathway inhibition via the targeting of Frizzled receptors results in decreased growth and tumorigenicity of human tumors." Proceedings of the National Academy of Sciences **109**(29): 11717-11722.

Hall, A. C., F. R. Lucas and P. C. Salinas (2000). "Axonal remodeling and synaptic differentiation in the cerebellum is regulated by WNT-7a signaling." Cell **100**(5): 525-535.

- Hamblet, N. S., N. Lijam, P. Ruiz-Lozano, J. Wang, Y. Yang, Z. Luo, L. Mei, K. R. Chien, D. J. Sussman and A. Wynshaw-Boris (2002). "Dishevelled 2 is essential for cardiac outflow tract development, somite segmentation and neural tube closure." Development **129**(24): 5827-5838.
- Harland, R. and J. Gerhart (1997). "Formation and function of Spemann's organizer." Annual review of cell and developmental biology **13**(1): 611-667.
- Hartmann, C. and C. J. Tabin (2000). "Dual roles of Wnt signaling during chondrogenesis in the chicken limb." Development **127**(14): 3141-3159.
- He, X., J.-P. Saint-Jeannet, Y. Wang, J. Nathans, I. Dawid and H. Varmus (1997). "A member of the Frizzled protein family mediating axis induction by Wnt-5A." Science **275**(5306): 1652-1654.
- He, X., M. Semenov, K. Tamai and X. Zeng (2004). "LDL receptor-related proteins 5 and 6 in Wnt/ $\beta$ -catenin signaling: arrows point the way." Development **131**(8): 1663-1677.
- Helms, A. W. and J. E. Johnson (2003). "Specification of dorsal spinal cord interneurons." Current opinion in neurobiology **13**(1): 42-49.
- Herrera, A., M. Saade, A. Menendez, E. Marti and S. Pons (2014). "Sustained Wnt/ $\beta$ -catenin signalling causes neuroepithelial aberrations through the accumulation of aPKC at the apical pole." Nature communications **5**.
- Hofmeister, W. and B. Key (2013). "Frizzled-3a and Wnt-8b genetically interact during forebrain commissural formation in embryonic zebrafish." Brain research **1506**: 25-34.
- Holcombe, R., J. Marsh, M. Waterman, F. Lin, T. Milovanovic and T. Truong (2002). "Expression of Wnt ligands and Frizzled receptors in colonic mucosa and in colon carcinoma." Molecular Pathology **55**(4): 220.
- Holowacz, T. and S. Sokol (1999). "FGF is required for posterior neural patterning but not for neural induction." Developmental biology **205**(2): 296-308.
- Houston, D. W. and C. Wylie (2002). "Cloning and expression of Xenopus Lrp5 and Lrp6 genes." Mechanisms of development **117**(1): 337-342.
- Hsieh, J.-C., A. Rattner, P. M. Smallwood and J. Nathans (1999). "Biochemical characterization of Wnt-frizzled interactions using a soluble, biologically active vertebrate Wnt protein." Proceedings of the National Academy of Sciences **96**(7): 3546-3551.
- Hua, Z. L., S. Jeon, M. J. Caterina and J. Nathans (2014). "Frizzled3 is required for the development of multiple axon tracts in the mouse central nervous system." Proceedings of the National Academy of Sciences **111**(29): E3005-E3014.
- Hua, Z. L., P. M. Smallwood and J. Nathans (2013). "Frizzled3 controls axonal development in distinct populations of cranial and spinal motor neurons." Elife **2**: e01482.
- Huang, H.-C. and P. S. Klein (2004). "The Frizzled family: receptors for multiple signal

transduction pathways." Genome biology **5**(7): 234.

Ikeya, M., S. M. Lee, J. E. Johnson, A. P. McMahon and S. Takada (1997). "Wnt signalling required for expansion of neural crest and CNS progenitors." Nature **389**(6654): 966-970.

Ille, F., S. Atanasoski, S. Falk, L. M. Ittner, D. Märki, S. Büchmann-Møller, H. Wurdak, U. Suter, M. M. Taketo and L. Sommer (2007). "Wnt/BMP signal integration regulates the balance between proliferation and differentiation of neuroepithelial cells in the dorsal spinal cord." Developmental biology **304**(1): 394-408.

Inestrosa, N. C. and L. Varela-Nallar (2014). "Wnt signaling in the nervous system and in Alzheimer's disease." Journal of molecular cell biology **6**(1): 64-74.

Ishikawa, T.-o., Y. Tamai, A. M. Zorn, H. Yoshida, M. F. Seldin, S.-i. Nishikawa and M. M. Taketo (2001). "Mouse Wnt receptor gene *Fzd5* is essential for yolk sac and placental angiogenesis." Development **128**(1): 25-33.

Jacob, J. and J. Briscoe (2003). "Gli proteins and the control of spinal-cord patterning." EMBO reports **4**(8): 761-765.

Janda, C. Y., D. Waghray, A. M. Levin, C. Thomas and K. C. Garcia (2012). "Structural basis of Wnt recognition by Frizzled." Science **337**(6090): 59-64.

Janssens, N., L. Andries, M. Janicot, T. Perera and A. Bakker (2004). "Alteration of frizzled expression in renal cell carcinoma." Tumor Biology **25**(4): 161-171.

Janssens, N., M. Janicot and T. Perera (2006). "The Wnt-dependent signaling pathways as target in oncology drug discovery." Investigational new drugs **24**(4): 263-280.

Jessell, T. M. (2000). "Neuronal specification in the spinal cord: inductive signals and transcriptional codes." Nature Reviews Genetics **1**(1): 20-29.

Kadzik, R. S., E. D. Cohen, M. P. Morley, K. M. Stewart, M. M. Lu and E. E. Morrisey (2014). "Wnt ligand/Frizzled 2 receptor signaling regulates tube shape and branch-point formation in the lung through control of epithelial cell shape." Proceedings of the National Academy of Sciences **111**(34): 12444-12449.

Karasawa, T., H. Yokokura, J. Kitajewski and P. J. Lombroso (2002). "Frizzled-9 is activated by Wnt-2 and functions in Wnt/ $\beta$ -catenin signaling." Journal of Biological Chemistry **277**(40): 37479-37486.

Kawakami, Y., N. Wada, S.-i. Nishimatsu, C. Komaguchi, S. Noji and T. Nohno (2000). "Identification of chick frizzled-10 expressed in the developing limb and the central nervous system." Mechanisms of development **91**(1): 375-378.

Kawakami, Y., N. Wada, S. i. Nishimatsu and T. Nohno (2000). "Involvement of Frizzled-10 in Wnt-7a signaling during chick limb development." Development, growth & differentiation **42**(6): 561-569.

Kawano, Y. and R. Kypta (2003). "Secreted antagonists of the Wnt signalling pathway."

Journal of cell science **116**(13): 2627-2634.

Kemp, C. R., E. Willems, D. Wawrzak, M. Hendrickx, T. Agbor Agbor and L. Leyns (2007). "Expression of Frizzled5, Frizzled7, and Frizzled10 during early mouse development and interactions with canonical Wnt signaling." Developmental Dynamics **236**(7): 2011-2019.

Kengaku, M., V. Twombly and C. Tabin (1997). Expression of Wnt and Frizzled genes during chick limb bud development. Cold Spring Harbor symposia on quantitative biology, Cold Spring Harbor Laboratory Press.

Kiecker, C. and C. Niehrs (2001). "A morphogen gradient of Wnt/ $\beta$ -catenin signalling regulates anteroposterior neural patterning in Xenopus." Development **128**(21): 4189-4201.

Kohn, A. D. and R. T. Moon (2005). "Wnt and calcium signaling:  $\beta$ -catenin-independent pathways." Cell calcium **38**(3): 439-446.

Koike, J., A. Takagi, T. Miwa, M. Hirai, M. Terada and M. Katoh (1999). "Molecular cloning of Frizzled-10, a novel member of the Frizzled gene family." Biochemical and biophysical research communications **262**(1): 39-43.

Komiya, Y. and R. Habas (2008). "Wnt signal transduction pathways." Organogenesis **4**(2): 68-75.

Le Douarin, N. and C. Kalcheim (1999). The neural crest, Cambridge University Press.

Le Dréau, G., L. Garcia-Campmany, M. A. Rabadán, T. Ferronha, S. Tozer, J. Briscoe and E. Martí (2012). "Canonical BMP7 activity is required for the generation of discrete neuronal populations in the dorsal spinal cord." Development **139**(2): 259-268.

Le Dréau, G. and E. Martí (2012). "Dorsal–ventral patterning of the neural tube: a tale of three signals." Developmental neurobiology **72**(12): 1471-1481.

Lee, H.-Y., M. Kléber, L. Hari, V. Brault, U. Suter, M. M. Taketo, R. Kemler and L. Sommer (2004). "Instructive role of Wnt/ $\beta$ -catenin in sensory fate specification in neural crest stem cells." Science **303**(5660): 1020-1023.

Lee, K. J., P. Dietrich and T. M. Jessell (2000). "Genetic ablation reveals that the roof plate is essential for dorsal interneuron specification." Nature **403**(6771): 734-740.

Li, G., C. Luna, J. Qiu, D. L. Epstein and P. Gonzalez (2011). "Role of miR-204 in the regulation of apoptosis, endoplasmic reticulum stress response, and inflammation in human trabecular meshwork cells." Investigative ophthalmology & visual science **52**(6): 2999.

Li, Y. and G. Bu (2005). "LRP5/6 in Wnt signaling and tumorigenesis."

Linker, C., C. Lesbros, M. R. Stark and C. Marcelle (2003). "Intrinsic signals regulate the initial steps of myogenesis in vertebrates." Development **130**(20): 4797-4807.

Liu, C. and J. Nathans (2008). "An essential role for frizzled 5 in mammalian ocular development." Development **135**(21): 3567-3576.

- Liu, G., A. Bafico, V. K. Harris and S. A. Aaronson (2003). "A novel mechanism for Wnt activation of canonical signaling through the LRP6 receptor." Molecular and cellular biology **23**(16): 5825-5835.
- Liu, H., O. Mohamed, D. Dufort and V. A. Wallace (2003). "Characterization of Wnt signaling components and activation of the Wnt canonical pathway in the murine retina." Developmental dynamics **227**(3): 323-334.
- Logan, C. Y. and R. Nusse (2004). "The Wnt signaling pathway in development and disease." Annu. Rev. Cell Dev. Biol. **20**: 781-810.
- Lu, C., E. Robertson and J. Brennan (2004). "The mouse frizzled 8 receptor is expressed in anterior organizer tissues." Gene expression patterns **4**(5): 569-572.
- Lu, D., Y. Zhao, R. Tawatao, H. B. Cottam, M. Sen, L. M. Leoni, T. J. Kipps, M. Corr and D. A. Carson (2004). "Activation of the Wnt signaling pathway in chronic lymphocytic leukemia." Proceedings of the National Academy of Sciences of the United States of America **101**(9): 3118-3123.
- Luo, J., J. Chen, Z.-L. Deng, X. Luo, W.-X. Song, K. A. Sharff, N. Tang, R. C. Haydon, H. H. Luu and T.-C. He (2007). "Wnt signaling and human diseases: what are the therapeutic implications?" Laboratory investigation **87**(2): 97-103.
- Lyuksytova, A. I., C.-C. Lu, N. Milanesio, L. A. King, N. Guo, Y. Wang, J. Nathans, M. Tessier-Lavigne and Y. Zou (2003). "Anterior-posterior guidance of commissural axons by Wnt-frizzled signaling." Science **302**(5652): 1984-1988.
- MacDonald, B. T. and X. He (2012). "Frizzled and LRP5/6 receptors for Wnt/ $\beta$ -catenin signaling." Cold Spring Harbor perspectives in biology **4**(12): a007880.
- MacDonald, B. T., K. Tamai and X. He (2009). "Wnt/ $\beta$ -catenin signaling: components, mechanisms, and diseases." Developmental cell **17**(1): 9-26.
- Mahmood, R., P. Kiefer, S. Guthrie, C. Dickson and I. Mason (1995). "Multiple roles for FGF-3 during cranial neural development in the chicken." Development **121**(5): 1399-1410.
- Malaterre, J., R. G. Ramsay and T. Mantamadiotis (2006). "Wnt-Frizzled signalling and the many paths to neural development and adult brain homeostasis." Frontiers in bioscience: a journal and virtual library **12**: 492-506.
- Mao, B., W. Wu, G. Davidson, J. Marhold, M. Li, B. M. Mechler, H. Delius, D. Hoppe, P. Stanek and C. Walter (2002). "Kremen proteins are Dickkopf receptors that regulate Wnt/ $\beta$ -catenin signalling." Nature **417**(6889): 664-667.
- Marchant, L., C. Linker, P. Ruiz, N. Guerrero and R. Mayor (1998). "The inductive properties of mesoderm suggest that the neural crest cells are specified by a BMP gradient." Developmental biology **198**(2): 319-329.
- Marti, E., D. A. Bumcrot, R. Takada and A. P. McMahon (1995). "Requirement of 19K form of

- Sonic hedgehog for induction of distinct ventral cell types in CNS explants." Nature **375**(6529): 322-325.
- Martí, E., R. Takada, D. A. Bumcrot, H. Sasaki and A. P. McMahon (1995). "Distribution of Sonic hedgehog peptides in the developing chick and mouse embryo." Development **121**(8): 2537-2547.
- Masckauchán, T. N. H. and J. Kitajewski (2006). "Wnt/Frizzled signaling in the vasculature: new angiogenic factors in sight." Physiology **21**(3): 181-188.
- Matise, M. P., D. J. Epstein, H. L. Park, K. A. Platt and A. L. Joyner (1998). "Gli2 is required for induction of floor plate and adjacent cells, but not most ventral neurons in the mouse central nervous system." Development **125**(15): 2759-2770.
- Matsumoto, K., R. Miki, M. Nakayama, N. Tatsumi and Y. Yokouchi (2008). "Wnt9a secreted from the walls of hepatic sinusoids is essential for morphogenesis, proliferation, and glycogen accumulation of chick hepatic epithelium." Developmental biology **319**(2): 234-247.
- Medina, A., W. Reintsch and H. Steinbeisser (2000). "Xenopus frizzled 7 can act in canonical and non-canonical Wnt signaling pathways: implications on early patterning and morphogenesis." Mechanisms of development **92**(2): 227-237.
- Medina, A. and H. Steinbeisser (2000). "Interaction of frizzled 7 and dishevelled in Xenopus." Developmental Dynamics **218**(4): 671-680.
- Megason, S. G. and A. P. McMahon (2002). "A mitogen gradient of dorsal midline Wnts organizes growth in the CNS." Development **129**(9): 2087-2098.
- Millonig, J. H., K. J. Millen and M. E. Hatten (2000). "The mouse Dreher gene *Lmx1a* controls formation of the roof plate in the vertebrate CNS." Nature **403**(6771): 764-769.
- Mo, S. and Z. Cui (2012). Regulation of canonical wnt signaling during development and diseases, INTECH Open Access Publisher.
- Momoi, A., H. Yoda, H. Steinbeisser, F. Fagotto, H. Kondoh, A. Kudo, W. Driever and M. Furutani-Seiki (2003). "Analysis of Wnt8 for neural posteriorizing factor by identifying Frizzled 8c and Frizzled 9 as functional receptors for Wnt8." Mechanisms of development **120**(4): 477-489.
- Moon, R. T., A. D. Kohn, G. V. De Ferrari and A. Kaykas (2004). "WNT and  $\beta$ -catenin signalling: diseases and therapies." Nature Reviews Genetics **5**(9): 691-701.
- Moriwaki, J., E. Kajita, H. Kirikoshi, J. Koike, N. Sagara, Y. Yasuhiko, T. Saitoh, M. Hirai, M. Katoh and K. Shiokawa (2000). "Isolation of Xenopus frizzled-10A and frizzled-10B genomic clones and their expression in adult tissues and embryos." Biochemical and biophysical research communications **278**(2): 377-384.
- Muller, H., R. Samanta and E. Wieschaus (1999). "Wingless signaling in the Drosophila embryo: zygotic requirements and the role of the frizzled genes." Development **126**(3): 577-586.

- Muñoz-Sanjuán, I. and A. H. Brivanlou (2002). "Neural induction, the default model and embryonic stem cells." Nature Reviews Neuroscience **3**(4): 271-280.
- Münsterberg, A., J. Kitajewski, D. A. Bumcrot, A. P. McMahon and A. B. Lassar (1995). "Combinatorial signaling by Sonic hedgehog and Wnt family members induces myogenic bHLH gene expression in the somite." Genes & development **9**(23): 2911-2922.
- Murdoch, J. N., D. J. Henderson, K. Doudney, C. Gaston-Massuet, H. M. Phillips, C. Paternotte, R. Arkell, P. Stanier and A. J. Copp (2003). "Disruption of scribble (Scrb1) causes severe neural tube defects in the circletail mouse." Human Molecular Genetics **12**(2): 87-98.
- Muroyama, Y., M. Fujihara, M. Ikeya, H. Kondoh and S. Takada (2002). "Wnt signaling plays an essential role in neuronal specification of the dorsal spinal cord." Genes & development **16**(5): 548-553.
- Muroyama, Y., H. Kondoh and S. Takada (2004). "Wnt proteins promote neuronal differentiation in neural stem cell culture." Biochemical and biophysical research communications **313**(4): 915-921.
- Nagayama, S., C. Fukukawa, T. Katagiri, T. Okamoto, T. Aoyama, N. Oyaizu, M. Imamura, J. Toguchida and Y. Nakamura (2005). "Therapeutic potential of antibodies against FZD10, a cell-surface protein, for synovial sarcomas." Oncogene **24**(41): 6201-6212.
- Nagayama, S., E. Yamada, Y. Kohno, T. Aoyama, C. Fukukawa, H. Kubo, G. Watanabe, T. Katagiri, Y. Nakamura and Y. Sakai (2009). "Inverse correlation of the up-regulation of FZD10 expression and the activation of  $\beta$ -catenin in synchronous colorectal tumors." Cancer science **100**(3): 405-412.
- Nakamura, H., T. Katahira, T. Sato, Y. Watanabe and J.-i. Funahashi (2004). "Gain-and loss-of-function in chick embryos by electroporation." Mechanisms of development **121**(9): 1137-1143.
- Nam, J.-S., T. J. Turcotte, P. F. Smith, S. Choi and J. K. Yoon (2006). "Mouse cristin/R-spondin family proteins are novel ligands for the Frizzled 8 and LRP6 receptors and activate  $\beta$ -catenin-dependent gene expression." Journal of Biological Chemistry **281**(19): 13247-13257.
- Nasevicius, A., T. M. Hyatt, S. B. Hermanson and S. C. Ekker (2000). "Sequence, expression, and location of zebrafish frizzled 10." Mechanisms of development **92**(2): 311-314.
- Neumann, C. J. and S. M. Cohen (1997). "Long-range action of Wingless organizes the dorsal-ventral axis of the *Drosophila* wing." Development **124**(4): 871-880.
- Nikaido, M., E. Law and R. N. Kelsh (2013). "A systematic survey of expression and function of zebrafish frizzled genes." PloS one **8**(1): e54833.
- Nohno, T., Y. Kawakami, N. Wada, C. Komaguchi and S. Nishimatsu (1999). "Differential expression of the frizzled family involved in Wnt signaling during chick limb development." Cellular and molecular biology (Noisy-le-Grand, France) **45**(5): 653-659.
- Parr, B. A., M. J. Shea, G. Vassileva and A. P. McMahon (1993). "Mouse Wnt genes exhibit

discrete domains of expression in the early embryonic CNS and limb buds." Development **119**(1): 247-261.

Pei, J.-J., E. Braak, H. Braak, I. Grundke-Iqbal, K. Iqbal, B. Winblad and R. F. Cowburn (1999). "Distribution of Active Glycogen Synthase Kinase 3 [beta](GSK-3 [beta]) in Brains Staged for Alzheimer Disease Neurofibrillary Changes." Journal of Neuropathology & Experimental Neurology **58**(9): 1010-1019.

Persson, M., D. Stamatakis, P. te Welscher, E. Andersson, J. Böse, U. Rütter, J. Ericson and J. Briscoe (2002). "Dorsal-ventral patterning of the spinal cord requires Gli3 transcriptional repressor activity." Genes & development **16**(22): 2865-2878.

Piccolo, S., Y. Sasai, B. Lu and E. M. De Robertis (1996). "Dorsoventral patterning in *Xenopus*: inhibition of ventral signals by direct binding of chordin to BMP-4." Cell **86**(4): 589-598.

Pinson, K. I., J. Brennan, S. Monkley, B. J. Avery and W. C. Skarnes (2000). "An LDL-receptor-related protein mediates Wnt signalling in mice." Nature **407**(6803): 535-538.

Placzek, M. (1995). "The role of the notochord and floor plate in inductive interactions." Current opinion in genetics & development **5**(4): 499-506.

Placzek, M., M. Tessier-Lavigne, T. Yamada, T. Jessell and J. Dodd (1990). "Mesodermal control of neural cell identity: floor plate induction by the notochord." Science **250**(4983): 985-988.

Popperl, H., C. Schmidt, V. Wilson, C. Hume, J. Dodd, R. Krumlauf and R. Beddington (1997). "Misexpression of *Cwnt8C* in the mouse induces an ectopic embryonic axis and causes a truncation of the anterior neuroectoderm." Development **124**(15): 2997-3005.

Purro, S. A., E. M. Dickins and P. C. Salinas (2012). "The secreted Wnt antagonist Dickkopf-1 is required for amyloid  $\beta$ -mediated synaptic loss." The Journal of Neuroscience **32**(10): 3492-3498.

Qiang, Y.-W., Y. Endo, J. S. Rubin and S. Rudikoff (2003). "Wnt signaling in B-cell neoplasia." Oncogene **22**(10): 1536-1545.

Quinlan, R., M. Graf, I. Mason, A. Lumsden and C. Kiecker (2009). "Complex and dynamic patterns of Wnt pathway gene expression in the developing chick forebrain." Neural development **4**(1): 1.

Ranheim, E. A., H. C. Kwan, T. Reya, Y.-K. Wang, I. L. Weissman and U. Francke (2005). "Frizzled 9 knock-out mice have abnormal B-cell development." Blood **105**(6): 2487-2494.

Rasmussen, J. T., M. A. Deardorff, C. Tan, M. S. Rao, P. S. Klein and M. L. Vetter (2001). "Regulation of eye development by frizzled signaling in *Xenopus*." Proceedings of the National Academy of Sciences **98**(7): 3861-3866.

Reya, T. and H. Clevers (2005). "Wnt signalling in stem cells and cancer." Nature **434**(7035): 843-850.

- Rodriguez, J., P. Esteve, C. Weinl, J. M. Ruiz, Y. Fermin, F. Trousse, A. Dwivedy, C. Holt and P. Bovolenta (2005). "SFRP1 regulates the growth of retinal ganglion cell axons through the Fz2 receptor." Nature neuroscience **8**(10): 1301-1309.
- Roelink, H., J. Porter, C. Chiang, Y. Tanabe, D. Chang, P. Beachy and T. Jessell (1995). "Floor plate and motor neuron induction by different concentrations of the amino-terminal cleavage product of sonic hedgehog autoproteolysis." Cell **81**(3): 445-455.
- Rulifson, E. J., C.-H. Wu and R. Nusse (2000). "Pathway specificity by the bifunctional receptor frizzled is determined by affinity for wingless." Molecular cell **6**(1): 117-126.
- Salinas, P. C. (2012). "Wnt signaling in the vertebrate central nervous system: from axon guidance to synaptic function." Cold Spring Harbor perspectives in biology **4**(2): a008003.
- Sato, A., T. Kojima, K. Ui-Tei, Y. Miyata and K. Saigo (1999). "Dfrizzled-3, a new Drosophila Wnt receptor, acting as an attenuator of Wingless signaling in wingless hypomorphic mutants." Development **126**(20): 4421-4430.
- Schulte, G. (2015). "Frizzleds and WNT/ $\beta$ -catenin signaling—the black box of ligand-receptor selectivity, complex stoichiometry and activation kinetics." European journal of pharmacology.
- Seifert, J. R. and M. Mlodzik (2007). "Frizzled/PCP signalling: a conserved mechanism regulating cell polarity and directed motility." Nature Reviews Genetics **8**(2): 126-138.
- Shamim, H. and I. Mason (1999). "Expression of Fgf4 during early development of the chick embryo." Mechanisms of development **85**(1): 189-192.
- Shi, D.-L. and J.-C. Boucaut (2000). "Xenopusfrizzled 4 is a maternal mRNA and its zygotic expression is localized to the neuroectoderm and trunk lateral plate mesoderm." Mechanisms of development **94**(1): 243-245.
- Shi, D.-L., C. Goisset and J.-C. Boucaut (1998). "Expression of Xfz3, a Xenopus frizzled family member, is restricted to the early nervous system." Mechanisms of development **70**(1): 35-47.
- Slusarski, D. C., V. G. Corces and R. T. Moon (1997). "Interaction of Wnt and a Frizzled homologue triggers G-protein-linked phosphatidylinositol signalling." Nature **390**(6658): 410-413.
- Stamatakis, D., F. Ulloa, S. V. Tsoni, A. Mynett and J. Briscoe (2005). "A gradient of Gli activity mediates graded Sonic Hedgehog signaling in the neural tube." Genes & development **19**(5): 626-641.
- Stark, M. R., J. J. Biggs, G. C. Schoenwolf and M. S. Rao (2000). "Characterization of avian frizzled genes in cranial placode development." Mechanisms of development **93**(1): 195-200.
- Stark, M. R., M. S. Rao, G. C. Schoenwolf, G. Yang, D. Smith and T. J. Mauch (2000). "Frizzled-4 expression during chick kidney development." Mechanisms of development **98**(1): 121-125.

- Stern, C. D. (2005). "Neural induction: old problem, new findings, yet more questions." Development **132**(9): 2007-2021.
- Storey, K. G., A. Goriely, C. M. Sargent, J. M. Brown, H. D. Burns, H. M. Abud and J. K. Heath (1998). "Early posterior neural tissue is induced by FGF in the chick embryo." Development **125**(3): 473-484.
- Streit, A., A. J. Berliner, C. Papanayotou, A. Sirulnik and C. D. Stern (2000). "Initiation of neural induction by FGF signalling before gastrulation." Nature **406**(6791): 74-78.
- Streit, A. and C. D. Stern (1999). "Establishment and maintenance of the border of the neural plate in the chick: involvement of FGF and BMP activity." Mechanisms of development **82**(1): 51-66.
- Sumanas, S., P. Strege, J. Heasman and S. C. Ekker (2000). "The putative wnt receptor *Xenopus* frizzled-7 functions upstream of beta-catenin in vertebrate dorsoventral mesoderm patterning." Development **127**(9): 1981-1990.
- Summerhurst, K., M. Stark, J. Sharpe, D. Davidson and P. Murphy (2008). "3D representation of Wnt and Frizzled gene expression patterns in the mouse embryo at embryonic day 11.5 (Ts19)." Gene Expression Patterns **8**(5): 331-348.
- Sun, T., H. Dong, L. Wu, M. Kane, D. H. Rowitch and C. D. Stiles (2003). "Cross-repressive interaction of the Olig2 and Nkx2. 2 transcription factors in developing neural tube associated with formation of a specific physical complex." The Journal of neuroscience **23**(29): 9547-9556.
- Tamai, K., X. Zeng, C. Liu, X. Zhang, Y. Harada, Z. Chang and X. He (2004). "A mechanism for Wnt coreceptor activation." Molecular cell **13**(1): 149-156.
- Tao, Q., C. Yokota, H. Puck, M. Kofron, B. Birsoy, D. Yan, M. Asashima, C. C. Wylie, X. Lin and J. Heasman (2005). "Maternal wnt11 activates the canonical wnt signaling pathway required for axis formation in *Xenopus* embryos." Cell **120**(6): 857-871.
- Terasaki, H., T. Saitoh, K. Shiokawa and M. Katoh (2002). "Frizzled-10, up-regulated in primary colorectal cancer, is a positive regulator of the WNT- $\beta$ -catenin-TCF signaling pathway." International journal of molecular medicine **9**(2): 107-112.
- Theodosiou, N. A. and C. J. Tabin (2003). "Wnt signaling during development of the gastrointestinal tract." Developmental biology **259**(2): 258-271.
- Thiele, S., M. Rauner, C. Goettsch, T. D. Rachner, P. Benad, S. Fuessel, K. Erdmann, C. Hamann, G. B. Baretton and M. P. Wirth (2011). "Expression profile of WNT molecules in prostate cancer and its regulation by aminobisphosphonates." Journal of cellular biochemistry **112**(6): 1593-1600.
- Timmer, J. R., C. Wang and L. Niswander (2002). "BMP signaling patterns the dorsal and intermediate neural tube via regulation of homeobox and helix-loop-helix transcription factors." Development **129**(10): 2459-2472.

- Tufan, A. C., K. M. Daumer and R. S. Tuan (2002). "Frizzled-7 and limb mesenchymal chondrogenesis: Effect of misexpression and involvement of N-cadherin." Developmental dynamics **223**(2): 241-253.
- Ueno, K., H. Hirata, Y. Hinoda and R. Dahiya (2013). "Frizzled homolog proteins, microRNAs and Wnt signaling in cancer." International Journal of Cancer **132**(8): 1731-1740.
- Ueno, K., M. Hiura, Y. Suehiro, S. Hazama, H. Hirata, M. Oka, K. Imai, R. Dahiya and Y. Hinoda (2008). "Frizzled-7 as a potential therapeutic target in colorectal cancer." Neoplasia **10**(7): 697-705.
- Ulloa, F. and E. Martí (2010). "Wnt won the war: Antagonistic role of Wnt over Shh controls dorso-ventral patterning of the vertebrate neural tube." Developmental dynamics **239**(1): 69-76.
- Umbhauer, M., A. Djiane, C. Goisset, A. Penzo-Méndez, J. F. Riou, J. C. Boucaut and D. L. Shi (2000). "The C-terminal cytoplasmic Lys-Thr-X-X-X-Trp motif in frizzled receptors mediates Wnt/ $\beta$ -catenin signalling." The EMBO journal **19**(18): 4944-4954.
- van Amerongen, R. and A. Berns (2006). "Knockout mouse models to study Wnt signal transduction." TRENDS in Genetics **22**(12): 678-689.
- van Amerongen, R. and R. Nusse (2009). "Towards an integrated view of Wnt signaling in development." Development **136**(19): 3205-3214.
- van Gijn, M. E., W. M. Blankesteyn, J. F. Smits, B. Hierck and A. C. Gittenberger-de Groot (2001). "Frizzled 2 is transiently expressed in neural crest-containing areas during development of the heart and great arteries in the mouse." Anatomy and embryology **203**(3): 185-192.
- Villanueva, S., A. Glavic, P. Ruiz and R. Mayor (2002). "Posteriorization by FGF, Wnt, and retinoic acid is required for neural crest induction." Developmental biology **241**(2): 289-301.
- Vinson, C. R. and P. N. Adler (1987). "Directional non-cell autonomy and the transmission of polarity information by the frizzled gene of *Drosophila*."
- Wallingford, J. B. and R. Habas (2005). "The developmental biology of Dishevelled: an enigmatic protein governing cell fate and cell polarity." Development **132**(20): 4421-4436.
- Wang, B., J. F. Fallon and P. A. Beachy (2000). "Hedgehog-regulated processing of Gli3 produces an anterior/posterior repressor gradient in the developing vertebrate limb." Cell **100**(4): 423-434.
- Wang, H.-q., M.-l. Xu, J. Ma, Y. Zhang and C.-h. Xie (2012). "Frizzled-8 as a putative therapeutic target in human lung cancer." Biochemical and biophysical research communications **417**(1): 62-66.
- Wang, H.-y., T. Liu and C. C. Malbon (2006). "Structure-function analysis of Frizzleds." Cellular signalling **18**(7): 934-941.

Wang, Y., N. Guo and J. Nathans (2006). "The role of Frizzled3 and Frizzled6 in neural tube closure and in the planar polarity of inner-ear sensory hair cells." The Journal of neuroscience **26**(8): 2147-2156.

Wang, Y., D. Huso, H. Cahill, D. Ryugo and J. Nathans (2001). "Progressive Cerebellar, Auditory, and Esophageal Dysfunction Caused by Targeted Disruption of the frizzled-4 Gene." The Journal of Neuroscience **21**(13): 4761-4771.

Wang, Y., J. P. Macke, B. S. Abella, K. Andreasson, P. Worley, D. J. Gilbert, N. G. Copeland, N. A. Jenkins and J. Nathans (1996). "A large family of putative transmembrane receptors homologous to the product of the Drosophila tissue polarity gene frizzled." Journal of Biological Chemistry **271**(8): 4468-4476.

Wang, Y., N. Thekdi, P. M. Smallwood, J. P. Macke and J. Nathans (2002). "Frizzled-3 is required for the development of major fiber tracts in the rostral CNS." The Journal of neuroscience **22**(19): 8563-8573.

Wang, Y., J. Zhang, S. Mori and J. Nathans (2006). "Axonal growth and guidance defects in Frizzled3 knock-out mice: a comparison of diffusion tensor magnetic resonance imaging, neurofilament staining, and genetically directed cell labeling." The Journal of neuroscience **26**(2): 355-364.

Wheeler, G. N. and S. Hoppler (1999). "Two novel Xenopus frizzled genes expressed in developing heart and brain." Mechanisms of development **86**(1): 203-207.

Wilson, L. and M. Maden (2005). "The mechanisms of dorsoventral patterning in the vertebrate neural tube." Developmental biology **282**(1): 1-13.

Wilson, S. I. and T. Edlund (2001). "Neural induction: toward a unifying mechanism." nature neuroscience **4**: 1161-1168.

Wodarz, A. and R. Nusse (1998). "Mechanisms of Wnt signaling in development." Annual review of cell and developmental biology **14**(1): 59-88.

Wu, C.-h. and R. Nusse (2002). "Ligand receptor interactions in the Wnt signaling pathway in Drosophila." Journal of Biological Chemistry **277**(44): 41762-41769.

Xu, Q., Y. Wang, A. Dabdoub, P. M. Smallwood, J. Williams, C. Woods, M. W. Kelley, L. Jiang, W. Tasman and K. Zhang (2004). "Vascular development in the retina and inner ear: control by Norrin and Frizzled-4, a high-affinity ligand-receptor pair." Cell **116**(6): 883-895.

Yamaguchi, T. P. (2001). "Heads or tails: Wnts and anterior-posterior patterning." Current Biology **11**(17): R713-R724.

Yan, Y., Y. Li, C. Hu, X. Gu, J. Liu, Y.-A. Hu, Y. Yang, Y. Wei and C. Zhao (2009). "Expression of Frizzled10 in mouse central nervous system." Gene Expression Patterns **9**(3): 173-177.

Yang-Snyder, J., J. R. Miller, J. D. Brown, C.-J. Lai and R. T. Moon (1996). "A frizzled

- homolog functions in a vertebrate Wnt signaling pathway." Current Biology **6**(10): 1302-1306.
- Yoshikawa, Y., T. Fujimori, A. P. McMahon and S. Takada (1997). "Evidence that absence of Wnt-3a signaling promotes neuralization instead of paraxial mesoderm development in the mouse." Developmental biology **183**(2): 234-242.
- Yu, H., P. M. Smallwood, Y. Wang, R. Vidaltamayo, R. Reed and J. Nathans (2010). "Frizzled 1 and frizzled 2 genes function in palate, ventricular septum and neural tube closure: general implications for tissue fusion processes." Development **137**(21): 3707-3717.
- Zecca, M., K. Basler and G. Struhl (1996). "Direct and long-range action of a wingless morphogen gradient." Cell **87**(5): 833-844.
- Zechner, D., T. Müller, H. Wende, I. Walther, M. M. Taketo, E. B. Crenshaw, M. Treier, W. Birchmeier and C. Birchmeier (2007). "Bmp and Wnt/ $\beta$ -catenin signals control expression of the transcription factor Olig3 and the specification of spinal cord neurons." Developmental biology **303**(1): 181-190.
- Zhang, H., Y. Hao, J. Yang, Y. Zhou, J. Li, S. Yin, C. Sun, M. Ma, Y. Huang and J. J. Xi (2011). "Genome-wide functional screening of miR-23b as a pleiotropic modulator suppressing cancer metastasis." Nature communications **2**: 554.
- Zhang, J. and R. W. Carthew (1998). "Interactions between Wingless and Dfz2 during Drosophila wing development." Development **125**(16): 3075-3085.
- Zhang, Z., S. A. Rankin and A. M. Zorn (2013). "Different thresholds of Wnt-Frizzled 7 signaling coordinate proliferation, morphogenesis and fate of endoderm progenitor cells." Developmental biology **378**(1): 1-12.
- Zhao, T., Q. Gan, A. Stokes, R. N. Lassiter, Y. Wang, J. Chan, J. X. Han, D. E. Pleasure, J. A. Epstein and C. J. Zhou (2014). " $\beta$ -catenin regulates Pax3 and Cdx2 for caudal neural tube closure and elongation." Development **141**(1): 148-157.
- Zhuang, B. and S. Sockanathan (2006). "Dorsal–ventral patterning: a view from the top." Current opinion in neurobiology **16**(1): 20-24.
- Zimmerman, L. B., J. M. De Jesús-Escobar and R. M. Harland (1996). "The Spemann organizer signal noggin binds and inactivates bone morphogenetic protein 4." Cell **86**(4): 599-606.

# Appendixes

## Appendix A

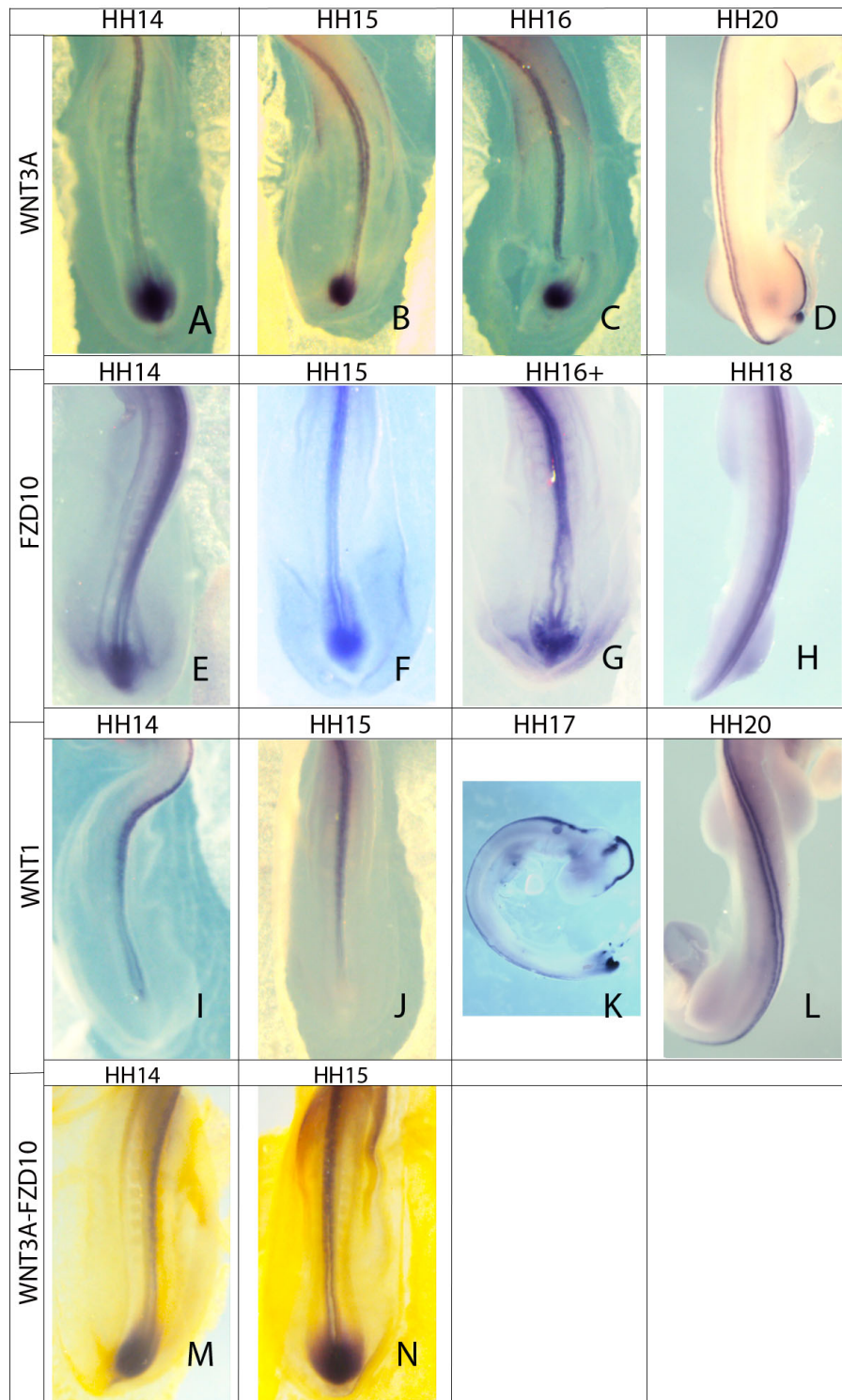


**Fig. A.1 - Whole mount in situ hybridization for Wnt3a, FZD10 and Wnt1 at different stages. Wnt3a (A,B,C and D). FZD10 (E,F,G and H). Wnt1 (I,J,K and L). (M and N) show double in situ for Wnt3a and FZD10.**

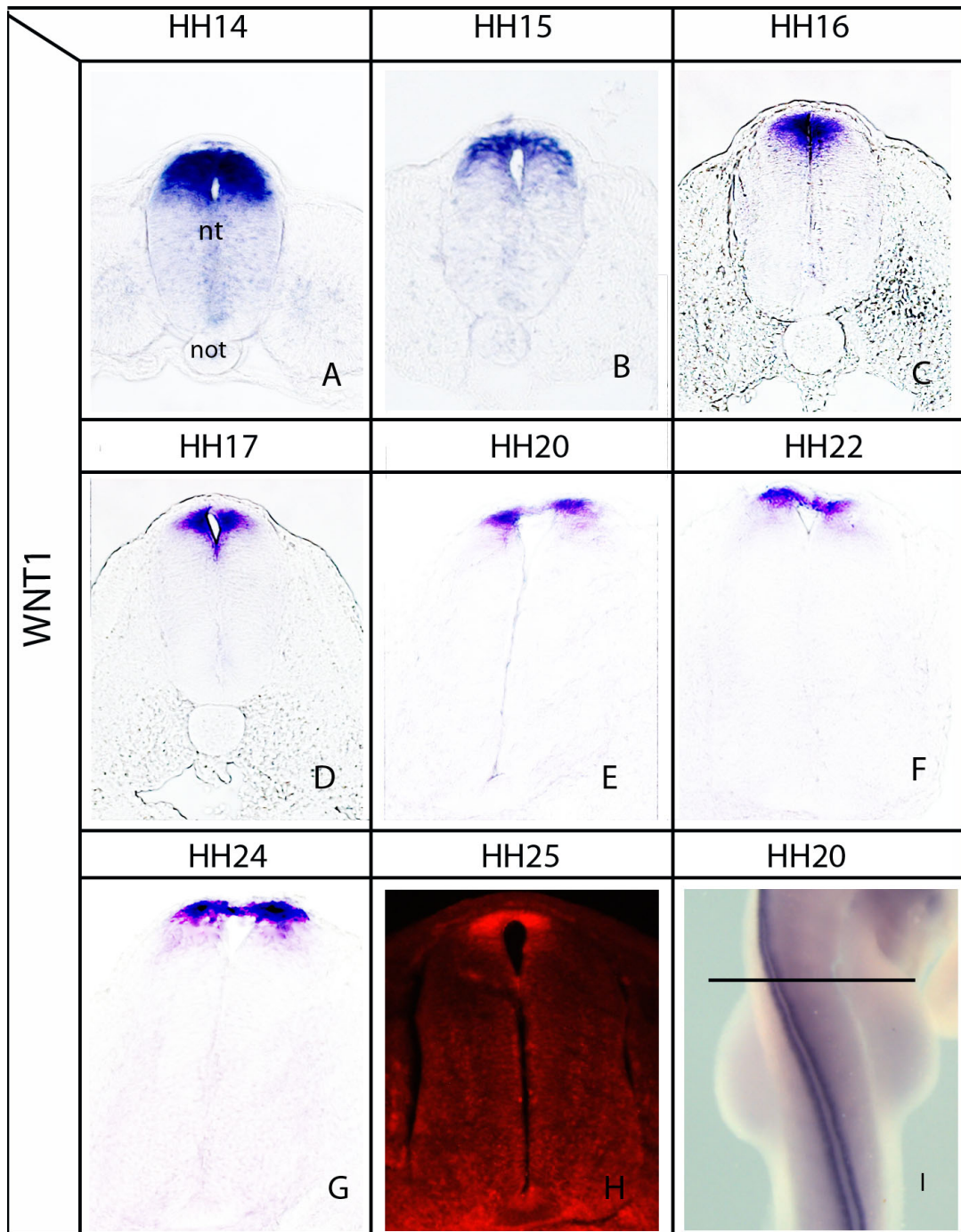


**Fig. A.2** In situ expression profile of Wnt1 in the developing spinal cord at different stages HH14 to HH25. Dorsal-ventral sections show Wnt1 expression (A-H).

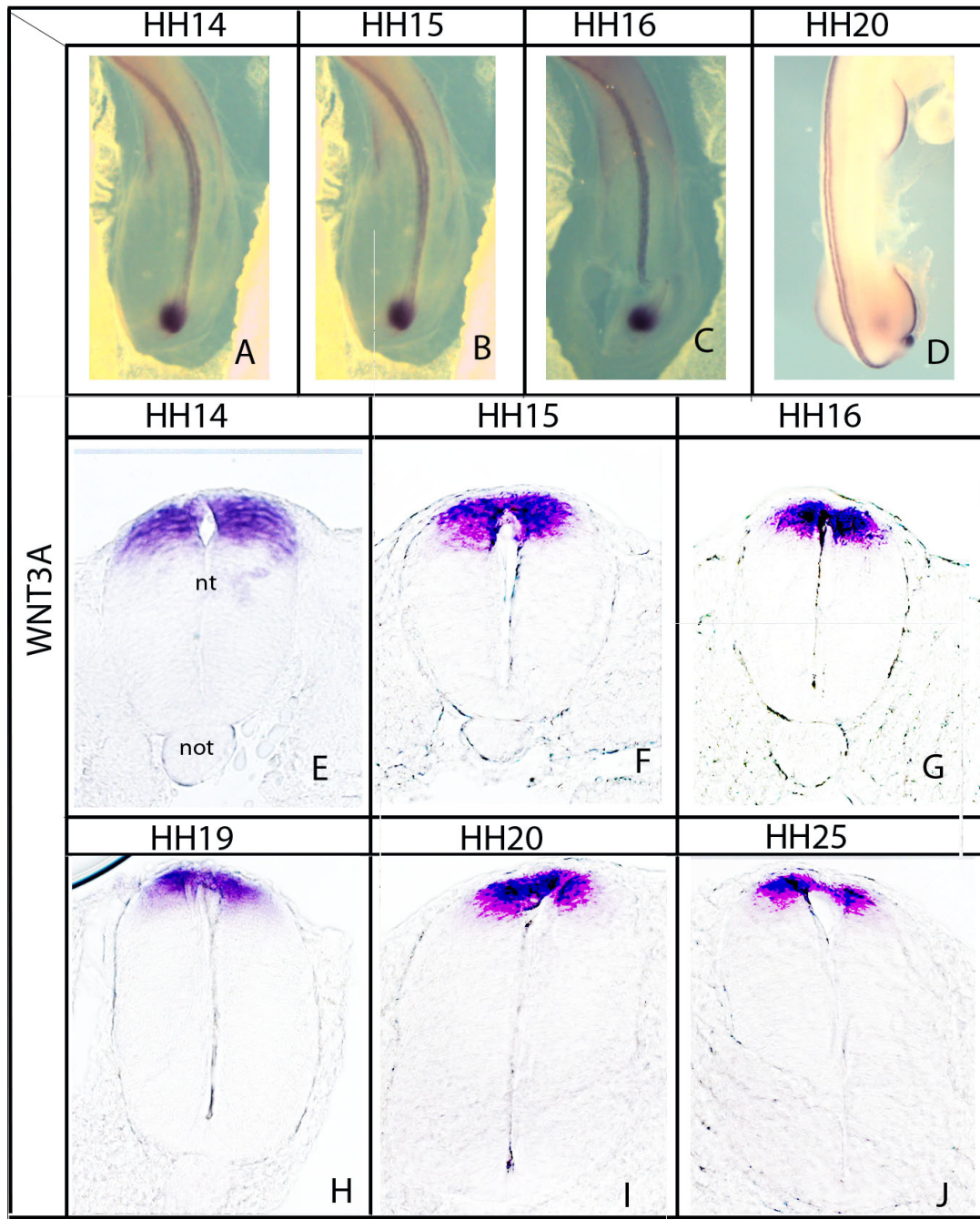


**Fig. A.3 In situ expression profile of Wnt3a at different stages.** A-D show whole mount in situ at HH14 to HH20. E-J shows the expression pattern of Wnt3a during the development of the spinal cord at stage HH14 to HH25.

## Appendix B

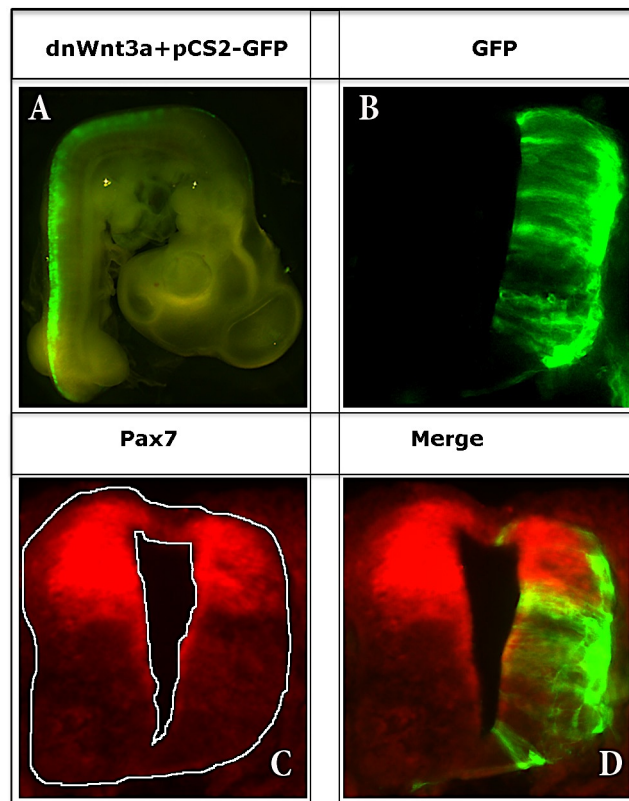


**Fig B.1 DnWnt3a** affects spinal cord size and reduces Pax7 expression domain (48hours PE). (A) Whole mount picture of electroporated embryo with dnWnt3a and pCS2-GFP. (B) Transverse section of spinal cord showing GFP expression in the electroporated side. (C) Electroporated side is smaller when compared to the control and Pax7 expression is inhibited as well as its expression domain is reduced. (D) GFP expression in the electroporated side of the spinal cord. Embryos number was 3/4.

## Appendix C

**Fig. C.2 comparing human Lrp6 protein sequence to predicted chick Lrp6.** Human Lrp6 were blasted against chick genomic sequence in NCBI; it was found that they share 93% amino acid identity, suggesting that Human and chick Lrp6 are conserved and may play same roles.

PREDICTED: LOW QUALITY PROTEIN: low-density lipoprotein receptor-related protein 6 [Gallus gallus]

Sequence ID: [ref|XP\\_417286.3|](#) Length: 1625 Number of Matches: 1

**Related Information**

[Gene-associated gene details](#)

[Map Viewer-aligned genomic context](#)

**Range 1: 26 to 1625** [GenPeptGraphics](#)

[Next Match](#)

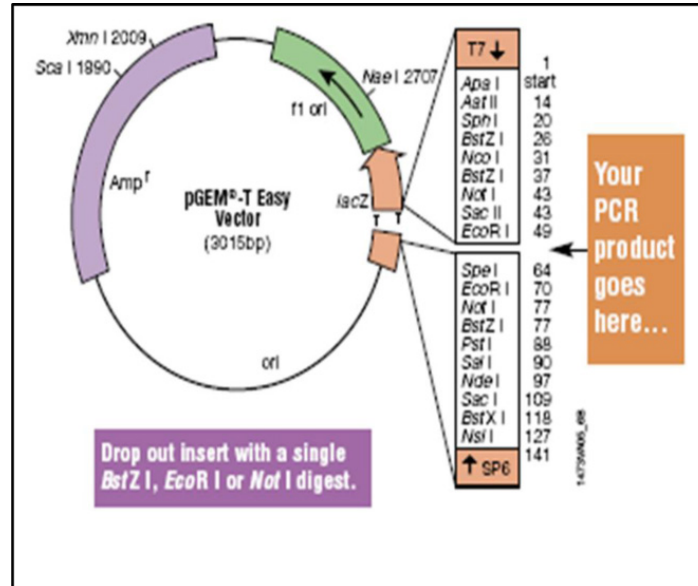
[Previous Match](#)

	Identities 1489/1601(93%)	Positives 1555/1601(97%)	Gaps 1/1601(0%)	
Query	13	FCVLLRAAPLLLYANRRDLRLVDATNGKENATIVVGGLEDAAAVDFVFSHGLIYWSVDVSE		72
		+CVLLR+APLLLYANRRDLRLVDA NGKENAT++VGGLEDAAAVDFVF GLIYWSVDVSE		
Sbjct	26	YCVLLRSAPLLLYANRRDLRLVDAANGKENATVI VGGLEDAAAVDFVFKGLIYWSVDVSE		85
Query	73	EAIKRTEFNKTESVQN VVVSGLLSPDGLACDWLGEKLYWTDSETNRIEVS NLDGSLRKVL		132
		EAIKRTEFNK+ SVQNVV+SGLLSPDGLACDWLGEKLYWTDSETNRIEVS NLDGSLRKVL		
Sbjct	86	EAIKRTEFNKSGSVQNVVISGLLSPDGLACDWLGEKLYWTDSETNRIEVS NLDGSLRKVL		145
Query	133	FWQELDQPRAIALDPSSGFMYWTDWGEVVKIERAGMDGSSRFIIINSEIYWPNGLTLDYE		192
		FWQELDQPRAIALDP+ GFMYWTDWGEVVKIERAGMDGSSR II+N++IYWPNGLTLDYE		
Sbjct	146	FWQELDQPRAIALDPARGFMYWTDWGEVVKIERAGMDGSSRSIIIVNTDIYWPNGLTLDYE		205
Query	193	EQKLYWADAKLNF IHKSNLDGTRQAVVKGSLPHPFALTLFEDILYWTDWSTH SILACNK		252
		EQKLYWADAKLNF IHKSNLDG++RQAVVKGSLPHPFALTLF D LYWTDW+THSILAC+K		
Sbjct	206	EQKLYWADAKLNF IHKSNLDGSHRQAVVKGSLPHPFALTLFGDTLYWTDWNTHSILACSK		265
Query	253	YTGEGLREIHSDFISPMDIHAFSQQRQPNATNPCGIDNGGCSHLCLMSPVKPFYQCACPT		312
		Y+GE LREIHS+IFSPMDIHAFSQ+RQPNATNPCGI+NGGCSHLCLMSP KP YQCACPT		
Sbjct	266	YSGEDLREIHSNIFISPMDIHAFSQQRQPNATNPCGINNGGCSHLCLMSPTKPSYQCACPT		325
Query	313	GVKLENGKTCCKDGATELLLLARRTDLRRISLDTPDFTDIVLQLEDIRHAI AIDYDPVEG		372
		GVKLENGKTCCKDGATELLLLARRTDLRRISLDTPDFTDIVL LEDIRHAI AID+DP+EG		
Sbjct	326	GVKLENGKTCCKDGATELLLLARRTDLRRISLDTPDFTDIVLPLEDIRHAI AIDFDPLEG		385
Query	373	YIYWTDDVEVRAIRRSFIDGSGSQFVVTAQIAHPDGI AVDWARNLYWTDGTDRIEVTRL		432
		YIYWTDDVEVRAIRRSF+DGSQSQFVVTAQIAHPDGI AVDWARNLYWTDGTDRIEVTRL		
Sbjct	386	YIYWTDDVEVRAIRRSFVDGSGSQFVVTAQIAHPDGI AVDWARNLYWTDGTDRIEVTRL		445
Query	433	NGTMRKILISEDLEEPRAIVLDPVMGYMYWTDWGEIPKIERAALDGS DRVVLVNTSLGWP		492
		NGTMRKILISEDLEEPRAIVLDPVMGYMYWTDWGEIPKIERAALDGS DR+VLVNTSLGWP		
Sbjct	446	NGTMRKILISEDLEEPRAIVLDPVMGYMYWTDWGEIPKIERAALDGS DRIVLVNTSLGWP		505
Query	493	NGLALDYDEGKIYWGDAKTDKIEVMNTDGTGRRVLVEDKIPHIFGF TLLGDYVYWTDWQR		552
		NGLALDY E KIYWGDAKTDKIEVMN DGTGRRVLVEDK+PHIFGF TLLGDYVYWTDWQR		
Sbjct	506	NGLALDYAESKIYWGDAKTDKIEVMNADGTGRRVLVEDKLP HIFGF TLLGDYVYWTDWQR		565
Query	553	RSIERVHKRSAREEVIIDQLPDLMLGKATNVHRVIGSNPCAENG GCSHLCLYRPQGLRC		612
		RSIERVHKR+AERE+IIDQLPDLMLGKATNVH++IG+NPCA E+NGGCSHLCLYRPQGLRC		
Sbjct	566	RSIERVHKRTAEREIIDQLPDLMLGKATNVHQIIGTNP CAEDNGGCSHLCLYRPQGLRC		625
Query	613	ACPIGFELISDMKTCIVPEAFLLFSRRADIRRI SLETNNNNVAIPLTG VKEASALDFDVT		672
		ACPIG ELI+DMKTCIVPEAFLLFSRRADIRRI SLETNNNNVAIPLTG VKEASALDF		
Sbjct	626	ACPIGELIINDMKTCIVPEAFLLFSRRADIRRI SLETNNNNVAIPLTG VKEASALDFXCD		685
Query	673	DNRIYWTDISLKTISR AFMNGSALEHVVEFGLDYPEGMAVDWL GKNLYWADTGTNRIEVS		732
		YWTDISLKTISR AFMNGSALEHVVEFGLDYPEGMAVDWL GKNLYWADTGTNRIEVS		
Sbjct	686	RQSNYWTDISLKTISR AFMNGSALEHVVEFGLDYPEGMAVDWL GKNLYWADTGTNRIEVS		745
Query	733	KLDGQHRQVLVWKDL DSPRALALDPAEGFMYWTEWGGKPKIDRAAMD GSERTTLVVPNVGR		792
		KLDGQHRQVLVWKDL DSPRALALDPAEGFMYWTEWGGKPKI DRA+MDGSERTTLVVPNVGR		
Sbjct	746	KLDGQHRQVLVWKDL DSPRALALDPAEGFMYWTEWGGKPKI DRAAMDGSERTTLVVPNVGR		805
Query	793	ANGLTIDYAKRRLYWTDLDTNLIESSNMLGLNREVIADDLPHPFGLTQYQDYIYWTDWSR		852
		ANGLTIDYAKRRLYWTDLDTNLIESSNMLGL+RE+IADDLPHPFGLTQYQDYIYWTDWSR		
Sbjct	806	ANGLTIDYAKRRLYWTDLDTNLIESSNMLGLDREI IADDLPHPFGLTQYQDYIYWTDWSR		865
Query	853	RSIERANKTSGQNRTIIQGHLDYVMDILVFHSSRQSGWNECASSNGHC SHLCLAVPVGGF		912
		RSIERANKTSGQNRTIIQGHLDYVMDILVFHSSRQ+GWNECASSNGHC SHLCLAVPVGGF		
Sbjct	866	RSIERANKTSGQNRTIIQGHLDYVMDILVFHSSRQAGWNECASSNGHC SHLCLAVPVGGF		925
Query	913	VCGCPAHYSLNADNRTCSAPTTFLFSQKSAINRMVIDEQSPDIILPIHSLRN VRAIDY		972
		VCGCPAHYSLN+DNRTCSAPTTFLFSQK+A INRMVIDEQSPDIILPIHSLRN VRAIDY		
Sbjct	926	VCGCPAHYSLNSDNRTCSAPTTFLFSQKNA INRMVIDEQSPDIILPIHSLRN VRAIDY		985
Query	973	DPLDKQLYWIDSRQNMIRKAQEDGSGQFTVVVSSVPSQNL EIQPYDLSIDIYSRIYWTCT		1032

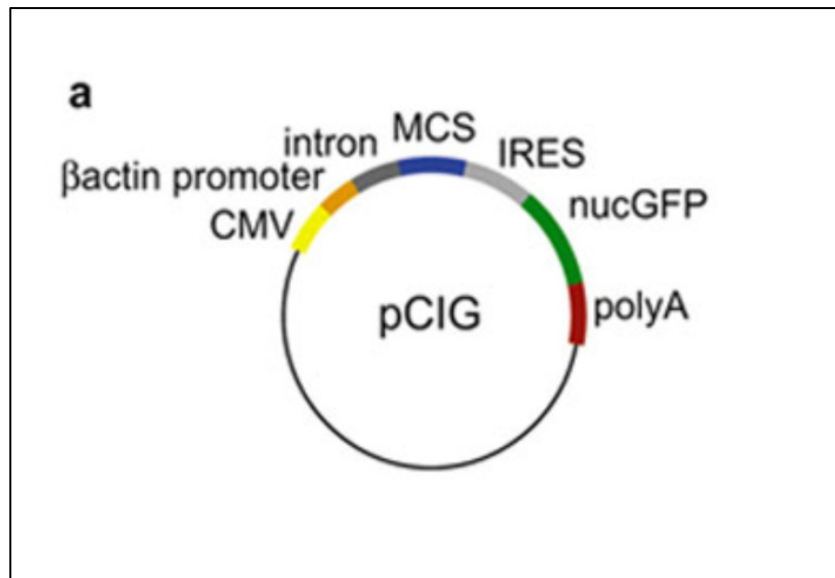
Sbjct	986	DPLDKQLYWIDSRQN+IRKAQEDGSQ TVV+S VP+QNL++QPYDLSIDIYSRYIYWTC DPLDKQLYWIDSRQNIIRKAQEDGSQSLTVVISFPVNPQNLDMQPYDLSIDIYSRYIYWTC	1045
Query	1033	EATNVINVTRLDGRSVGVVLKGEQDRPRAVVVNPEKGYMYFTNLQERSPKIERAALDGT EATNVINVTRLDGR +GVVLKG+QDRPRA+VVNPEKGYMYFTNLQERSPKIERAALDGT	1092
Sbjct	1046	EATNVINVTRLDGRPMGVVLKGDQDRPRAIVVNPEKGYMYFTNLQERSPKIERAALDGT	1105
Query	1093	REVLFFSGLSKPIALALDSRLGKLFWADSDLRRIESDLSGANRIVLEDSNILQPVGLTV REVLFFSGLSKPIALA+DS+LGKLFWADSDLRRIESDLSGANR+VLEDSNILQPVGLTV	1152
Sbjct	1106	REVLFFSGLSKPIALALDSRLGKLFWADSDLRRIESDLSGANRVVLEDSNILQPVGLTV	1165
Query	1153	FENWLYWIDKQQMIEKIDMTGREGRTKVQARIAQLSDIHAVKELNLQEYRQHPAQDNG FENWLYWID+QQMIEKIDMTGREGRTKVQARIAQLSDIHAVKELN+QEYRQHPC+QDNG	1212
Sbjct	1166	FENWLYWIDRQQMIEKIDMTGREGRTKVQARIAQLSDIHAVKELNLQEYRQHPCSQDNG	1225
Query	1213	GCSHICLVKGDGTRCSCPMLVLLQDELSCGEPPTCSPQQFTCFTGEIDCIPVAWRCDG GCSHIC+VKGDGTRCSCP+HLVLLQDELSCGEPPTCSPQQFTCFTGEIDCIPVAWRCDG	1272
Sbjct	1226	GCSHICIVKGDGTRCSCPVHLVLLQDELSCGEPPTCSPQQFTCFTGEIDCIPVAWRCDG	1285
Query	1273	FTECEDHSDELNCPVCSSESQFCASGQCIDGALRCNGDANCQDKSDEKNCVCLIDQFR FTECEDHSDE NCPVCS++QFQC SGQCID ALRCNG+ANCQD SDEKNCVCL QFR	1332
Sbjct	1286	FTECEDHSDEKNCPVCSDTQFQCESGQCIDSALRCNGEANCQDNSDEKNCVCLTSQFR	1345
Query	1333	CANGQCIGKHKKCDHNVDKSDKDELDCYPTTEEPAPQATNTVGSVIGVIVTIFVSGTVYF CA+GQCIGK KKCDHN+DCSD SDE CY TEEPAPQ NT+GS+IGVI+T+FV G +YF	1392
Sbjct	1346	CASGQCIGKSKKCDHNLDKSDSSDEQGCYTTEEPAPQPNNTIGSIIIGVILTLFVVGAMYF	1405
Query	1393	ICQRMLCPRMKGDGETMTNDYVVHGPASVPLGYVPHPSLGSGLPGMSRGKSMISLSIM ICQR+LCPRMKGDGETMTNDYVVHGPASVPLGYVPHPSLGSGLPGMSRGKS+ISSLSIM	1452
Sbjct	1406	ICQRVLCPRMKGDGETMTNDYVVHGPASVPLGYVPHPSLGSGLPGMSRGKSVISSLSIM	1465
Query	1453	GGSSGPPYDRAHVTGASSSSSSSTKGTYPFPAILNPPSPATERSHYTMEFGYSSNSPSTH GGSSGPPYDRAHVTGASSSSSSSTKGTYPF ILNPPSPATERSHYTMEFGYSSNSPSTH	1512
Sbjct	1466	GGSSGPPYDRAHVTGASSSSSSSTKGTYPFPILNPPSPATERSHYTMEFGYSSNSPSTH	1525
Query	1513	RSYSYRPYSYRHFAPPTTPCSTDVCDSDYAPSRRTSVATAKGYTSDLNYDSEPVPVPPPT RSYSYRPYSYRHFAPPTTPCSTDVCDSDYAPSRRT+T+ AKGYTSDLNYDSEPVPVPPPT	1572
Sbjct	1526	RSYSYRPYSYRHFAPPTTPCSTDVCDSDYAPSRRTAT-MAKGYTSDLNYDSEPVPVPPPT	1584
Query	1573	PRSQYLSAEENYESCPPSPYTERSYSHHLYPPPPSPCTDSS 1613	
Sbjct	1585	PRSQYLSAEENYESCPPSPYTERSYSHHLYPPPPSPCTDSS 1625	

## APPENDIX D

-Vectors used in this study:

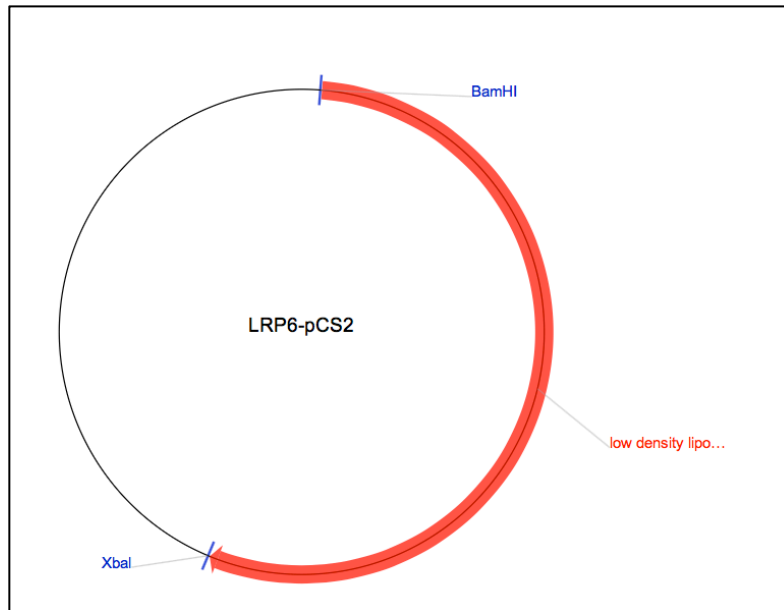


E.1 Schematic shows pGEM-T easy vector used for cloning and generating in situ probes.



E.2 Schematic representation of the pCIG-IRES-GFP vector used for overexpression of Wnt1 and Wnt3a in chick neural tube. (Adapted from Megason and McMahon, 2002).





**E.5** Schematic representation of the pCS2 vector used for overexpression of LRP6 in chick neural tube. (Adapted from Addgene).